# A DYNAMIC PROGRAM FOR MINIMUM COST SHIP ROUTING UNDER UNCERTAINTY

by

Henry H.T. Chen

B.Sc. University of Newcastle Upon Tyne, ENGLAND
(1973)

S.M. Massachusetts Institute of Technology
(1976)

SUBMITTED IN PARTIAL FULFILLMENT
OF THE REQUIREMENTS FOR THE
DEGREE OF
DOCTOR OF PHILOSOPHY

at the

MASSACHUSETTS INSTITUTE OF TECHNOLOGY
February, 1978

Signature redacted

Signature of Author.....
Department of Ocean Engineering, Febuary, 1978

Signature redacted

Certified by.....
Thesis Supervisor

Signature redacted

Accepted by.....
Chairman, Departmental Committee ~~on Graduate~~ Students

# A DYNAMIC PROGRAM FOR MINIMUM COST SHIP ROUTING UNDER UNCERTAINTY

by

Henry H.T. Chen

Submitted to the Department of Ocean Engineering on February 24, 1978 in partial fulfillment of the requirements for the Degree of Doctor of Philosophy.

## ABSTRACT

The minimum cost ship routing system, consisting of a series of computer programs to prepare the input data, perform route optimization and retrieve the expected trajectories was developed around a stochastic dynamic programming algorithm.

The input environmental data is derived from the directional wave spectra and other weather products forecasted by the Fleet Numerical Central of the U.S. Navy. The ship motion response characteristics are in the form of Response Amplitude Operators calculated by the M.I.T. 5-D ship motion program developed at the Department of Ocean Engineering.

The routing optimization program implemented on an IBM 370/168 computer at the Information Processing Center requires 170 K core region and 2.5 CPU minutes which amounts to $40 per run at M.I.T. price for a typical Trans-Atlantic voyage. By incorporating a modified open-loop control strategy to update the recommended route several times during a voyage, the system is economically feasible if 1% of the fuel cost saving can be realized.

The algorithm has retained enough flexibility for carrying out sensitivity studies on the feasible state space discretization. Ways and means for model calibration under real operating conditions are outlined. Test and evaluation methods are also recommended for future real-time implementation.

Thesis Committee: Devanney,III, John W., Assoc.Prof. Ocean Eng.
Frankel, Ernst G., Prof., Ocean Eng.
Simpson, Robert W., Prof, Aero.& Astro.Eng.
Wilson, Nigel H.M. Assoc. Prof. Civil Eng.

## ABSTRACT

This thesis summarizes an approach to the problem of minimum cost ship routing under uncertainty. The problem is essentially treated as a multi-stage stochastic dynamic control process under the constraint of ship operational requirements, probablistic ocean environmental conditions and ship dynamic response characteristics in seaways. A stochastic dynamic programming algorithm was developed to compute the ship's trajectory and its corresponding power output and heading based on the minimization of the expected total voyage cost.

The ship routing system consists of a series of computer programs to prepare the input data, perform optimization and retrieve the expected ship trajectories. The input environmental data is derived from the directional wave spectra and other weather products forecasted by the Fleet Numerical Weather Central of the U.S. Navy. The ship motion response characteristics are in the form of Response Amplitude Operator calculated by the MIT 5-D ship motion program developed at the Department of Ocean Engineering. The routing optimization program developed on an IBM 370/168 computer at the Information Processing Center requires 170 K core region and 2.5 minutes of CPU time which amounts to $40 per run for a typical Trans-Atlantic voyage at M.I.T. price. By incorporating a modified open-loop control strategy to update the recommended route several times during a voyage, the system is economically feasible if 1% of the fuel saving can be realized.

The algorithm has retained enough flexibility for carrying out sensitivity studies on the feasible state space discretization. Ways and means for model calibration under real operating conditions are outlined. Test and evaluation methods are also recommended for future real-time implementation.

ACKNOWLEDGEMENT

I wish to express my sincere gratitude to my advisor, Professor Ernst Frankel for his continuous encouragement and guidance during my studies at M.I.T.

Thanks are also due to Professors J.W. Devanny III, R.W. Simpson and N.H.M. Wilson of Center of Transportation Studies for their contributions and interests as thesis committee members. I am particularly indebted to Prof. Devanny for his valuable suggestions and criticism in developing the routing algorithm.

The data concerning wave information and LASH ship characteristics were kindly provided by Dr. Dan Hoffman, Hoffman Maritime Consultant. Thanks are also due to Mr. Norm Stevenson of Fleet Numerical Weather Central of the U.S. Navy for his interest and valuable discussions on ocean wave spectra forecasts.

The use of M.I.T. 5-D Ship Motion Program was kindly provided by Prof. C.Chryssostomidis, his assistance in running the program is also acknowledged.

The present research is under the sponsorship of National Maritime Research Center, Kings Point, MARAD, whose financial support is greatly appreciated.

Last but not least, I would like to thank my wife Ailene for her understanding and encouragement throughout the entire effort.

TABLE OF CONTENTS

LIST OF TABLES

LIST OF FIGURES

# Chapter 1

# INTRODUCTION

## 1.1 BACKGROUND

Historically, the concept of ship weather routing has been practiced for a long time. Navigators and explorers who had sailed a particular route would select a track on the basis of the expected weather pattern rather than following standard or seasonal tracks. The first weather routed voyage could conceivably be dated back to the fourteenth century when Henry the Navigator learned how to benefit from the Trade Winds. He led his fleet to the equator while trying to find a way around the Cape into the Indian Ocean in order to oust the Venetians and Arabs from their lucrative trading position in that area.

Over the past decade, there have been some advances in the state-of-the-art of ship weather routing. Various manual and computer aided weather routing methods have been practiced and some of them are commercially available at the present.

These methods* usually work on the principle of minimum time of transit and storm avoidance, rely largely on human experiences and empirical data to derive the best ship trajectories with the limited available resources. Even though some of the models tend to be simplistic and do not guarantee the optimal track, the strategic and economic advantages of ship routing are obviously recognized and confirmed by the large number of ship operators who subscribe to the services.

More recently, there are several major advances in the field of ocean wave forecasting, naval architecture and shipboard

---

* For an excellent review of the history and recent development of weather routing techniques please refer to James' paper, Ref. [1]. The reference list starts on page

instrumentation which have enabled us to realistically and accurately predict the ship speedkeeping and seakeeping performance at sea. Specifically, the sophisticated Spectral Ocean Wave Model (SOWM) developed by the U.S. Navy's Fleet Numerical Weather Central (FNWC) forecasts ocean wave spectra at 12 hour intervals up to 72 hours. The forecasted directional wave spectra in fifteen frequency bands and twelve directions are now available on a regular basis for the major oceans in the world [2].

In parallel to this major development, the studies sponsored by the U.S. Maritime Administration (MARAD) on seakeeping performance of ship carried out by the Massachusetts Institute of Technology (M.I.T.) has resulted in the successful development of a computer program to predict ship motion responses and seakeeping characteristics at sea [3]. For a given ship geometry, the program can predict the magnitude of bending moment, absolute or relative motion, velocity and acceleration in five degrees of freedom plus the added resistance in head seas, in long crested regular sea as well as in irregular seas described by their wave spectra.

In view of these major developments, it is believed that further advances in ship routing techniques are possilbe. In particular, it is hoped to develop a powerful ship routing algorithm which will account for the stochastic variations in the forecasted environment and be adaptable to satisfy a variety of pre-selected ship motion criteria and set functions related to ship's safety and operation at sea.

## 1.2 SHIP ROUTING AS AN OPTIMIZATION PROBLEM

When a ship sails in the open seas, it encounters various environmental disturbances such as wind, wave, current, ice fog, etc. which will effect its safety and operating performance. For the merchant marine, this results in changes of ship operating economy, while for military application, it changes the vessel's tactical effectiveness.

Ship routing is concerned with the choice of the most suitable strategic trajectory or route and the corresponding control options from the voyage origin to destination so that a desired objective function or performance index is optimized.

In the modern commercial ship operation, the following is a list of criteria that are most commonly used:

1. Ship safety
2. Prevention of damage to hull, cargo, deck equipment, etc.
3. Economy in navigation, e.g. Minimum cost, transit time,etc.
4. Crew/passenger comfort
5. Maintenance of fleet schedule

Other criteria in logistics of interests to military operations may include:

1. Minimum probability of detection
2. Minimum time of intercept
3. Maximum combat effectiveness
4. Optimum search and rescue effectiveness

In practice, more than one of the above criteria are relevant, as a result, we have to select the most suitable one as our objective function to be optimized while the other criteria would serve as system constraints in our optimization problem.

In commercial applications, usually, the most important objective function for the ship routing problem is to minimize the total voyage cost. The voyage cost may consists of two parts, operating cost (mainly fuel cost) and terminal cost (cost of delay at the destination). The system constraints in this case relate to ship motion seakeeping criteria which ensures crew/passenger comfort and avoids cargo ship damages. From this viewpoint, the problem is to find the ship route and the corresponding controls such that the total voyage cost is minimized while all the constraints on the ship motion limits are satisfied.

## 1.3 NEED FOR A REALISTIC ROUTING ALGORITHM

The major part of research and development in mathematical ship routing has been performed in the United States by the U.S. Navy (at the Naval Post-graduate School in Monterey, California) [4,5,6,7,8], and the Fleet Numerical Weather Central [9]. Commercial services based on manual or semi-manual routing methods are also available from Oceanroutes [10], Bendix[11] and other routing companies.

Considerable amount of work has similarly been done abroad. Fugitsu Company, Ltd. of Japan [12] has developed an onboard Optimum Ship Route Setting System complete with hardware. With the help of French Bureau Veritas, Empresa Nacional Elcano, also equipped one of its ships with a system for route optimization [13]. In Britian, a team of scientists and engineers is working on Weather Routing of Ships in the North Atlantic [14]. On the software side, two major studies were cited; one by a Dutch engineer, deWit [15], and the other by an Italian, Zoppoli [16].

Table 1.3-1

COMPARISON OF SOLUTION METHODS FOR OPTIMUM SHIP ROUTING PROBLEM

| CLASS | METHOD | HANDLING CONSTRAINTS | OBJECTIVE FUNCTION | EXTENSION TO STOCHASTIC MODEL | COMPUTATION REQUIREMENTS |
|---|---|---|---|---|---|
| I | Mathematical Heuristics | As part of the method | Minimum time only | Lack of mathematical proof | Minimal, should be completed with graphic display |
| II | Variational calculus 2nd derivative methods | Imbeddedin the speed function then use feasible direction search | Minimum time | Stochastic programming techniques available but the complexity of mathematics puts restriction on the objective function and type of constraints | Sometimes convergence problem particularly when there are high seas which vary rapidly with time |
| | 1st Derivative Methods | As above or use penalty function | Minimum time or simple cost function | | Slow convergence require substantial CPU time. |
| III | Scatter-gunning extremals | Feasible direction search and interpolation | Minimum time only | Same as above | Faster convergenc |
| IV | Dynamic Programming | Checked directly | Any functional that can be decomposed into a multi-stage form | Basic recursion functional form remains the same for Expected value decision making. | May require substantial CPU time if full model is desired |

Generally speaking, the methods that have been developed so far can be classified into four categories . Table 1.3-1 shows the comparison of various solution methods for the ship routing problem. At present, all the models are deterministic which may be unrealistic in view of the uncertainties in the wind and wave conditions along the route. Furthermore, because of the difficulties in handling complex functional forms, the models has been restricted to the minimization of transit time rather than that of cost, thus completely ignoring the real tactical and economic reasons for ship routing from an operator's point of view.

## 1.4 OUTLINE OF THE THESIS

An algorithm for solving the stochastic minimum cost ship routing is described in this thesis. In chapter 2, the problem is formulated as a dynamic program or a multi-stage decision process. The deterministic and stochastic equations are then derived and their properties are discussed in the context of overall uncertainties and accuracies of the input data. Based on the discussions, a closed open-loop control stragegy was adopted for the proposed ship routing system. Finally, sensitivity studies in state space discretization were performed on a Trans-Atlantic voyage using simulated data, their implications on computing cost, solution accuracy and overall uncertainty are also presented in the section on model calibration.

Chapters 3 and 4 treat the two major required input data sources in detail. First, various Dynamic Ocean Environmental Conditions which have significant effects on ship performance are outlined and their final level of detials as well as the suitable data format for the routing model are recommended.

Following the specification of the input environmental parameters, a methodology for analyzing the ship seakeeping, speedkeeping characteristics is proposed.

A summary of available seakeeping criteria recommended for commercial operation is also presented and their lack of causal contents to ship, cargo, damages are discussed. It is hoped that with the help of onboard ship instrumentation, a set of new seakeeping statistics will be developed in the future to realistically reflect a ship operator's criteria for voluntary speed reduction.

Finally, a computerized Ship Routing System is proposed in Chapter 5 with a complete systems programming structure and data management consideration. Based on the preliminary experiences of running the model, Chapter 6 contains a conclusion and recommendations for a three step test and evaluation procedure before future real-time implementation.

# CHAPTER 2

# A DYNAMIC PROGRAMMING APPROACH TO SHIP ROUTING PROBLEM

## 2.1 PROBLEM FORMULATION

### 2.1.1 PROBLEM STATEMENT

The kinematics of a ship sailing in the ocean can be basically described in terms of its position as time progresses. The ship's position as specified by the longitude X and latitude Y plus the time T determines the ship's trajectory in a ship routing problem. To completely describe the ship system, however, we need to introduce the dynamic responses of a ship in a seaway. They are introduced into the system by a control vector, $\vec{U}$ specifying the ship's heading $\psi$ and the power output P, plus a generalized ship motion seakeeping constraint vector $\vec{M}$.

It follows therefore, the evolution or DYNAMICS of the system can be expressed in a general functional form as:

$$( X,Y,T ) = f( X',Y',T',\vec{U},\vec{M} ) \qquad \ldots\ldots (2.1)$$

where $T' = T - \Delta T$. Or in words: The ship would arrive at the present position X,Y, and present time T if controls $\vec{U}$ were applied $\Delta T$ units of time ago, provided that during the transition ship motion did not exceed the limit $\vec{M}$.

Thus the minimum cost ship routing problem can be simply expressed in mathematical terms as:

Minimize :

$$C(X_D, Y_D, T) = \int_{T_0}^{T} \alpha[X, Y, U, M, \tau]d\tau + \beta[X_D, Y_D, T]$$

for all possible time of arrival T

.....(2.2)

where,

$T_0$ = starting time

$\tau$ = dummy variable for integration

$\alpha$ = scaler functional for cost per unit time before arrival

$\beta$ = vector functional for cost of arrival at various time T

$X_D, Y_D$ = coordinates of the destination

The optimization problem can now be stated as following:

Given:
1. An initial ship position specified by its longitude and latitude, and initial time $T_0$;
2. Constraints on inadmissible areas such as land mass, shallow water, navigation hazards, etc; on admissible controls $P_{min} \leq P \leq P_{max}$ and $0^o \leq \psi \leq 360^o$; and on admissible ship motion seakeeping limits;
3. A function describing the ship's transition from one position to another, i.e., eq. (2.1);
4. An operating cost function $\alpha$, and a terminal cost function $\beta$

Find: The ship trajectory or route which comprised of $(X, Y, T)_k$ for k = 1,2,...N and the corresponding controls $\vec{U}_k$ so that the total voyage cost is minimized, while all the constraints on admissibility are satisfied.

### 2.1.2 CHOICE OF STAGE VARIABLE

Let us now see the problem graphically. Fig. 2.1-1 shows a grid covering a band along a typical Trans-Atlantic great circle route. The vertical and horizontal axis describe the increments in latitude and longitude respectively. The other dimension, time, is not shown here, but one can picture similar grids staged on top of another representing different time increments. Our mission is then to find the ship trajectory which comprised of a set of feasible grid points linking origin to destination through time and position so that the sum of operating cost and terminal cost is minimized.

To solve the ship routing problem via dynamic programming approach [20], we have to formulate the problem as a multi-stage decision problem. There are clearly two choices of stage variable, time and a measure of progress of the voyage. Both of them are monotonically increasing and would lead to the derivation of a recursive computation procedure which can be implemented on a digital computer. However, the recursion equations do have some distinct differences regarding the limitation and interpretation of the control policies in the respective feasible state spaces and the resulting computation efficiency.

Let us first consider the choice of time as the stage variable. This has been often used in solving many classical optimal control problems via the dynamic programming approach. [22,77] The choice is a logical one when observations or control changes in the system are limited at regualr intervals and the performance of the system is state dependent (eg. chemical plants).

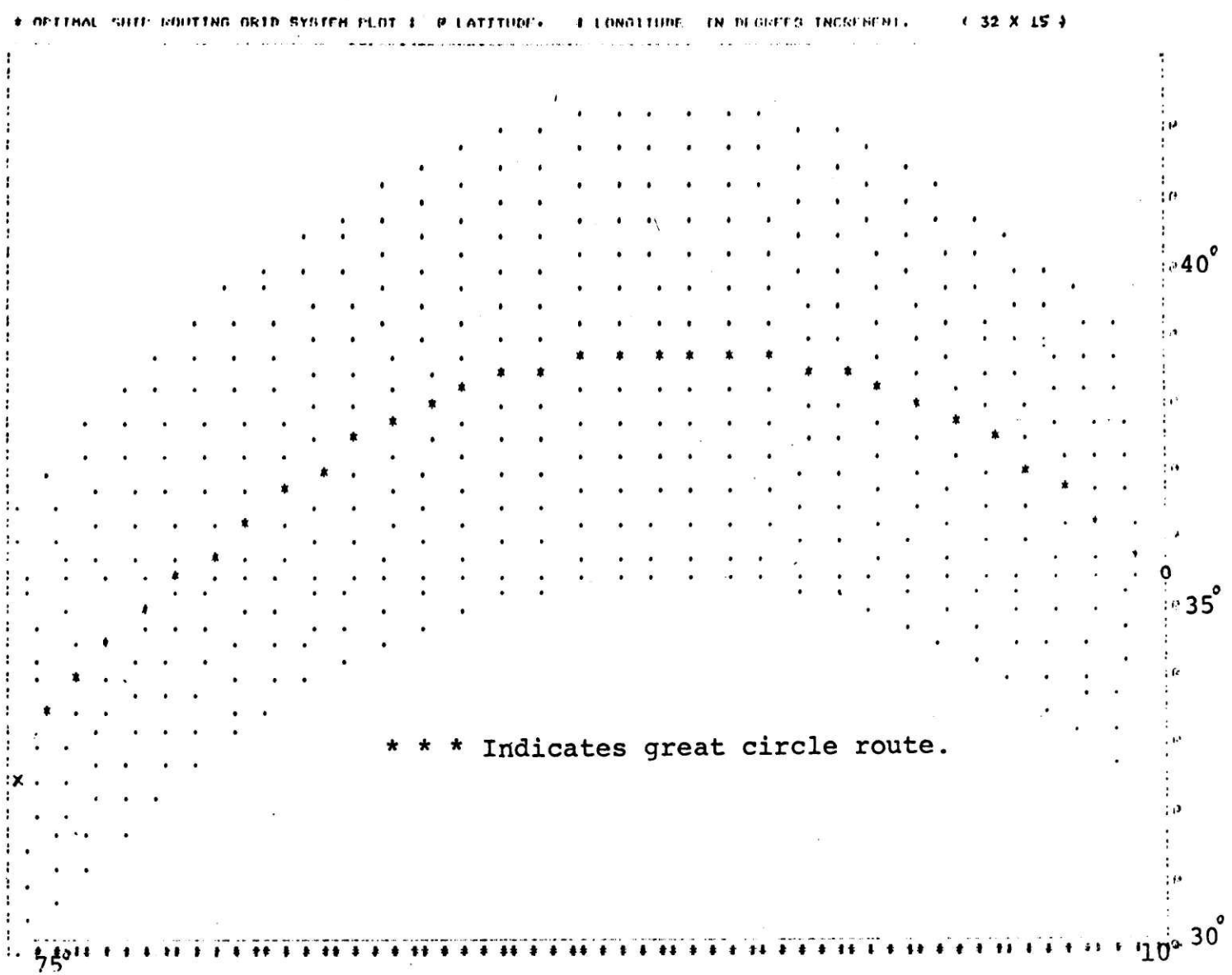


Figure 2.1-1 An example of computer generated grid system for a Trans-Atlantic voyage.

For the ship routing problem, however, the situation is quite different. First of all, we do not have the problem of limited state observations or control modifications. In fact, with modern navigation equipments and powerful ship control devices, the state of the system can be continuously monitored and changed if necessary. Secondly, recalling eq.(2.2) the operating cost is only dependent on the controls $\vec{U}$ and dT, the length of time during which $\vec{U}$ were executed, but explicitly independent of the state ( X,Y ) until the ship reaches its destination, ( $X_D$, $Y_D$ ) as a boundary condition. This property of our problem unfortunately leads to serious consequences in the required computation efforts to solve the recursion equation.

Since the operating cost cannot be explicitly expressed as function of the state variables (i.e. ship's position X,Y), it creates serious difficulties and ambiguity in interpolating the optimal value function between the discrete grid points. In other words, we have no way of finding how the optimal value function would behave over a large area represented by a grid point. As a result, we may be forced to use a finer grid system and assume the optimal value function remains constant over a representative area of each individual grid point.

To get a rough estimate of the required computation effort, let us consider a typical Trans-Atlantic voyage of around 3,500 nautical miles by a 20 knot ship which takes less than 200 hours of voyage time. If we make the stage variable at a 2 hour interval, the feasible state space has 100 stages. At each stage, the area of interests is again described by a grid covering a bound, say, 500 nautical miles across the great circle route. Suppose, we use

a grid system so that each grid point represents a 20 x 20 square miles area or require less than 1 hour to sail from one boundary to another, then the total number of states would add up to 200,000[1]. At each state, if 15 sets of control options (5 heading times 3 power settings) are applied, it would result in a total of 3 million calculations. Suppose each calculation requires 100 computer operations or approximately $10^{-4}$ CPU seconds, then to solve the deterministic ship routing problem, it would require about 5 minutes of CPU time.

As far as the core memory requirements are concerned, it has not yet caused any problem. The main obstacle seems to be the excessive computation burden, expecially if we extend it to the stochastic ship routing problem. It seems, therefore, that the multi-stage decision problem formulation using time as the stage variable would not yield fruitful results for our stochastic ship routing problem.

The next choice of the stage variable is a measure of the voyage progress. This choice is perhaps more subtle since it is not explicitly defined. Let us again refer to the grid system in fig. 2.1-1. Suppose, we let the changes in the X direction (i.e. longitude) be considered as a measure of the voyage progress and we allow transitions to be taking place from one longitude to another, then we have in effect defined the latitude Y and time T as state variables. More generally, we may use the incremental distances in the general direction of travel (e.g. using the great circle route as a reference) as the stage variable and the incremental distance perpendicular to the reference route together with time as state variables.

---

[1] The number of grid points increases from stage to stage as the voyage progresses. On the average, the feasible state space per stage is half the size of the entire area.

Again, we have formulated the ship routing process as a multi-stage decision problem as shown in figure 2.1-2.

Notice that we now have a more restrictive problem formulation than the previous one. First of all, by predefining the allowable transitions, we can not specify the headings explicitly. Since the ship's headings are determined by the grid point spacings DX and DY from one stage to another and the number of such transitions allowed,[1] the level of ship's power output becomes the only explicitly defined control variable. In comparison, the previous formulation allows any combination of power and heading as control polices.

In practice, this limitation on allowable transitions means that the ship will travel in a forward direction. No matter how severe the sea condition is, it will not turn back and attempt to run away from the storm, except to reduce speed and maintain steerage (i.e. directional controlability). Such policy has traditionally been taken and is believed to be effective from past experiences.

Secondly, since the ship trajectory is now comprised of a sequence of predefined grid points rather than the discretized longitudes and latitudes in the feasible state space, the formulation further requires the system to be perfectly controlable in the transition between grid points. In other words, with the continuous dead-reckoning of its track by modern navigation equipments and the ability of feedback control modifications by the onboard crew, a modern ship with powerful control devices should be able to reach the next grid point sooner or later.

---

[1] In rectangular coordinate system, $\Delta\psi = \tan^{-1}(DY/DX)$. Under normal operating conditions, the maximum course changing is less than 35° from ship's original heading.

[2] Private communication with Captain A. Fiore, head of Nautical Science department, U.S. Merchant Marine Academy, Kings Point.

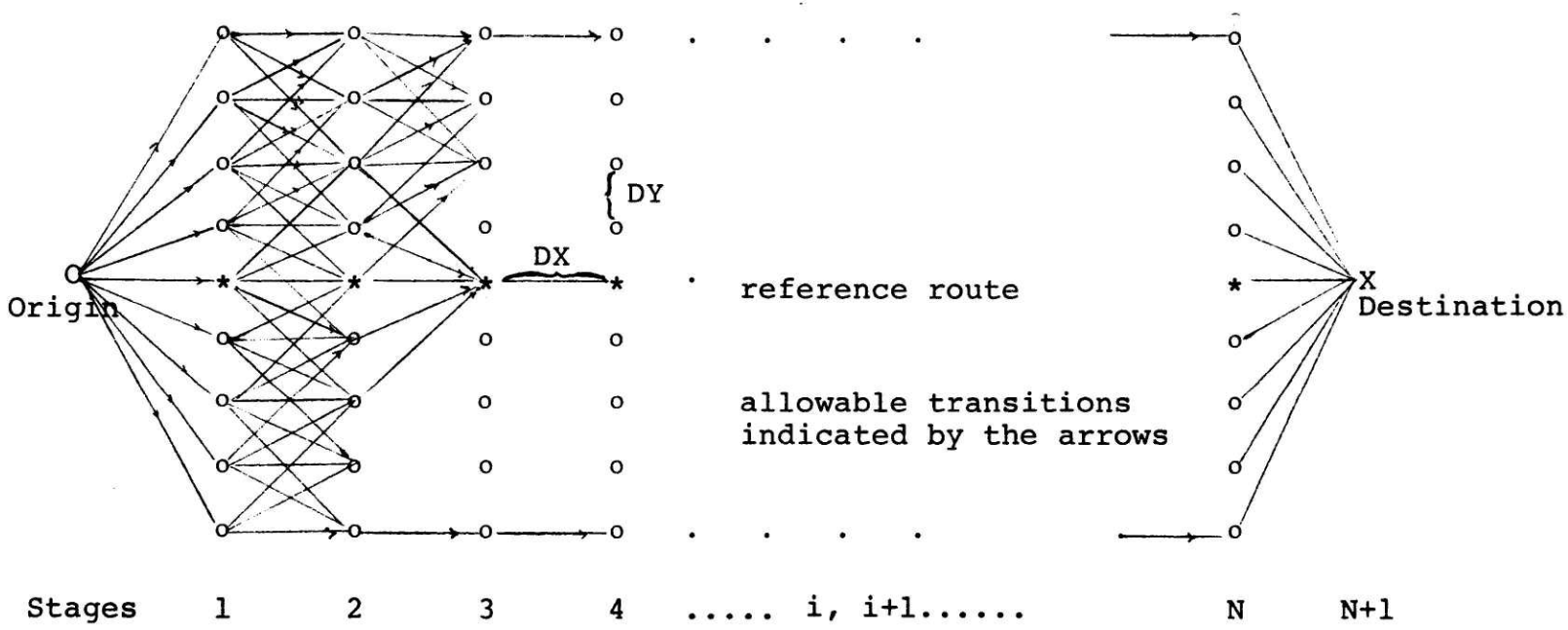


Fig. 2.1-2 Ship routing as a multi-stage decision problem using a predefined grid system.

On the positive side, by defining **arrival** time at a grid point as a state variable, we have effectively removed the ambiguity and difficulty of interpolating the optimal value function in the feasible state space. Since both of our cost functions (operating cost as well as terminal cost function) are time dependent with ship positions appearing only in the state transition equation (2.1), a simple one dimensional interpolation scheme in the time domain would be sufficient to determine the optimal value function between the discretized time intervals at each grid point.

More importantly, since we can generate different grid system by using different values of the spacings DX and DY, sensitivity studies can be performed to calibrate the routing algorithm. For example, the size of DX determines the total number of stages or decision points to change controls in order to ensure the cost minimization during a voyage. Together with DY, they also determine the number of control options and magnitude of course diversion to ensure a smooth trajectory. Obviously both DX and DY as well as the time step will have major effects on the accuracy of the solution which will be investigated later.

To repeat, with the second choice of the stage variable, we have defined:

**STAGE Variable:** **i = A monotonically increasing integer variable related to the headway and consistent with the set of allowable forward transitions at each stage.**

STATE Variable: $\vec{X} = (G,t)$, where G denotes the navigational coordinates of a grid point on a predefined grid system; t is a quantized state variable for time.

CONTROL Variable: $\vec{U} = (\psi,P)$ where $\psi$ now becomes a set of allowable forward transitions between present state and the states in next stage; P is a set of discretized power output.

CONSTRAINTS: $\vec{M}$ = A generalized ship motion and seakeeping index same as before.

OBJECTIVE FUNCTION: Minimize the total voyage cost

$$C(\vec{X}, N+1) = \sum_{i=1}^{N} \alpha_i[\vec{X}(i), \vec{U}(i), \vec{M}(i)] + \beta[\vec{X}_{N+1}] \quad \ldots(2.3)$$

Subject to constraints:

$\vec{X} \in \vec{X}_a(i)$ Within the predefined grid system

$\vec{U} \in \vec{U}_a(i)$ Allowable transitions between grids

$\vec{M} \in \vec{M}_a(i)$ Allowable motion

## 2. 2 SOLUTION ALGORITHM

### 2.2.1 DETERMINISTIC DYNAMIC PROGRAMMING RECURSION EQUATION

Having formulated the ship routing problem as a dynamic programming problem, we are now in a position to derive the recursive computation procedure for finding the optimum solution based on Bellman's Principle of Optimality

Recall that equation (2.3), our objective is to minimize the total voyage cost.

$$C(\vec{X},N+1) = \sum_{i=1}^{N} \alpha_i [\vec{X},\vec{U},\vec{M},] + \beta [\vec{X}_{N+1}]$$

Where the first term represents the operating cost and the second represents the terminal cost.

Let us define the minimum cost function:

$$C(\vec{X},\ k) = \min_{\vec{U}\ (k)} \{\sum_{i=k}^{N} \alpha_i [\vec{X},\vec{U},\vec{M}]\} \qquad k=N,N-1....3,2,1 \quad ....(2.4)$$

We can also rewrite the expression as the following:

$$C(\vec{X},\ k) = \min_{\vec{U}(k)} \{\alpha_k [\vec{X},\vec{U},\vec{M}] + \sum_{i=k+1}^{N} \alpha_i [\vec{X},\vec{U},\vec{M}]\}.$$

According to the Principle of Optimality, the minimization operation can be split into two parts. One involving the present stage k, the other over the remaining stages k+1, k+2.....N.

$$C(\vec{X},k) = \min_{\vec{U}(k)} \min_{\substack{\vec{U}(i) \\ i=k+1...N}} \{\alpha_k(\vec{X},\vec{U},\vec{M}) + \sum_{i=k+1}^{N} \alpha_i (\vec{X},\vec{U},\vec{M})\}$$

It can be seen that the first term in the brackets depends only on $\vec{U}(k)$ and not on any other $\vec{U}(i)$, i=k+1....N. Therefore, the minimization over $\vec{U}(i)$ for i<k has no effect on this term

$$\min_{\vec{U}(k)} \min_{\substack{\vec{U}(i) \\ i=k+1\ldots N}} \{\alpha_k(\vec{X},\vec{U},\vec{M},)\} = \min_{\vec{U}(k)} \{\alpha_k(\vec{X},\vec{U},\vec{M})\}$$

For the second term, on the other hand, it does not explicitly depend on $\vec{U}(k)$. It is only related to $\vec{U}(k)$ through the state transition Dynamics of eq. (2.1).

$$\vec{X}_{k+1} = f_k(\vec{X},\vec{U},\vec{M},k)$$

Therefore it reduces to:

$$\min_{\substack{\vec{U}(i) \\ i=k+1\ldots N}} \{\sum_{i=k+1}^{N} \alpha_i(\vec{X},\vec{U},\vec{M})\}$$

But this is exactly the definition of our minimum cost function for $C(\vec{X},k+1)$. Hence, we have derived the recursive relationship which enables us to find the minimum cost function at the present stage based on the minimum cost function derived at one stage ago.

$$C(\vec{X},k) = \min_{\vec{U}_k \epsilon \vec{U}_a} \{\alpha_k[\vec{X},\vec{U},\vec{M}] + C(\vec{X},k+1)\} \qquad \ldots (2.5)$$

$$k=N,N-1\ldots 2,1$$

To carry out the computation of the optimal value function $C(\vec{X},k)$, we must also prescribe a boundary condition at N+1 and that is our terminal cost function on arrival at the destination.

$$C(\vec{X}_f,N+1) = \beta(\vec{X}_f, N+1) \qquad \ldots (2.6)$$

By using equations (2.5) and (2.6), the minimum cost from any state defined by the grid point as well as time of arrival to the final destination can be calculated by stepping backwards stage by stage to the original position and starting time. Once the entire optimal value function has been evaluated, the minimum cost route and its corresponding controls at each stage can be easily traced out by going forward.

## 2.2.2 EXTENSION TO STOCHASTIC SHIP ROUTING MODEL

The stochastic routing model is a direct extension to the deterministic model presented in the previous sections. The major difference is that it takes into account some of the uncertainties in ocean environment forecasting and hence the resulting probablistic travel time. Since our objective is to minimize the total operating cost plus a terminal cost,both of which is a function of time, the stochastic variation of the forecasted environment and the resulting distribution of time may significantly effect the choice of optimal control policies as compared with deterministic models.

In order to introduce the stochastic variation of ocean environment into the model, let us assume that the seaway may be characterized by a random vector $\vec{R}$, where $\vec{R}$ is defined as a set of parameters which will sufficiently describe the sea severity in which the ship is operating[1]. The state vector $\vec{X}$ (position as well as time) thus becomes a random vector as a function of $\vec{R}$ and a given set of control $\vec{U}$.

The resulting stochastic variations in the state variables have also changed our objective function which is no longer the minimization of deterministic costs. There are several types of decision criteria which can be incorporated in Dynamic Programming algorithm without expanding the state

---

[1]For example, the parameters may be significant wave height, peak frequency which are often used to fit a two parameter spectra;plus a predominant wave direction. More detailed representation is possible at the expense of more computing effort.

space . They are the expected value and constant risk aversion decision making. Both these decision rules are of interest to us in the stochastic ship routing problem. The former assumes that the ship-owner is an Expected Value Decision Maker who would like to minimize his total voyage cost 'on the average', see Ref. [23] whereas the latter takes account of his risk preference behavior and requires the calibration of his utility function in an exponential form.[1] The general recursion equation has been developed for this type of problem, see reference [24].

For the purpose of our study, we will use the former decision rule. i.e. to minimize the expected value of the total voyage cost over the probability distribution of $\vec{R}$ at all stages i = 1,2...N. state j = 1, 2.....M.

$$\tilde{C}(\vec{X},k) = \underset{\vec{U}}{\text{Min}} \; \underset{\vec{R}_{ij}}{E} \left[\sum_{i=k}^{N} \alpha_i \; (\vec{X}_j, \vec{U}, \vec{M})\right] \qquad \ldots.(2.7)$$

To derive the stochastic recursion equation, it is necessary to assume that the state of the system (grid position as well as the time in getting there) at any stage depends only on the state of the system at the previous stage and on known probabilities. This is essentially a first degree dependence property similar to the first order, time invariant Markov Process, Ref. [25]. In which case the probability distribution of $\vec{X}_i$ is given by $P_i(\vec{X}_i, \vec{X}_{i+1})$ i = 1,2....N. Each degree of dependence adds another state variable and makes the recursion equation more unwieldly. For our ship routing problem involving many states it seems suitable to use the first order model which does not increase the original state space in the deterministic model.

---

[1] The linearity of expected value operation and the separable property of the constant risk aversion allows us to retain the original state space.

The first order model assumes that the random variables $R_k$ are independent from one stage to another. Under this assumption, the joint probability density function $P(R_1, R_2 \ldots R_k)$ can be written as the product of the individual probability density functions.

$$P[\vec{R}_1, \vec{R}_2 \ldots \vec{R}_k] = P(\vec{R}_1) P(\vec{R}_2) \ldots P(\vec{R}_k) \quad \ldots (2.8)$$

The dynamics which describe the state transition become in this case:

$$\vec{X}_{k+1} = \tilde{f}_k[\vec{X}, \vec{U}, \vec{M}, \vec{R},] \quad \ldots (2.9)$$

Notice that it is no longer possible to minimize the original deterministic cost function, because the present state $\vec{X}_k$ and the controls from thereon $\vec{U}_j, k \leq j \leq N$ do not completely specify the future states $\vec{X}_j$, $k+1 \leq j \leq N$ but instead determines only the probability distribution of these states. The objective function in this case has to become the minimization of the expected value of the total voyage cost as specified in the equation (2.7).

More importantly, the first order model also implies that our control algorithm is a non-adaptive one. This is a so called "open-loop" control stragegy which determines the entire ship trajectory based on the forecast environmental condition $R_{1,2 \ldots N+1}$. Any observation of the sea severity during a voyage after deriving the minimum cost control policies will not change the probabilistic distribution of future states or their corresponding controls and minimum expected costs. The use of the observed sea severity and

and system responses can only be made at the next update of the entire optimal value function using the most recent information of the actual ship position, time and the revised forecasts of environmental conditions. The "continuous" update of the "open-loop" control stragegy is sometimes called a Closed Open-Loop Control. Fig. 2.2-1 shows a flow chart of this kind of strategy.

The derivation of stochastic recursion equation follows very similiarly as in the deterministic case. First, let us define the expected minimum cost function:

$$\tilde{C}(\vec{X},k) = \min_{\substack{\vec{U}(i) \\ i=k\ldots N}} \{ E_{\substack{\vec{R}_{ij} \\ i=k\ldots N \\ j=1\ldots M}} [\sum_{i=k}^{N} \alpha_i(\vec{X}_{ij},\vec{U},\vec{M},\vec{R}_{ij})]\} \qquad \ldots(2.10)$$

Since the probability density function of $\vec{R}_i$ is independent from one stage to another we may rewrite the expression..

$$\tilde{C}(\vec{X},k)=\min_{\substack{\vec{U}(i) \\ i=k..N}} \{E_{R_{kj}} \cdot E_{\substack{R_{ij} \\ i=k+1..N \\ j=1,\ldots M}} [\alpha_k(\vec{X}_{kj},\vec{U},\vec{M},\vec{R}_{kj})+\sum_{i=k+1}^{N} \alpha_i(\vec{X}_{ij},\vec{U},\vec{M},\vec{R}_{ij})]\}$$

Since the expectation is a linear operator and also the independence assumptions in equation (3.5), it may be carried out inside the bracket term by term. By applying the Principle of Optimality to the minimum expected cost function, and proceed very much as in the deterministic case except the deterministic cost becomes the expected cost. We may derive the stochastic recursion equation as the following:

$$\tilde{C}(\vec{X},k) = \min_{\vec{U}_k} E_{\vec{R}_{kj}} [\alpha_k(\vec{X},\vec{U},\vec{M},\vec{R})+\tilde{C}(\vec{X}_j,k+1)] \qquad \ldots.(2.11)$$

Fig.2.2-1 Closed Open-Loop Control Strategy
for minimum cost ship routing under uncertainty

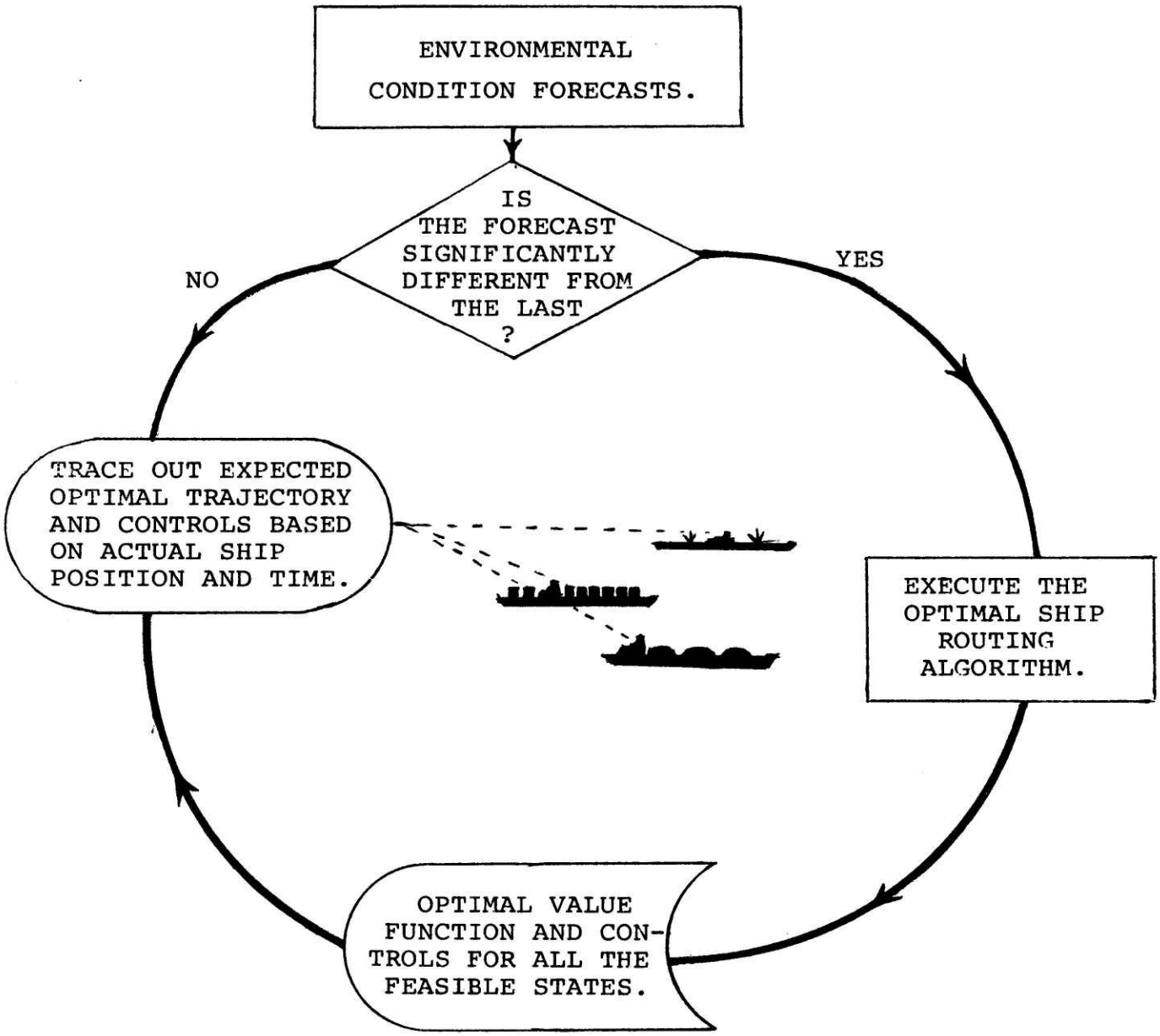

The computation procedure is very similar to that of the deterministic model. The random vector $\vec{R}$ is quantized with corresponding discrete probability densities $P(r_\ell)$, $\ell = 1,2,3\ldots L$; $r_\ell \in \vec{R}$, then the expected value operation is just a simple summation:

$$\underset{\vec{R}_k}{E} [\alpha_k(\vec{X},\vec{U},\vec{M},\vec{R}) + \tilde{C}(\vec{X},k+1)]$$

$$= \sum_{\ell=1}^{L} p(r_\ell) \cdot [\alpha_k(\vec{X},\vec{U},\vec{M},r_\ell) + \tilde{C}(\vec{X}(r_\ell),k+1)] \quad \ldots\ldots (2.12)$$

Once this quantity has been computed for each state and control, the procedure is exactly the same as in the deterministic case. It can be seen that the introduction of stochastic variation in the system increases the computation effort by a factor of L if we were using only one wave parameter, e.g. wave height, as a random variable; not increasing the original feasible state space.

To rewrite the stochastic equation more explicity we have:

$$\tilde{C}\left(\begin{matrix} G \\ t \end{matrix}, k\right) = \min_{\vec{U}_k} \{E_{R_{kj}} [\alpha_k\left(\begin{matrix} G \\ t \end{matrix}, \vec{U},\vec{M},\vec{R},\right) + \tilde{C}\left(\begin{matrix} G \\ t_j \end{matrix}, k+1\right)]\} \quad \ldots\ldots (2.13)$$

By assuming the ship's controls are powerful, G is no longer a random variable, only $t_j$ has a probability distribution depending on the stochastic sea severity $R_{kj}$ and the deterministic quantities of $G,\vec{U},\vec{M}$. However, $R_{kj}$ itself is time dependent and to a certain extent on $t_j$. To properly derive the probability density function of $t_j$, therefore, would involve as many simultaneous equations as the number of possible $t_j$s at every grid point. Obviously, such large computational undertaking would not be permitted for the size of our problem.

In order to carry out the expected value operation in the recursion equation and solve our optimization problem, we propose a method to derive an approximated probability density function using the expected value of arrival time $t_j$.

Recall that the major difficulty encountered in deriving the probability density function of $t_j$ was because of its interdependence with $R_{kj}$. In the deterministic case, obviously, we do not have the problem at all. Since the environmental condition is known for certain, there is a one to one correspondence of the environment and $t_j$ for a given set of $G, \vec{U}$ and $\vec{M}$. Now, let us bear in mind that the deterministic model is just a degenerated case of our stochastic model with known state transition probability of unity. Suppose we could relax this unit probability and assume that the variance assocoated with $t_j$ is small in the real stochastic environment, then we may be able to replace the random state variable $t_j$ by its expected value $\bar{t}_j$ thus avoiding the solution of large sets of simultaneous equations. (for mathematical justification see APPENDICES A).

In practice, to make the variance associate with $t_j$ small, it is necessary to reduce the required transition time between grid points or increase the number of stages[1].

Thus, we have finally derived the approximated recursion equation for the stochastic minimum cost ship routing problem.

$$\tilde{C}\left(\bar{\underset{t}{G}},k\right) = \min_{\vec{U}(k)} \; \underset{R_{kj}}{E} \left[\alpha_k\left(\bar{\underset{t}{G}}, \vec{U}, \vec{M}\right) + \tilde{C}\left(\bar{\underset{t_j}{G}}, k+1\right)\right] \qquad \ldots.(2.14)$$

[1] Here we assume that with the onboard feedback of the actual arrival time, the variance does not propagate from one stage to another.

By using the above recursion equation and the boundary conditions in eq. (2.6), the entire optimal value function can be evaluated in a manner similar to the deterministic case. However, since it is no longer possible to calculate the state transitions deterministically due to the stochastic variations of random environment, the derived control policy based on the expected cost is itself stochastic except for the first set of controls after the stochastic state variable__time of arrival at the grid point becomes known. The remaining control decisions obtained from the recursion equation cannot be expressed deterministically in terms of state variables until the stochastic states that proceeds them are revealed. In other words, there is no optimal trajectory as such in the stochastic model. The closest analogy to the optimal trajectory in the deterministic model is the track based on the expected state values. The practical implication is therefore to retain the entire optimal value function on a direct access disc file. The recommended control policies (heading and power output) are only revealed one at a time as the ship's actual progress have been identified. In our non-adaptive control algorithm, the optimal value function at all the states and the corresponding controls are retained until the next update with the new forecasted environmental conditions.

## 2.3 CALIBRATION OF THE STOCHASTIC MODEL

During the development of the stochastic ship routing algorthm, various simplification and assumptions have been made in order to make the problem solvable. Let us now see to what extent can these approaches be realistically used in reducing the computation effort and more importantly, what are their effects on the accuracy of the final solution.

To calibrate the model, the algorithm was programmed and sensitivity studies were carried out using simulated input data resembling a Trans-Atlantic voyage by a LASH ship. The ocean environmental conditions (only wave, height, and direction) were generated by a computer program. The following are some major results from the investigation.

1. Feasible State Space Reduction

A grid system was constructed covering a band of approximately 3,300 x 450 nautical miles along the great circle route from the strait of Gibraltar to Charleston U.S.A. See fig. 2.1-1. The width of the band should be a function of the length of the voyage and the expected wave conditions. If a widespread storm is expected during the voyage, it is necessary to increase the width of the band in order to include more alternatives for course diversion. On the other hand, when the voyage is short or the sea is rela--tively calm, then the band width may be reduced to save computation cost.

In the time domain, the same principle for state space reduction can be applied. By using the expected maximum and minimum ship speed along the voyage, the earliest and latest arrival time at a certain grid point can be calculated as a function of the distance from the origin. Figure 2.3-1 shows an example of the heuristically defined feasible time intervals as a function of voyage distance and max/min ship speed. Notice that the required time interval increases rapidly for the low ship speeds and the long voyage distances. Thus requiring more computing effort.

This set of heuristically generated bounds on feasible time of arrival at a certain grid point should be consistent with the available power output options and expected sea severity.

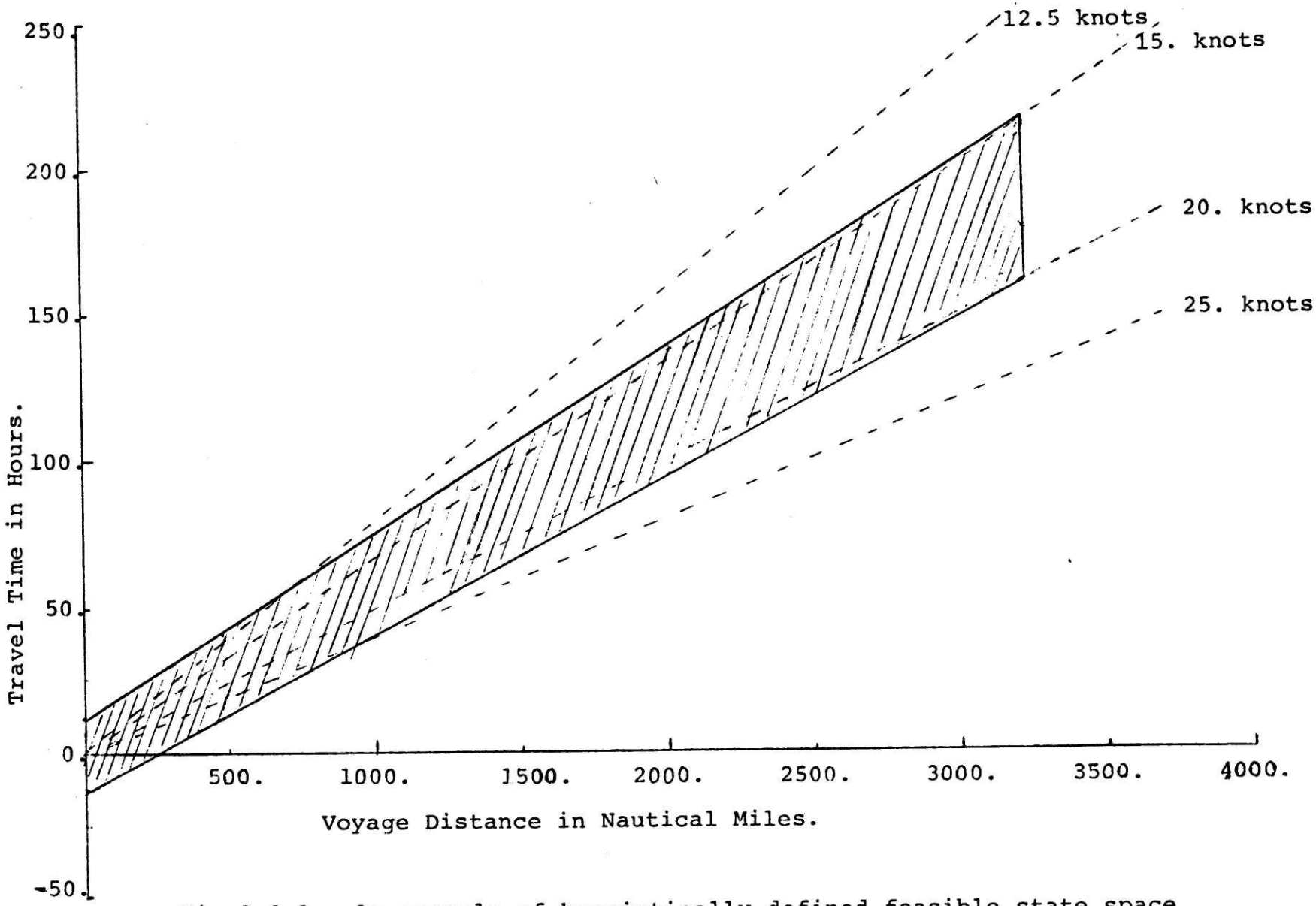


Fig.2.3-1 An example of heuristically defined feasible state space as a function of voyage distance and max/min ship speed.

Theorectically, there is always a possibility of arriving at the grid point later than the "latest time" due to the non-zero probabilities of extremely severe sea conditions. To ensure the bounds are large enough, a penalty method approach derived in APPENDIX B was carried out. Essentially, we impose a high penalty cost whenever the bound is exceeded in a single transition. In effect, by imposing a large penalty cost for the states that have non-zero probability of going outside the bounds, the algorithm will automatically force the controls of the previous stages to stay away from this state because of the potential high cost. However, due to the nature of the recursion equation, if the effect of the penalty did not diminish quickly and change a large part of the optimal value function, and hence the corresponding control policies, then it will introduce substantial error in the final solution. To check whether the bounds are large enough, we have derived the following set of necessary conditions:

i. The probability $P_{cr}$ of starting from an admissible state and ending outside the bounds after applying n successive control is small.

ii. The expected value of penalty i.e. $P_{cr} \cdot M$ is also small for sufficiently large penalty M.

In our test runs, we have allowed a time interval of 12 hours either earlier or later than the scheduled departure time. The extra computation effort was to make sure that the expected trajectory would stay within the bound as well as to facilitate sensitivity study of ship scheduling from the management point of view.

## 2. The Effect of Discretization in the Time Domain

Having defined the feasible state space by a band along the nominal track and a suitable time interval, the next step is to investigate the effect of different size of time steps (DT) in discretization of the state variable, time. Figure 2.3-2 shows a plot of the optimal value function along the great circle route at various time relative to the original departure schedule. The time bounds corresponding to the ones in Fig. 2.3-1 were set from -12 hours to +12 hours at the origin of the voyage and from 162 hours to 215 hours at the destination. Using the terminal cost function as derived in APPENDIX F, the optimal value function was evaluated for both the problems with 25 times steps[1] and 50 time steps. The doubling of the size of DT at this level did not introduce substantial changes in the optimal function as shown in Figure 2.3-3. This is perhpas due to the relatively smooth nature of the input terminal cost function and a slow moving storm system. Thus for a discontinuous terminal cost function or relatively fast moving storm system, it may be necessary to reduce the size of the time steps in order to closely approximate the optimal value function.

From the computation point of view, doubling the number of time steps would nearly double the required computation effort and core storage for the same problem. Evidently, the suitable choice of the discretization in the time domain will be one of the issues under actual implementation conditions when the ability to provide detailed forecasts, computer hardware availability etc. are taken into consideration.

---

[1] For our test runs, the time step size varies from 2.4 hours at the destination to 1.0 hour at the beginning of the voyage.

During the execution of the recursion equations, a large penalty cost of two orders of magnitude larger than the actual cost was imposed on the states which may have non-zero probability of going out of bounds in a single transition. The optimal value function was calculated with and without the expected penalty. The difference between the two were printed out for each state. For the present simulated routing exercise, the differences diminish rapidly with the number of stages away from the penalty states. At the origin, the optimal value function was completely unaffected by the penalties incurred in the previous stages. This shows that the probability of going out of the bounds from the initial position time is very small and the algorithm has forced the controls to stay away from the inadmissible states. Therefore, we can be relatively confident that our predefined bounds were large enough. However, when there are substantial effects of the penalty which still remains in the optimal value function, then the computation should be repeated by increasing the latest arrival time bound at each stage.

The same type of penalty method are also implemented for those states which exceed the ship motion constraints[1]. By the same token, if the probability of getting into one of these motion constraint states is high and the expected penalty cost has significantly changed the optimal value function and control policies, then the optimal value function should be recomputed using a different grid away from the expected storm area and perhaps with a larger time interval.

---

[1] At present, due to the lack of causal relationship between ship motion and damage cost, it is considered as hard constraints. Future effort is required to incorporate them into the operating cost function.

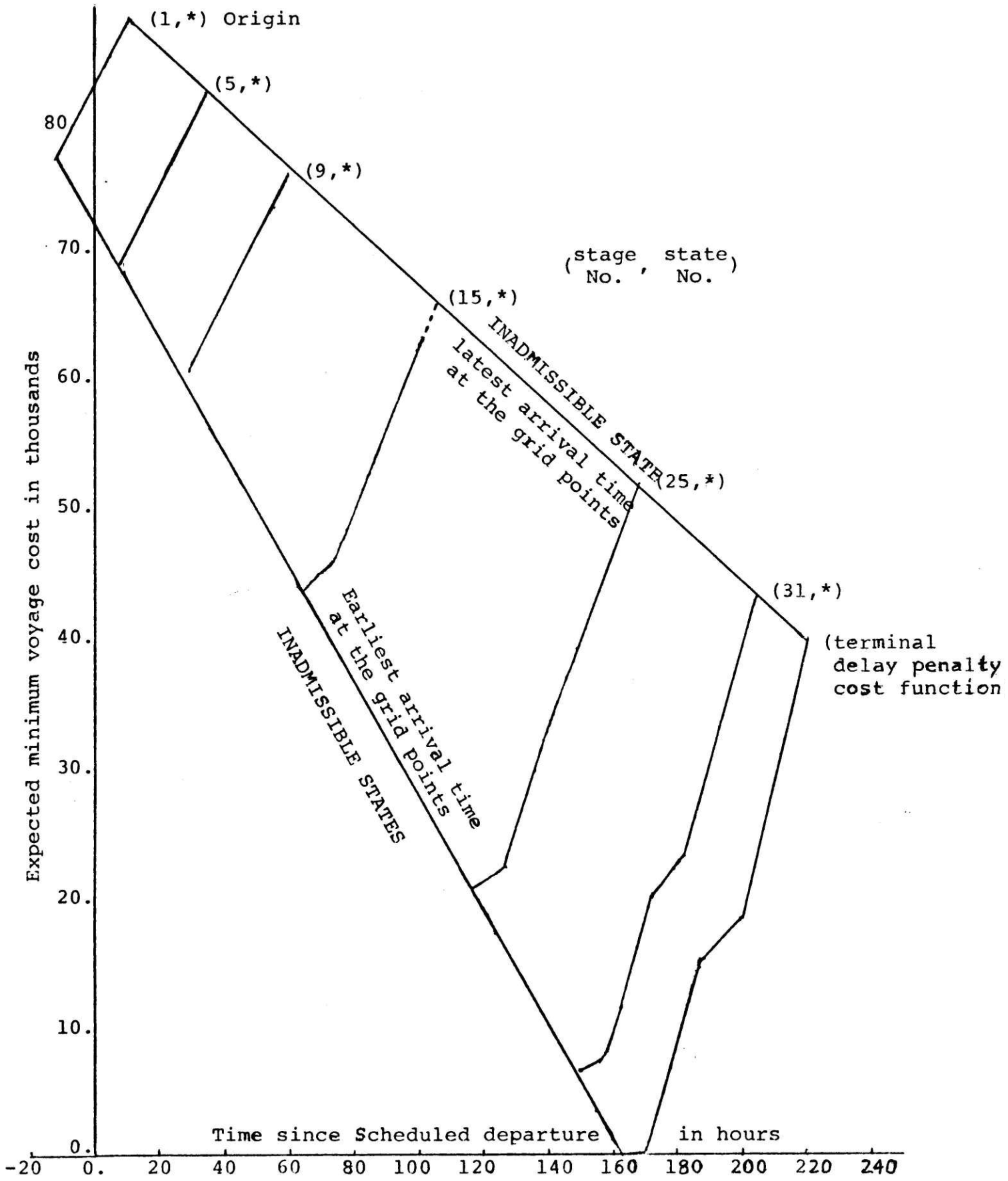


Fig. 2.3-2 A plot of the Optimal value function along the grid points on the Great Circle route.

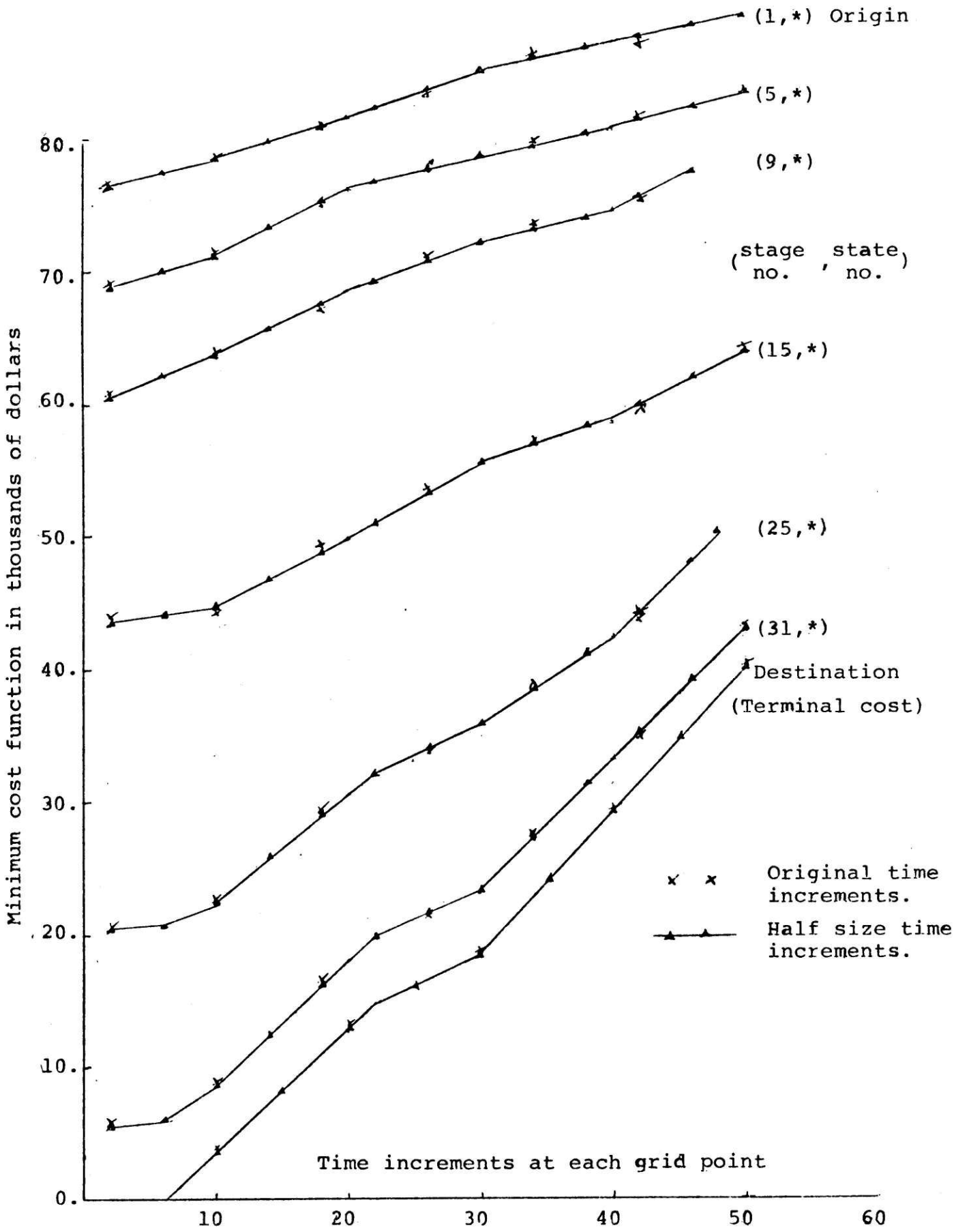


Fig. 2.3-3 Effect of reduce the size of state variable TIME by half on the Optimal Value function at variaous stages.

## 3. Effect of Discretization in the Space Domain

There are two dimensions which need to be discretized in the space domain for the ship routing problem. A simple algorithm was developed for automatically generating a grid covering the band of feasible state space. Two important inputs which specify the distances between grid points are DX and DY. DX may be considered as the average distance between grid points along the nominal track dscribed by the user in terms of a set of coordinates, and DY is the distance between grid points perpendicular to the track. Thus in our formulation, the number of increments in the DX direction becomes the stage variable and that of DY becomes one of the state variables (the other is time increments), see Figure 2.1-2.

Although both variables are used to discretize the feasible state space and approximate the optimal value function continuum by a grid system, the sizes of DX and DY have entirely different implications on the final solution in this formulation .

In the DX direction, since there are transitions taking place from stage to stage by using the optimal controls, the size of DX determines the accuracy of the solution. In other words, with the smaller values of DX, there would be more chances to modify the controls and ensure the minimization of the total voyage cost. On the other hand, there is no such transition taking place in the DY direction. Besides the accuracy of the solution the other concerns here are to provide sufficient number of control options for course diversion and ensure a smooth trajectory.

To show the sensitivity of the algorithm on state discretization, several test runs were carried out with different sizes of DX and DY using the same simulated environmental data. First, to investigative the effect of changing DX, two separate runs using DX = 100 nautical miles; DY = 30. n.m; and DX = 200 n.m; DY=30 n.m. were carried out. Figure 2.3-4 shows a comparison of the minimum cost function at various stages and time increments. Notice that the differences between the coarse grid (DX= 200 n.m. dotted line and the finer grid DX= 100.n.m. solid line) increases as the distances increases from the destination. For the example shown here, this difference amounts up to 5% of the total voyage cost at the beginning of the voyage. Aparantly, the case with the larger size of DX, hence fewer stages[1], did not provide enough opportunities for the control modifications to ensure the cost minimization in solving the recursion equation. This is also confirmed by the frequent jumps of the recommended power outputs along the ship trajectory. Theorectically, this 5% difference will diminish with the successively smaller DX when the actual minimum cost has been reached.

Two separate runs were also carried out for testing the sensitivity of the final solution to the size of DY. As mentioned before, besides the question of accuracy, the size of DY is also responsible for providing a smooth trajectory which is considered to be important by the on-board personnel.

To see the changes in the optimal value functions using the two different grid systems (DX=100, DY = 60) and (DX=100, DY=30), the minimum costs were plotted for various stages and a typical time interval as shown in figure 2.3-5.

[1]Total number of stage in the DX =200 n.m. case equals 16 versus 33 in the DX = 100 n.m. case.

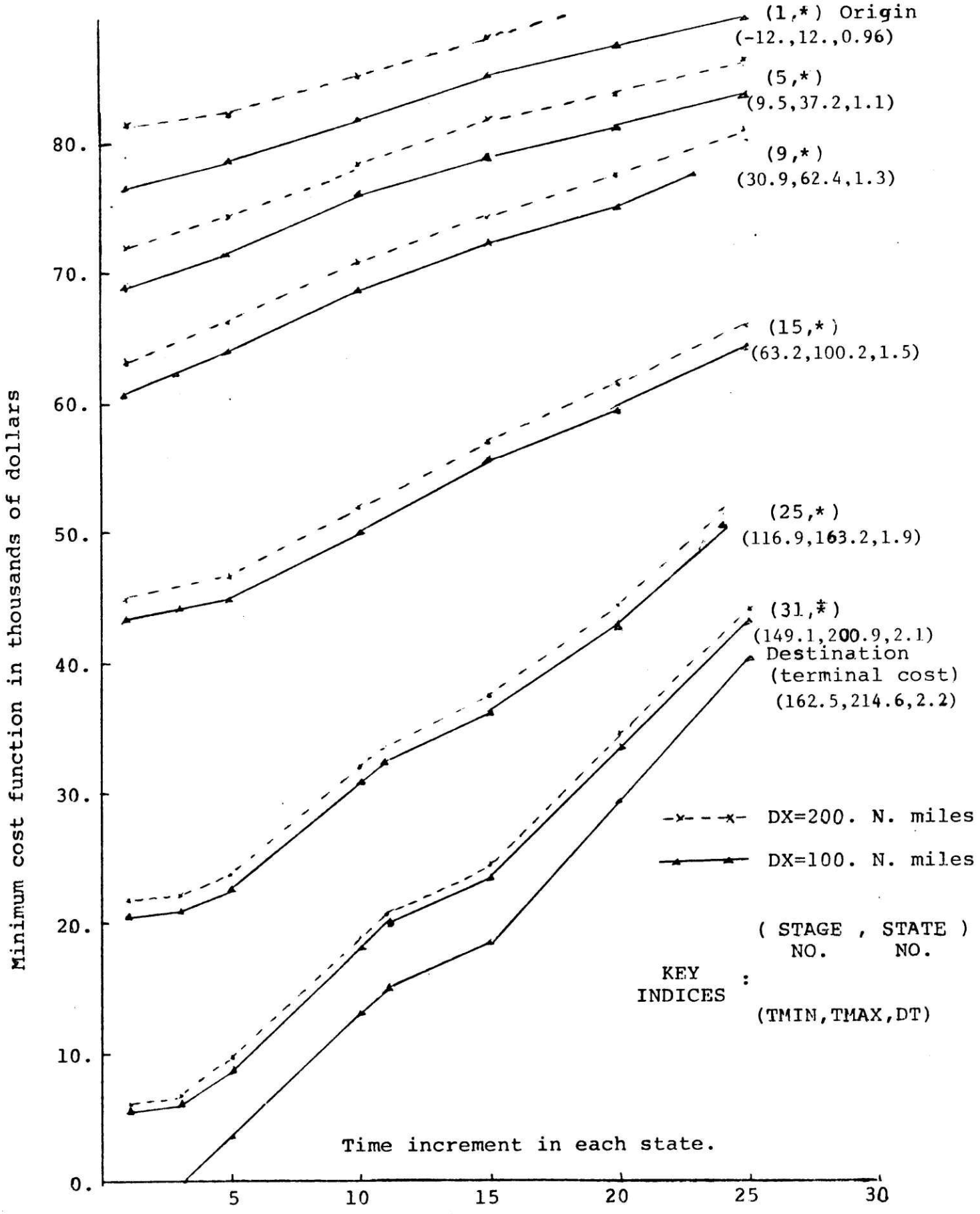


Fig. 2.3-4 Effect of reducing grid size DX by half on the Optimal value function at various stages.

Notice that the results are similar for the stages near the destination. The simulated storm was somewhere between the stages 10 and 15. The high waves forced the controls to divert from the original great circle route to a southern route as shown in Figure 2.3-5. In this case, there is a difference of up to 3% in the expected voyage cost at the beginning of the voyage.

Evidently, the size of DY also has a substantial effect on the final solution and the expected ship trajectory. The difference comes from the fact that we are approximating the optimal value function continuum by discrete points in the feasible state space. The limited power output and course changing options from a coaser grid system cannot accurately represent the actual optimal and its related controls. As a result, the expected ship trajectory may exhibit the zig-zag characteristics as shown in figure 2.3-6 for the DY=60. nautical miles case.

More importantly, this 3% or 5% changes in the objective function may seem small percentagewise. It really represents a large portion of what could have been saved when one realized that the minimum cost along the great circle route in calm water situation would amount to at least $70,000. In other words, it is actually a change of 25% of what could be saved. Furthermore, from a ship owner's point of view, this 5% saving, if realized, would translate into thousands of dollars. For comparision, even though the computation cost increased 100%,when the number of stages was doubled, it amounts to $40 from the original $20. Suppose the ship tracks requires updating once every day in our Closed open-loop control strategy. The total computing cost would be around $200[1]. It is quite obvious that the use of a finer

[1]The number of stages will decrease as the voyage continues, hence less computation effort for the later updates. The $200 is an average figure and would be substantially less if a special purpose computer is used.

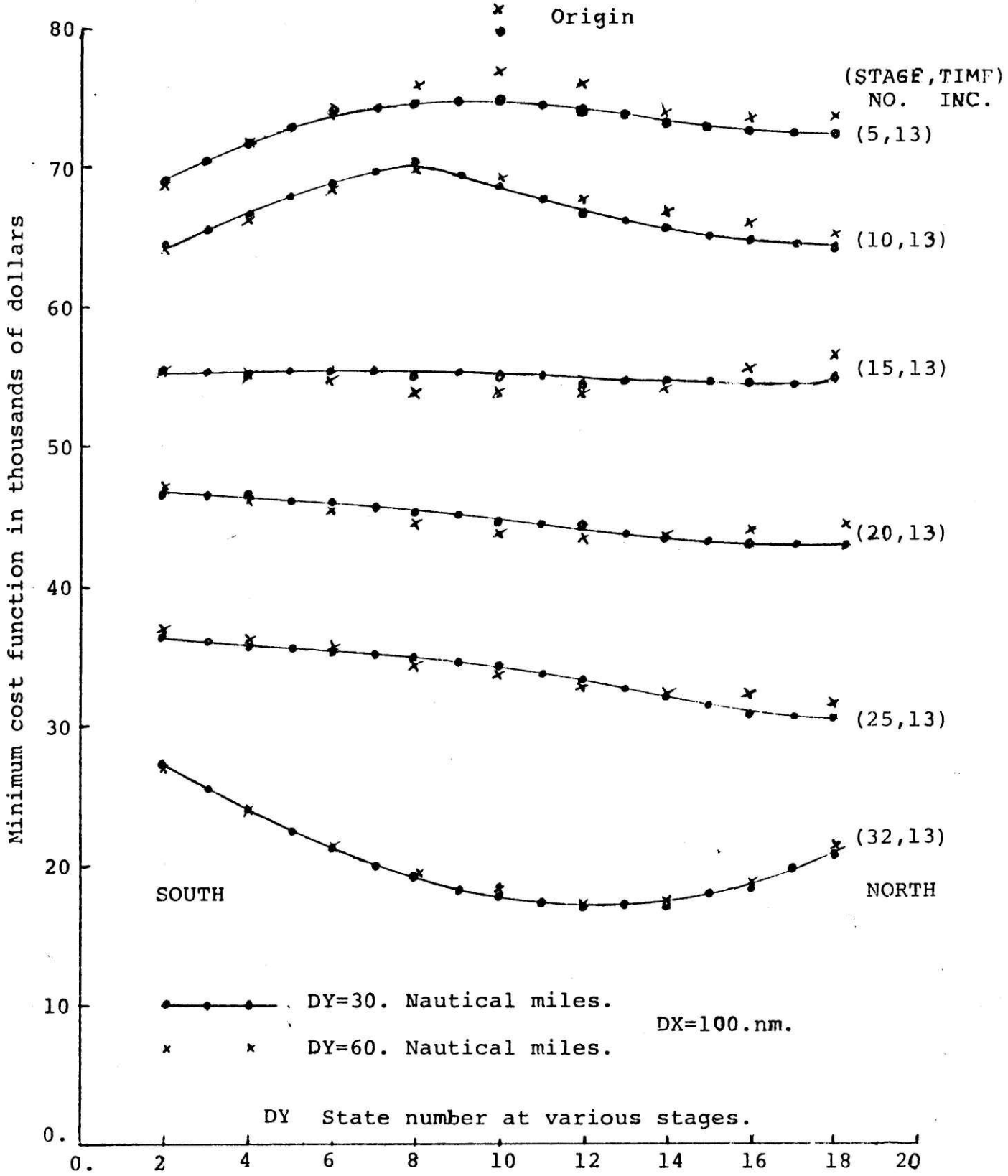


Fig.2.3-5 Effect of reducing grid spacing DY by half on the Optimal value function.

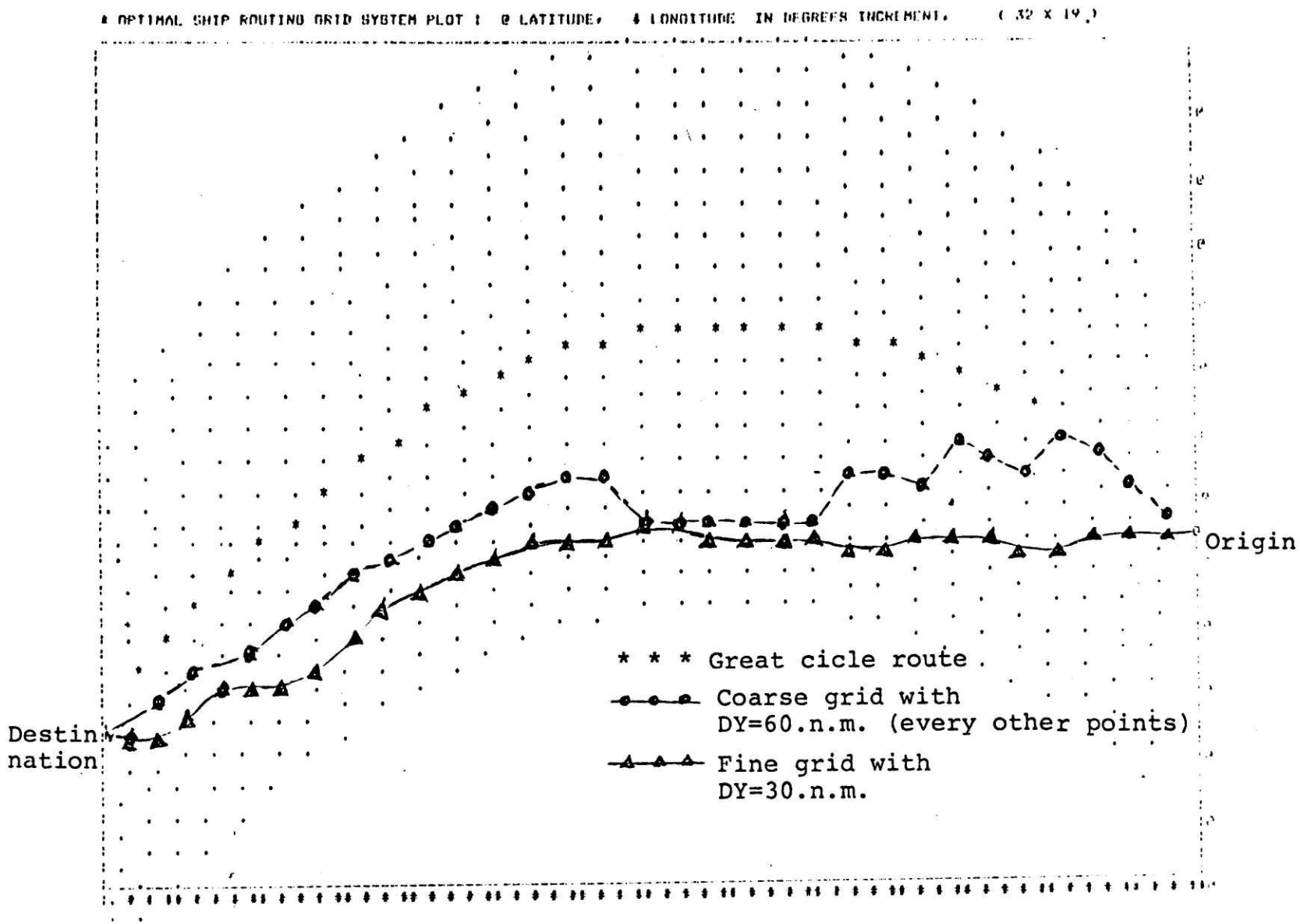


Fig. 2.3-6 Comparision of the expected ship trajectories using two different grid spacings.

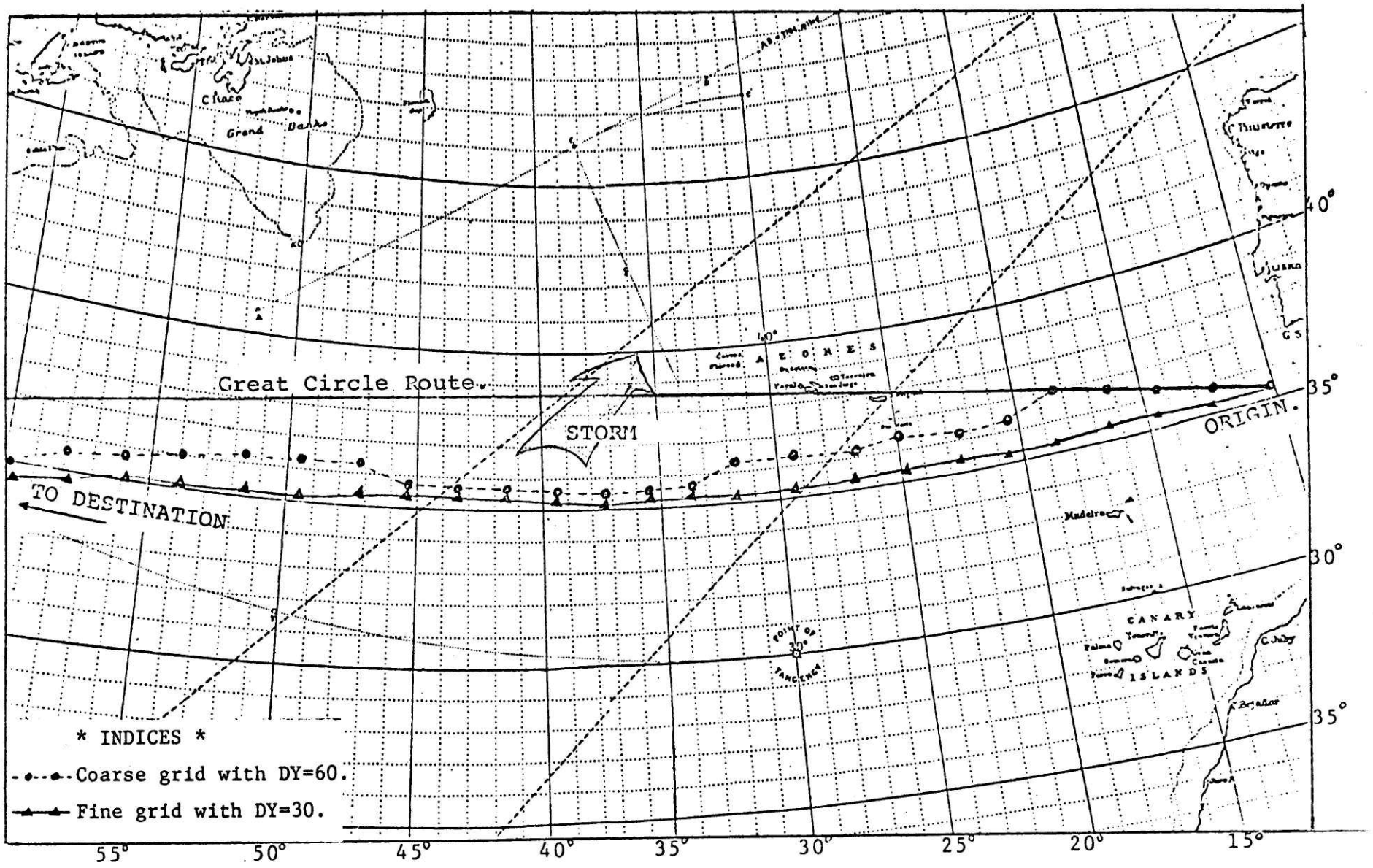


Fig. 2.3-7 Map plot of the expected ship trajectories using two different grid system.

grid system is always preferred even only 1% of the saving could be realized.

In conclusion, the calibration studies show that the algorithm is sensitive to the discretization in the space domain and less sensitive in the time domain for the type of cost function considered. The algorithm seems quite efficient when the required computing cost is compared to the expected savings in the actual voyage cost.

## 2.4 DISCUSSION

In this chapter, a Dynamic Programming algorithm using the closed open-loop control strategy has been developed for the ship routing problem under uncertainty. The results from the calibration exercise have shown that the algorithm is economically feasible for real-time implementation.

It is interesting to compare with the mathematically elegant Calculus of Variation approaches that have been investigated in many previous studies [4,5,6,7,8] for minimum time ship routing. In the Calculus of Variation methods, attention was focused upon the function that yields the minimum value rather upon the numerical values of the minimized functional itself. In these algorithms, any likely trajectory is chosen. The feasible solution then is improved according to the gradients of the objective function until the optimum has been reached and the boundary conditions are satisfied. The procedures require the solutions of either a set of linear homogeneous differential equations called ajoint or the Euler Hamiltonian equation in the vector form. One major difficulty of these methods

is the evaluation of the partial derivatives of the ship speed function with respect to the geographic positions and the ship's controls. The solution procedure generally breaks down (convergence problem) if the derivatives are mutually dependent as it is often the case in the ship routing problem.

Whereas from the dynamic programming viewpoint, the algorithm centers its attention upon the optimal value function and upon its attributes-optimal controls. When we adopt this point of view, the state variable becomes independent of each other. Any changes in the state variables during the recursion procedure means that we are changing the initial boundary conditions and consequently considering a new variational problem from there on. The procedure continues until the entire problem is solved.

From a theoretical point of view, the algorithm is, by definition, an approximated one. When comparing it to the classical optimal control approach using time as a stage variable, the algorithm is somewhat restrictive and relies quite heavily on assumptions with regard to modern ship control devices and operational practices. However, the present approach removes the ambiguity in the interpolation of the optimal value function between geographical position and more importantly, its lack of generality is far outweighted by the computation efficiency which makes the stochastic model to be economically attractive.

One of the very critical assumptions we made in deriving the stochastic recursion equation was the first order Markov property on the random environmental conditions. Such an assumption obviously is not realistic knowing that the ocean wave is naturally a correlated time and space process.

To avoid the use of higher order models and also account for the inaccuracy of the long range weather forecasts, we have recommended a so-called 'closed open-loop'control strategy, rather than going for an adaptive one. The choice was made in view of the limited computing capability onboard and our inability to specify the probablistic change of weather patterns in a quantitative manner.

The other less realistic assumption is the expected value decision-making rule we imposed on a ship owner. The criteria essentially assumes that he would like to minimize the total voyage cost on the average for the given uncertainty on the wave conditions. It does not imply any risk preference on the decision maker's part. i.e. he is risk neutral. He chooses his control policy by comparing the expected cost of the alternative policies under uncertainty[1]. Since the ship operating cost constitutes a relatively small portion of the multi-million dollar investment, the risk preference in making the ship routing decisions would not make much difference even for the most daring or the most conservative ship owner.

[1]For an axiomatic development of the utility theory and a vigorous justification of the expected value decision making criteria see Ref. [27].

# CHAPTER 3

# DYNAMIC ENVIRONMENTAL CONDITIONS

## 3.1 MODELLING OCEAN ENVIRONMENT

Both the atmosphere and ocean have dynamic properties that strongly influence the performance of a ship in a seaway. Sea severity not only effects the ship speed during a voyage, but also induces ship responses such as motion, acceleration, slamming, etc., which may violate the system constraints $\vec{M}$ of the routed ship for reasons of cargo, ship crew safety and other operation criteria. It is therefore most important that an accurate description of the ocean environmental condition is provided as inputs to our routing algorithm for evaluating ship speedkeeping, seakeeping responses.

To compute the ship response and seakeeping statistics, it requires a knowledge of the ship's responses to all individual wave components that may be encountered in the ocean. Since by linear theory, the response of the ship to any particular wave component is the product of the wave component times the corresponding frequency response of the ship, an adequate representation of the seaway is absolutely essential besides the characterization of the ship responses in the frequency domain. These two requirements can be pursued with varying degrees of sophistication depending upon the accuracy and resolution desired in the output data for a particular application.

The purpose of the chapter is to suggest various ways of modelling the dynamic ocean environments for ship routing. Starting from a full detailed approach to a much simplified parameter approach, the advantages and disadvantages of various

representations of seaways are discussed in view of the required data management, online computing time, interpolation scheme and other practical implications.

## 3.2 OCEAN WAVES

### 3.2.1. DIRECTIONAL SPECTRA REPRESENTATION

The most useful description of a seaway for evaluating ship responses by frequency domain analysis is in terms of its spectral representation. The most complete information on ocean waves for the purpose is in terms of its directional spectra, Fig. 3.2.-1 shows a three dimensional plot of the concept. To provide such information, FNWC of the U.S. Navy has developed an operational Spectral Ocean Wave Model (SOWM). Ref. [2] to forecast directional spectra at various ocean grid points up to 72 hours.

The model, was developed for Northern hemispheres and used an icosahedron to depict the shape of the globe as shown in Fig. 3.2-2. An icosahedron is a twenty sided polygon with equilateral triangles for its faces. The SOWM uses seven triangles for the North Pacific Ocean, six for the North Atlantic Ocean, and one for the Indian Ocean. Each triangle has 325 grid points with a spacing of approximately 350 km at the point of tangency and 194 km at the vertices. At each grid point, the wave energy is the sum of all the energy in terms of a twelve direction by fifteen frequency band matrix. Table 3.2-1 shows a typical output of the SOWM.

Each number represents the incremental mean square wave height $\Delta\overline{e}^2$ contained in an elemental band of wave frequency $\Delta\omega$ and direction $\Delta\chi$. The sum of the 12 x 15 elements gives the mean

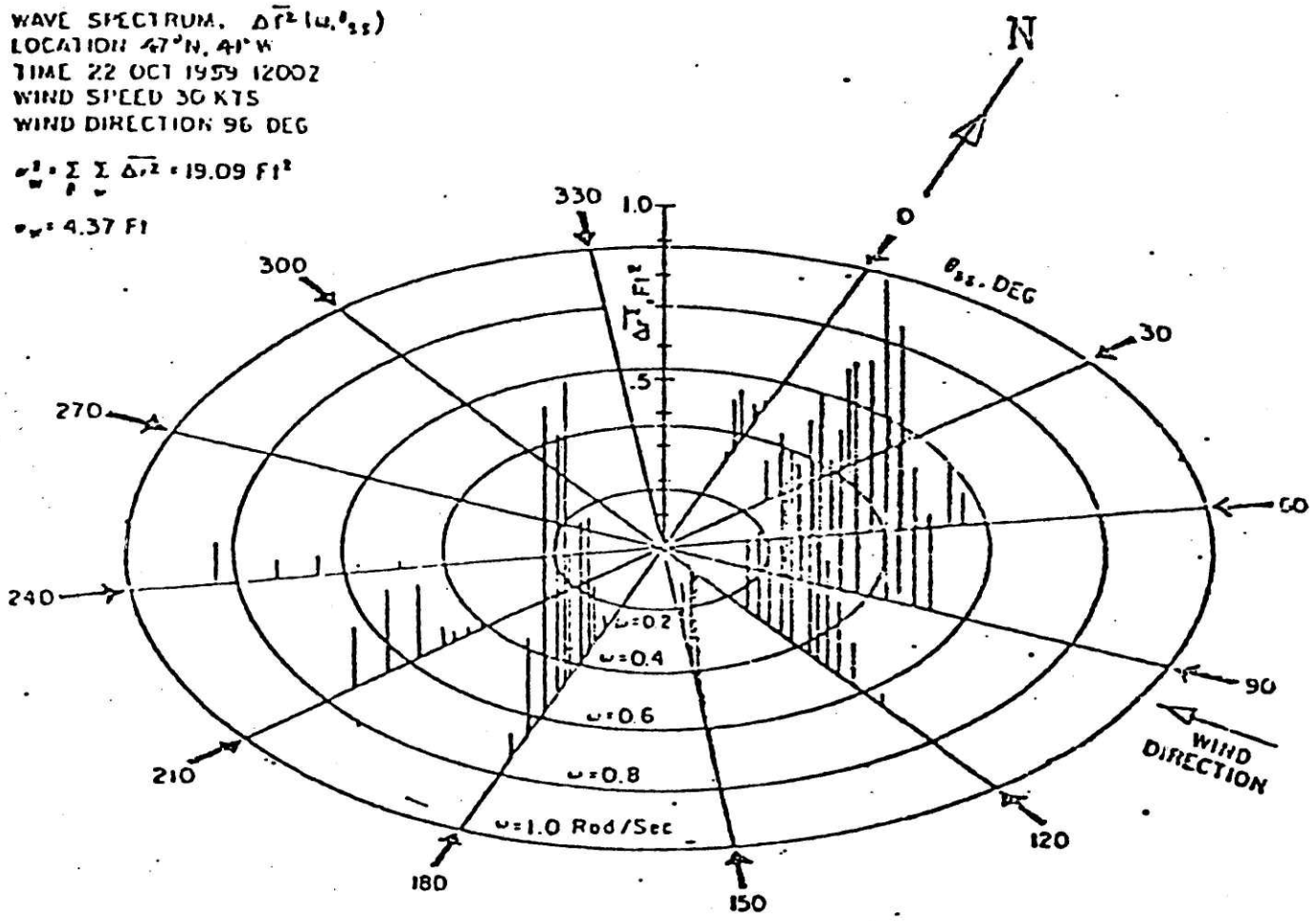


Figure 3.2-1 Three dimensional plot of the concept of directional spectra.

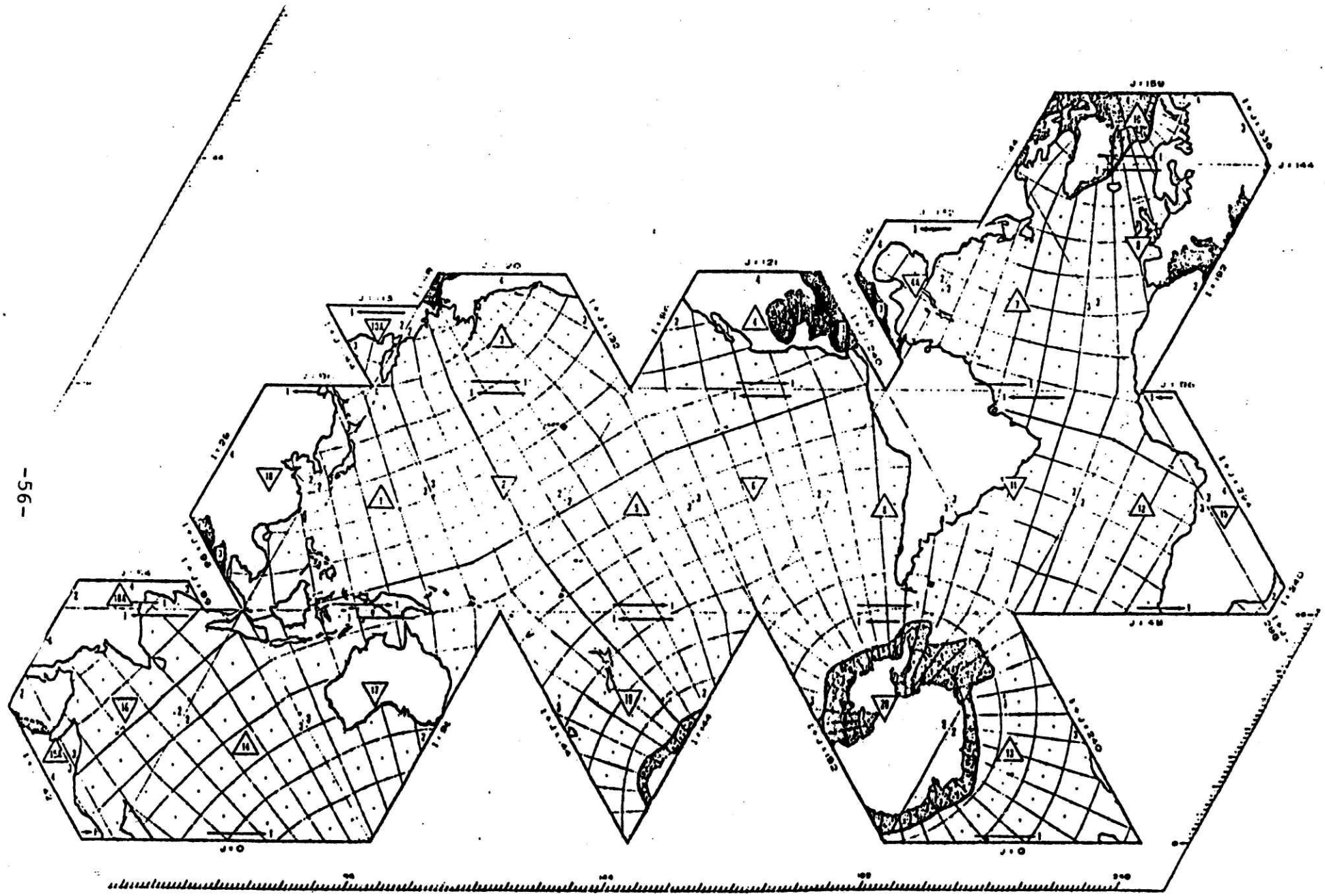

MAP OF THE WORLD OCEAN FOR WAVE STUDIES

Figure 3.2-2

JTG= 731,273, TAU= -6

TIME STEP 1 SUBPROJECTION 3 GRID PT 154 LAT 50.687 LONG (EAST) 214.354
WIND SPEED 13.74 WIND DIR 201.0 USTAR .49

| FREQ / DIR. | .164 | .153 | .133 | .117 | .103 | .092 | .083 | .076 | .072 | .067 | .061 | .056 | .050 | .044 | .039 | | (MET DI |
|---|---|---|---|---|---|---|---|---|---|---|---|---|---|---|---|---|---|
| 1 | 0.000 | 0.000 | 0.000 | 0.000 | 0.000 | 0.000 | 0.000 | 0.000 | 0.000 | 0.000 | 0.000 | 0.000 | 0.000 | 0.000 | 0.000 | 0.000 | 319.52 |
| 2 | 0.000 | 0.000 | 0.000 | .016 | .014 | 0.000 | .001 | 0.000 | .106 | 0.000 | 0.000 | 0.000 | 0.000 | 0.000 | 0.000 | .131 | 289.52 |
| 3 | .000 | .002 | .025 | .163 | .373 | .795 | .655 | 1.046 | 1.391 | .760 | .250 | .023 | .002 | 0.000 | 0.000 | 5.540 | 259.52 |
| 4 | .223 | .032 | .131 | .479 | .044 | .537 | .203 | .253 | .101 | .060 | 0.000 | .021 | 0.000 | 0.000 | 0.000 | 2.059 | 229.52 |
| 5 | .332 | .297 | .402 | .656 | .269 | .244 | .551 | .615 | .130 | .043 | .034 | .125 | .005 | .000 | 0.000 | 3.704 | 199.52 |
| 6 | .212 | .236 | .234 | .444 | .037 | .017 | .016 | .046 | .006 | .031 | .008 | .005 | .001 | 0.000 | 0.000 | 1.652 | 169.52 |
| 7 | .048 | .143 | .091 | .176 | .136 | .013 | .005 | 0.000 | 0.000 | 0.000 | 0.000 | 0.000 | 0.000 | 0.000 | 0.000 | .600 | 139.52 |
| 8 | 0.000 | 0.000 | .005 | .109 | .013 | .017 | .000 | .001 | .003 | 0.000 | 0.000 | 0.000 | 0.000 | 0.000 | 0.000 | .047 | 109.52 |
| 9 | 0.000 | 0.000 | 0.000 | .000 | .001 | 0.000 | 0.000 | 0.000 | 0.000 | 0.000 | 0.000 | 0.000 | 0.000 | 0.000 | 0.000 | .001 | 79.52 |
| 10 | 0.000 | 0.000 | 0.000 | 0.000 | .000 | .010 | 0.000 | 0.000 | 0.000 | 0.000 | 0.000 | 0.000 | 0.000 | 0.000 | 0.000 | .010 | 49.52 |
| 11 | 0.000 | 0.000 | 0.000 | 0.000 | 0.000 | 0.000 | 0.000 | 0.000 | 0.000 | 0.000 | 0.000 | 0.000 | 0.000 | 0.000 | 0.000 | 0.000 | 19.52 |
| 12 | 0.000 | 0.000 | 0.000 | 0.000 | 0.000 | 0.000 | 0.000 | 0.000 | 0.000 | 0.000 | 0.000 | 0.000 | 0.000 | 0.000 | 0.000 | 0.000 | 349.52 |
| **** | .881 | .707 | .947 | 1.936 | .867 | 1.628 | 1.434 | 1.961 | 2.037 | .944 | .292 | .174 | .007 | .000 | 0.000 | 13.785 | |

$\bar{H}$ 1/3=14.8 FT

TIME STEP 1 SUBPROJECTION 3 GRID PT 155 LAT 48.474 LONG (EAST) 217.473
WIND SPEED 26.03 WIND DIR 219.5 USTAR 1.05

| FREQ / DIR | .164 | .153 | .133 | .117 | .103 | .092 | .083 | .076 | .072 | .067 | .061 | .056 | .050 | .044 | .039 | | (MET DI |
|---|---|---|---|---|---|---|---|---|---|---|---|---|---|---|---|---|---|
| 1 | .032 | 0.000 | 0.000 | 0.000 | 0.000 | 0.000 | 0.000 | 0.000 | 0.000 | 0.000 | 0.000 | 0.000 | 0.000 | 0.000 | 0.000 | .002 | 321.81 |
| 2 | .143 | .002 | .000 | .014 | .007 | .000 | .004 | .013 | .017 | 0.000 | .002 | 0.000 | 0.000 | 0.000 | 0.000 | .734 | 291.81 |
| 3 | .297 | .297 | .331 | .656 | .664 | 1.093 | .803 | .951 | 1.052 | .521 | 0.000 | .003 | .000 | 0.000 | 0.000 | 6.729 | 261.81 |
| 4 | .451 | .301 | .427 | .766 | .772 | 1.334 | .350 | .377 | .278 | .269 | 1.930 | .139 | .058 | .001 | 0.000 | 7.939 | 231.81 |
| 5 | .441 | .311 | .441 | .775 | .917 | 1.184 | .615 | .399 | 1.509 | 1.051 | 1.253 | .023 | .015 | .001 | 0.000 | 8.918 | 201.81 |
| 6 | .263 | .229 | .274 | .480 | .453 | .593 | .275 | .281 | .443 | .329 | .053 | .024 | .001 | 0.000 | 0.000 | 3.432 | 171.81 |
| 7 | .026 | .044 | .001 | .123 | .101 | .062 | .007 | .004 | .002 | 0.000 | .002 | 0.000 | 0.000 | 0.000 | 0.000 | .433 | 141.81 |
| 8 | 0.000 | 0.000 | .000 | .002 | .000 | .029 | .001 | 0.000 | 0.000 | 0.000 | .001 | 0.000 | 0.000 | 0.000 | 0.000 | .042 | 111.81 |
| 9 | 0.000 | 0.000 | 0.000 | 0.000 | .017 | .001 | 0.000 | 0.000 | 0.000 | 0.000 | 0.000 | 0.000 | 0.000 | 0.000 | 0.000 | .017 | 81.81 |
| 10 | 0.000 | 0.000 | 0.000 | 0.000 | 0.000 | 0.000 | .010 | 0.000 | 0.000 | 0.000 | 0.000 | 0.000 | 0.000 | 0.000 | 0.000 | .000 | 51.81 |
| 11 | 0.000 | 0.000 | 0.000 | 0.000 | 0.000 | 0.000 | 0.000 | 0.000 | 0.000 | 0.000 | 0.000 | 0.000 | 0.000 | 0.000 | 0.000 | 0.000 | 21.81 |
| 12 | 0.000 | 0.000 | 0.000 | 0.000 | 0.000 | 0.000 | 0.000 | 0.000 | 0.000 | 0.000 | 0.000 | 0.000 | 0.000 | 0.000 | 0.000 | 0.000 | 351.81 |
| **** | 1.653 | 1.184 | 1.616 | 2.769 | 2.928 | 4.067 | 2.118 | 2.029 | 3.721 | 1.467 | 3.247 | .989 | .074 | .002 | 0.000 | 28.246 | |

$\bar{H}$ 1/3=21.3 FT

from [2] SOWM Two Dimensional Wave Spectra for 50°.89N, 145°.25W and 48°.47N, 142°.53W
October 26, 1973 18Z

Table 3.2-1 15X12 matrix of the wave energy content in a directional spectrum forecasted by SWOM of FNWC.

square wave height and is also related to the significant wave height, $H_{1/3}$ by definition :

$$H_{1/3} = 4.0 * \sqrt{E_{total}} \qquad ....(3.1)$$

The direction intervals $\Delta\chi$ corresponds to 30 degree of compass spread, the frequency interval is not uniform. The band width at the lower frequencies (may be interpreted as swell) are smaller than those at the high frequencies (sea). To incorporate the full directional spectra into our ship routing model, storage space must be provided for the 12 X 15 matrixes at all the wave grid points up to 72 hours in 12 hour intervals. For the North Atlantic which has a total of 1950 grid points, a disk data file of at least 10,000 k bytes of storage space must be available for updating and maintaining the directional spectra. During the computation of optimal value function for each state, the directional spectra is accessed and interpolated over space as well as time. Then, various ship motion indices can be calculated online according to the procedrues outlined in the next chapter.

The advantage of this approach using the full directional spectra representation in calculating the ship responses is that it provides the capability to obtain the complete power spectra and cross-spectra of the responses for ocean systems which are highly critical and sensitive to changes of encounter frequencies, e.g. drilling ship operation, aircraft carrier landing problems, the ability to predict the system responses at various wave frequencies and directions is absolutely essential. The disadvantage is obviously the excessive online computation and storage that are required to perform these calculations. In addition, due to the wide

| Central Frequency [$H_z$] | Central Frequency (rad/sec) | Central Period (Seconds) | Frequency Bandwidth [$H_z$] |
|---|---|---|---|
| 0.164 | 1.030 | 6.1 | .164 - ∞ |
| 0.153 | 0.961 | 6.5 | .142 - .164 |
| 0.133 | 0.836 | 7.5 | .125 - .142 |
| 0.117 | 0.735 | 8.6 | .108 - .125 |
| 0.103 | 0.647 | 9.7 | .097 - .108 |
| 0.092 | 0.578 | 10.9 | .086 - .097 |
| 0.083 | 0.522 | 12.0 | .080 - .086 |
| 0.078 | 0.490 | 12.9 | .075 - .080 |
| 0.072 | 0.452 | 13.8 | .069 - .075 |
| 0.067 | 0.421 | 15.0 | .064 - .069 |
| 0.061 | 0.383 | 16.4 | .058 - .064 |
| 0.056 | 0.352 | 18.0 | .053 - .058 |
| 0.050 | 0.314 | 20.0 | .047 - .053 |
| 0.044 | 0.276 | 22.5 | .042 - .047 |
| 0.039 | 0.245 | 25.7 | .036 - .042 |

Table 3.2-2 Frequency definition of SOWM Spectra Matrix

spacing between SOWM's grid systems as well as its large forecast interval, severe difficulty may be encountered in trying to derive the spectra for other non-standard time and positions.

In conclusion, it seems that while this full detailed approach would provide the most accurate evaluation of ship responses in a seaway, the amount of computation and storage requirements is not feasible at the present level of computer technology. Furthermore, such accuracy deteriorates rapidly due to the unavailability of sophisticated wave interpolation model and the present state-of-the-art of weather forecasting.

### 3.2.2 SWELL, SEA SPECTRA REPRESENTATION

One of the approaches to evaluate ship responses that is most commonly used in design studies is the utilization of theoretical sea spectral formulae. These formulations which were derived from a large number of measured point spectra, represents the most probable spectral shape for a given sea severity.

The most common form that has been widely accepted and recommended by the International Towing Tank Conference [30] is a two parameter Bretschneider spectral formulation:

$$s(\omega) = \alpha\omega^{-a} \exp(-\beta\omega^{-b}) \quad \ldots.(3.2)$$

$$\alpha = 5/16\ \omega_p^{\ 4}\ (H_{1/3})^2$$

$$\beta = 5/4\ \omega_p^{\ 4}$$

$$a = 5.0$$

$$b = 4.0$$

Where $S(\omega)$ is the spectral density as a function of wave frequency $\omega$. $H_{1/3}$ is the significant wave height as defined in eq. (3.1) and $\omega_p$ is the peak frequency often related to the characteristic wave period.

It follows therefore, by utilizing the two-parameter theoretical spectral formulation, we can summarize the full directional spectra by a few parameters. From eq. (3.1), the magnitude of significant wave height $H_{1/3}$ can be calculated. To locate the peak frequency, one simply has to search for the frequency band which contains the highest energy per unit frequency. To account for the directionality and shortcrestness, a spreading function is usually employed. One of the most common form is as follows:

$$S(\mu) = \frac{2}{\pi} \cos^2 \mu \qquad \ldots\ldots(3.3)$$

where $\mu$ wave direction relative to predominant wave direction.

Hence, the full directional spectrum is approximated by a point spectrum in conjunction with a spreading function.

$$S(\omega,\mu) = S_1(\omega) S_2(\mu) \qquad \ldots\ldots(3.4)$$

$$\text{for} \quad 0 \leq \omega \infty$$

$$-\pi/2 \leq \mu \pi/2$$

This data reduction procedure drastically reduces the storage requirement for the wave data file. Instead of storing 180 pieces of information, it only requires about four for each spectrum. Furthermore, since the spectra are

parameterized, we can pre-compute the responses for all combinations of $H_{1/3}$ $\omega_p$ and ship-wave angle, then store them offline. The comparison of the ship responses to a pre-defined motion constraint criteria $\vec{M}$ only involves a simple read operation online once the parameters are known.

Unfortunately, there are a couple of problems with this simple procedure. First, it is a single peaked spectrum which cannot realistically represent a seaway when distinct swells are present. Secondly, the formulation assumes a constant spectral broadness measure or shape. (i.e. the variability of the frequency content is constant). In reality, the shapes of wave spectra measured in the ocean vary considerably (even though the values of $H_{1/3}$ are the same) depending on environmental condition such as stage of growth and decay of a storm, duration and fetch of the prevailing wind, depth of the water etc.

Figure 3.2-3 from [69] illustrates dramatically the variability of spectral shapes which essentially have the same parameters.

One major improvement over the simple two-parameter spectra approach may be the use of separate spectral formulations and directions for the primary as well as the secondary wave components.

In most cases, when a point spectrum has double peaks, it usually indicates that there is two distinct trains of wave energy travelling in different directions. The concentration of energy in the area of low frequency bands especially in a direction greater than 30° from the existing wind direction would indicate the existence of swells. Whereas for high frequency components, the energy spreads over a larger band and it is usually referred to as sea.

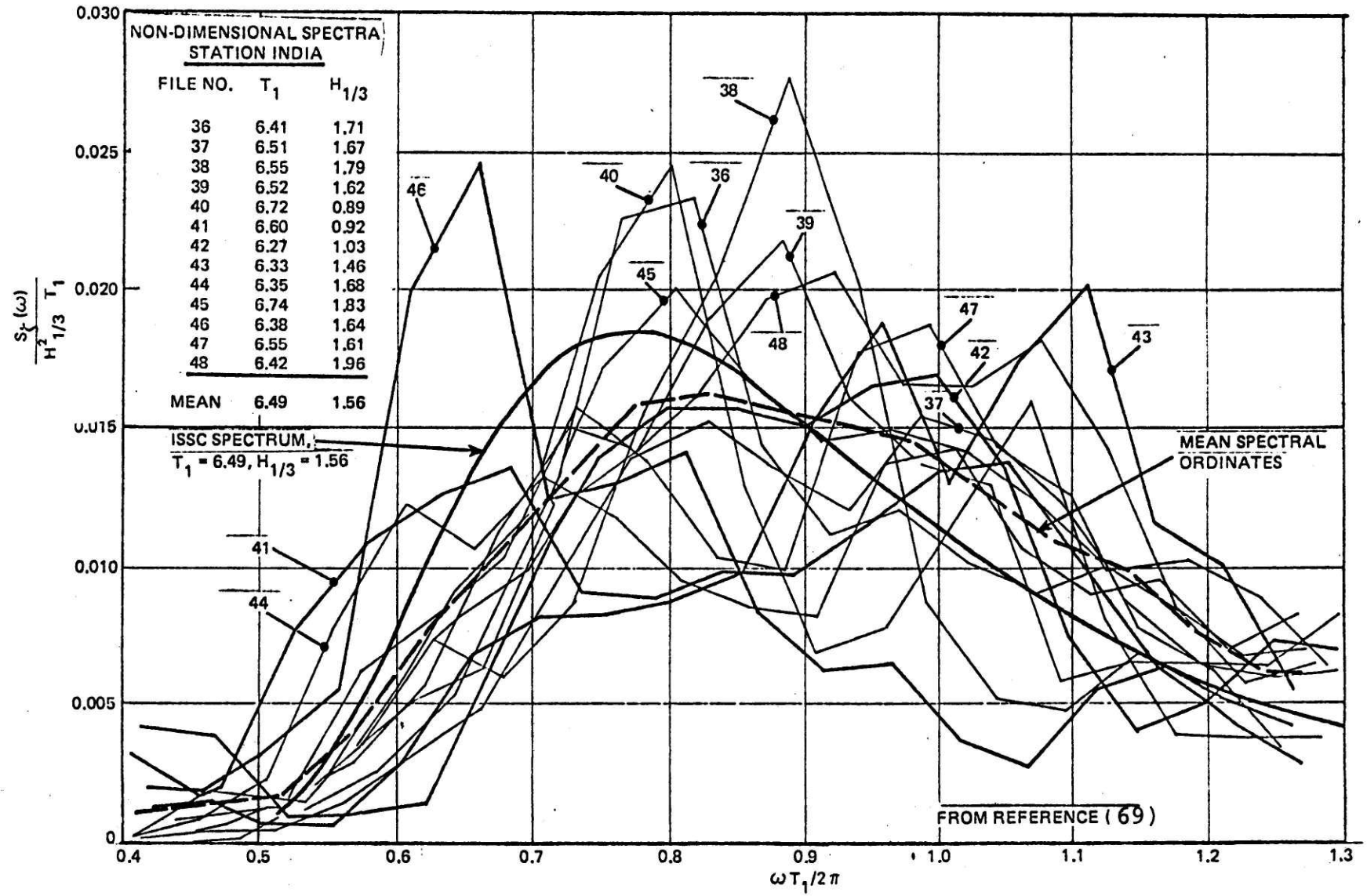


Fig.3.2-3 Non-Dimensional Plot of 13 Spectra of Approximately Equal Characteristics

SUMMARY OF SOME THEORETCIAL TWO PARAMETER SPECTRAL FORMULATION AND THEIR PROPERTIES

| SPECTRAL TYPES | $\alpha$ | $\beta$ | a | b | Spectral width or broadness measure | |
|---|---|---|---|---|---|---|
| | | | | | $\varepsilon$ | q |
| Bretschneider | $5/16 \cdot \omega_p^4 (H_{1/3})^2$ | $5/4\ \omega_p^4$ | 5 | 4 | 0.59 | 0.3908 |
| Neuman | $1.46\ \omega_p^5 (H_{1/3})^2$ | $3\ \omega p^2$ | 6 | 2 | 0.816 | 0.3888 |
| Noznesenski-Netsvetayev | $0.457\ \omega p^5 (H_{1/3})^2$ | $1.51\ \omega p^4$ | 6 | 4 | - | 0.3157 |
| Daviddan-Lopatukhin | $6\ Mo\ \omega p^5$ | $1.2\ \omega p^5$ | 6 | 5 | - | 0.2997 |
| Darbyshire | $s(\omega) = \alpha H_{1/3}^2 \exp\left\{-\left[\frac{(\omega-\omega_p)^2}{0.065(\omega-\omega_p+0.26)}\right]^{1/2}\right\}$ <br> $\alpha = 0.214 \qquad -0.26 < (\omega-\omega_p) < 1.65$ | | | | - | 0.47 |

Generalized Two-parameter Spectra

$$S(\omega) = \alpha\omega^{-a}\exp\ (-\beta\omega^{-b})$$

Spectral width or broadness measure : $\varepsilon = \left[1 - \frac{M_2^2}{M_o M_4}\right]^{1/2}$ ; $q = \left[1 - \frac{M_1^2}{M_o M_2}\right]^{1/2}$ .

To identify swell components in a directional spectrum, one must first locate the direction by inspecting the angular distribution of mean square wave heights. See Table 3.2-1. If there are two separate high energy components traveling at directions more than 30° apart. There is a high possibility of swell existence and the resulting double peakness in the point spectra.[1]

By finding the largest wave energy per unit frequency in each direction and choosing the one with lower frequency as swell components, the directional spectrum is represented by two parts: one swell component and one sea. Thus the original double peak point spectra is "decomposed" into a unidirectional long-crested swell spectra and a short crested single peak sea spectra.

The spectral density contribution from swell is given by

$$S_{Swell}(\omega,\chi) = \begin{cases} S(\omega_1\ \chi) & \text{for } \omega_1 - \frac{\Delta\omega}{2} \leq \omega \leq \omega_1 + \frac{\Delta\omega}{2} \\ 0 \end{cases} \quad \ldots\ldots(3.5)$$

where $\omega,\chi$ are the central frequency and direction; $\Delta\omega,\Delta\chi$ are the bandwidths respectively.

For the "sea", the usual two parameter Bretschneider spectral formulation may be used to fit the point spectrum and a simple cosine square spreading function to account for short crestness.

---

[1] Private communication with Mr. Norm Stevenson, FNWC.

Figure 3.2-4 shows an example of the above data reduction method applied to the directional spectrum presented in Table 3.2-1.

The advantage of the approach is that it reduces the effect of the two major shortcomings in the previous simple two parameter representation of ocean waves. By separating the sea and swell components according to their energy contents and directions, the directional ocean wave spectra is approximated more accurately. Although the question of spectral broadness or shape of the 'sea' spectra, still has to be resolved if a two parameter formulation is used to fit the remaining 'sea' spectrum, the variation due to swell components have been taken out.

The biggest advantage from data preparation point of view is that it not only reduces the input description of wave conditions to $[\omega,\chi,S(\omega,\chi)]$ swell, $[H_{1/3},\omega_p\chi]$ sea, six pieces of information, but also more importantly allows us to precompute the ship responses offline, and store them on a direct access disc file. Thus by using the two-parameter Bretschneider formulation in conjunction with a cosine square spreading function, the ship motion response may be calculated for the sea and tabulated according to combinations of the discrete intervals of significant wave height, peak frequency and wave direction. For the responses due to swell, since it is a unidirectional longcrested wave component, no spreading is required. Hence the combined response is given by the sum of the mean square responses due to sea and swell.[1] The details of ship motion analysis will be discussed in the next chapter.

---

[1]This is only true for linear systems. In ship motion theory, it is assumed that linear superposition is valid for most of the responses.

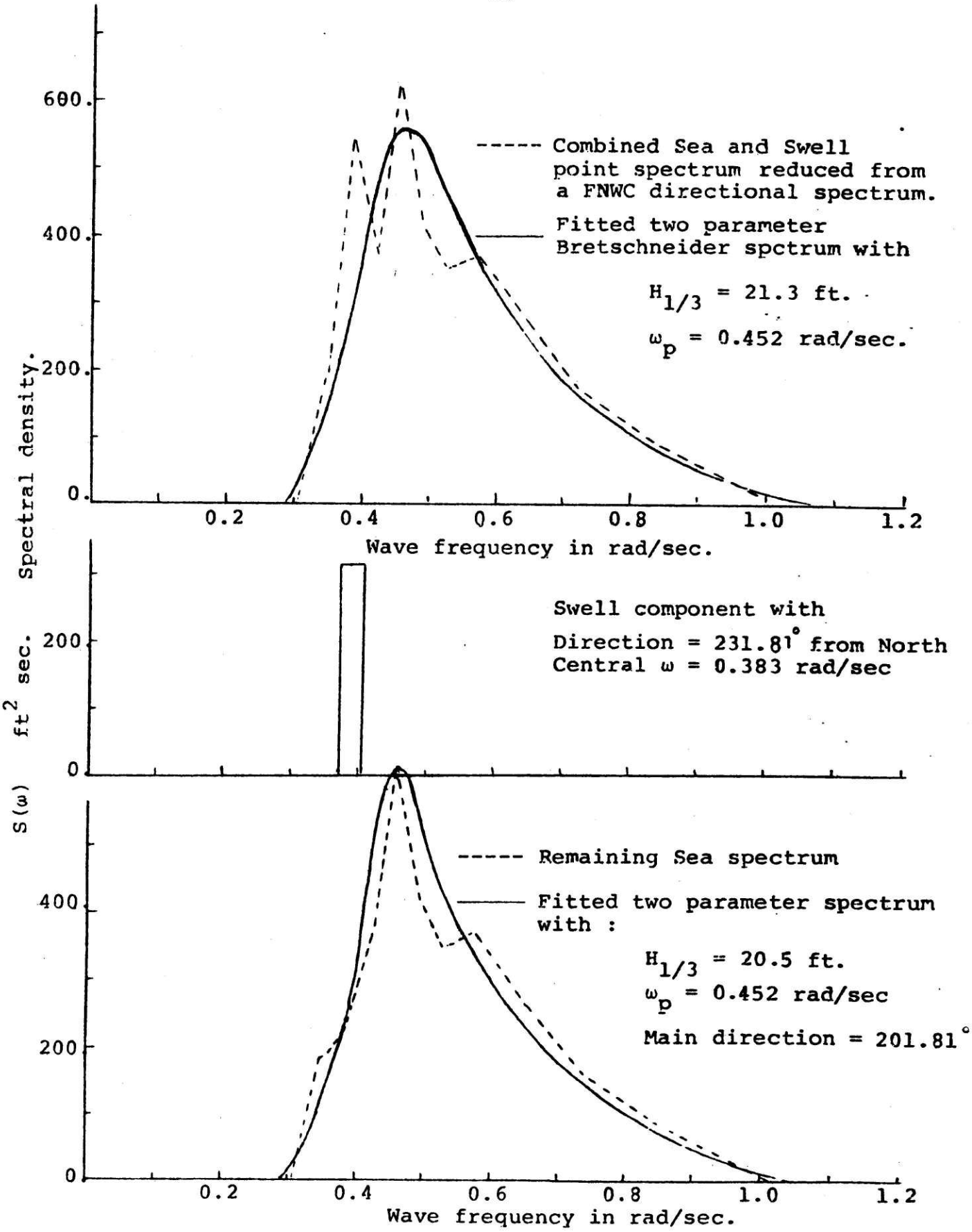


Fig. 3.2-4 An example of point spectra decomposition into Sea and Swell components.

### 3.2.3 CHARACTERIZING THE UNCERTAINTIES IN OCEAN WAVE FORECASTING

Having condensed our forecasted directional spectra into swell and sea spectral parameters, it is relatively easy to characterize the uncertainties in the wave forecasting from which the state transition probabilities are derived.

Recall that in section 2.2.2 , we defined $\vec{R}$ as a random vector describing the ocean wave conditions. Let us consider the following scenario: at the beginning of the voyage, the severities of the waves in the feasible state space have been forecasted by point estimates of $\vec{R}_{kj}$. For example, the vector $\vec{R}$ may be the significant wave height and peak frequency condensed from the directional spectra at various wave grids forecasted by FNWC at 12 hour intervals. As the time of forecasts increase into the future, the accuracy of the point estimates of $\vec{R}$ deteriorates and the uncertainty in terms of its variance also increases. Figure 3.2-4 shows a typical plot of the mean error and variance of forecasted significant wave heights.[1] The values also vary with the sea severity as shown explicitly in Fig. 3.2-6. The problem is how to characterize the distribution of R from which the probability density function of transition time is derived in order to carry out our stochastic recursion equation.

For the purpose of illustrating the mathematics and also due to the availability of data, let us only consider one parameter; the significant wave height H, and assume that H is normally distributed[1] for a given forecasted wave height parameter $\hat{H}$ at a particular forecast period DT(e.g. 0,12,24,36...hours later).

$$p(H \mid \hat{H}, DT) = \frac{1}{\sqrt{2}\sigma} \cdot \exp\left[ \frac{(H-\mu^2}{2\sigma^2} \right]$$

[1] This data was obtained from a wave buoy located somewhere in the North sea. Similar data should be obtained along commercial ship routes for verification of the wave model.

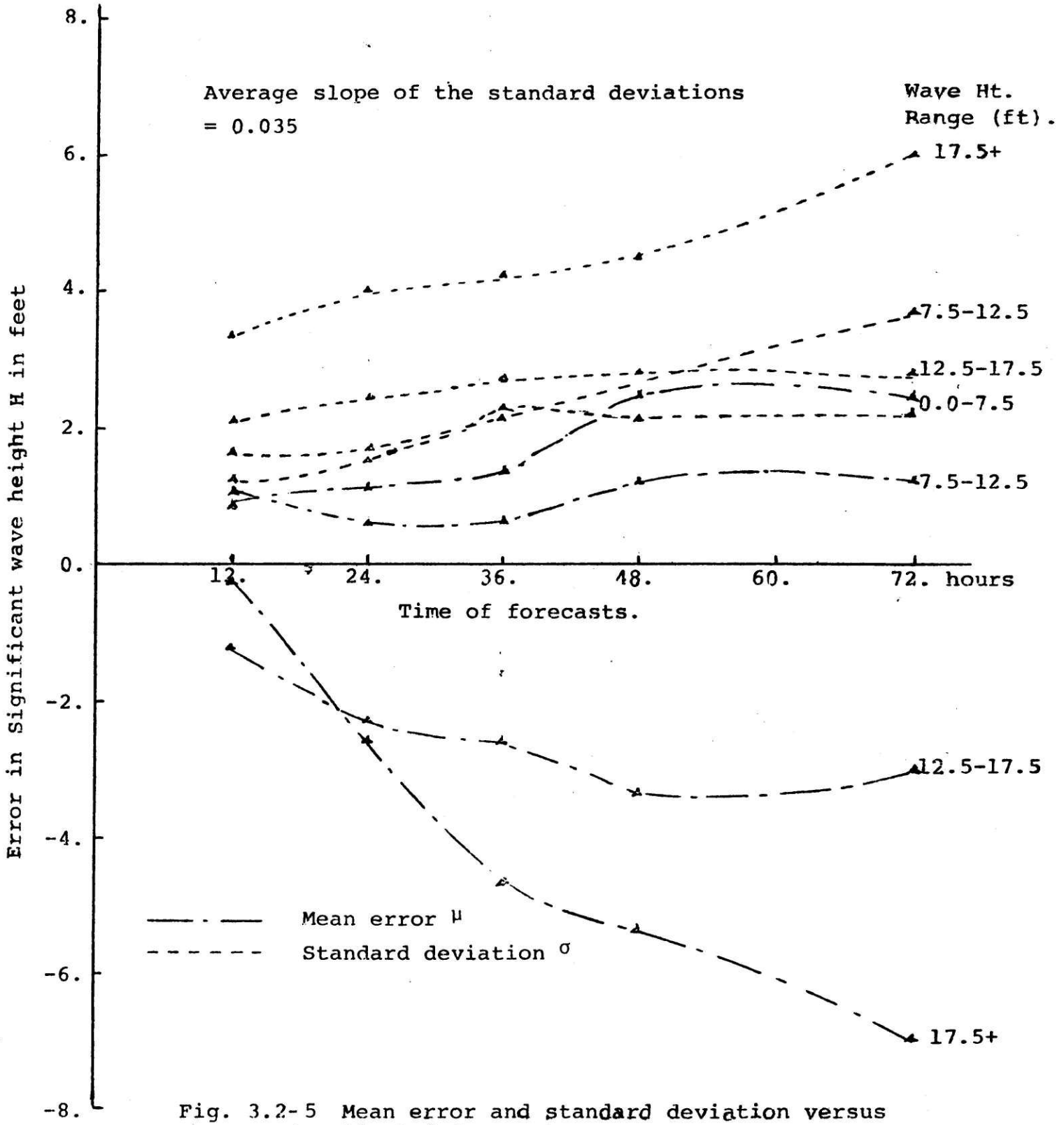


Fig. 3.2-5 Mean error and standard deviation versus time of forecasts.

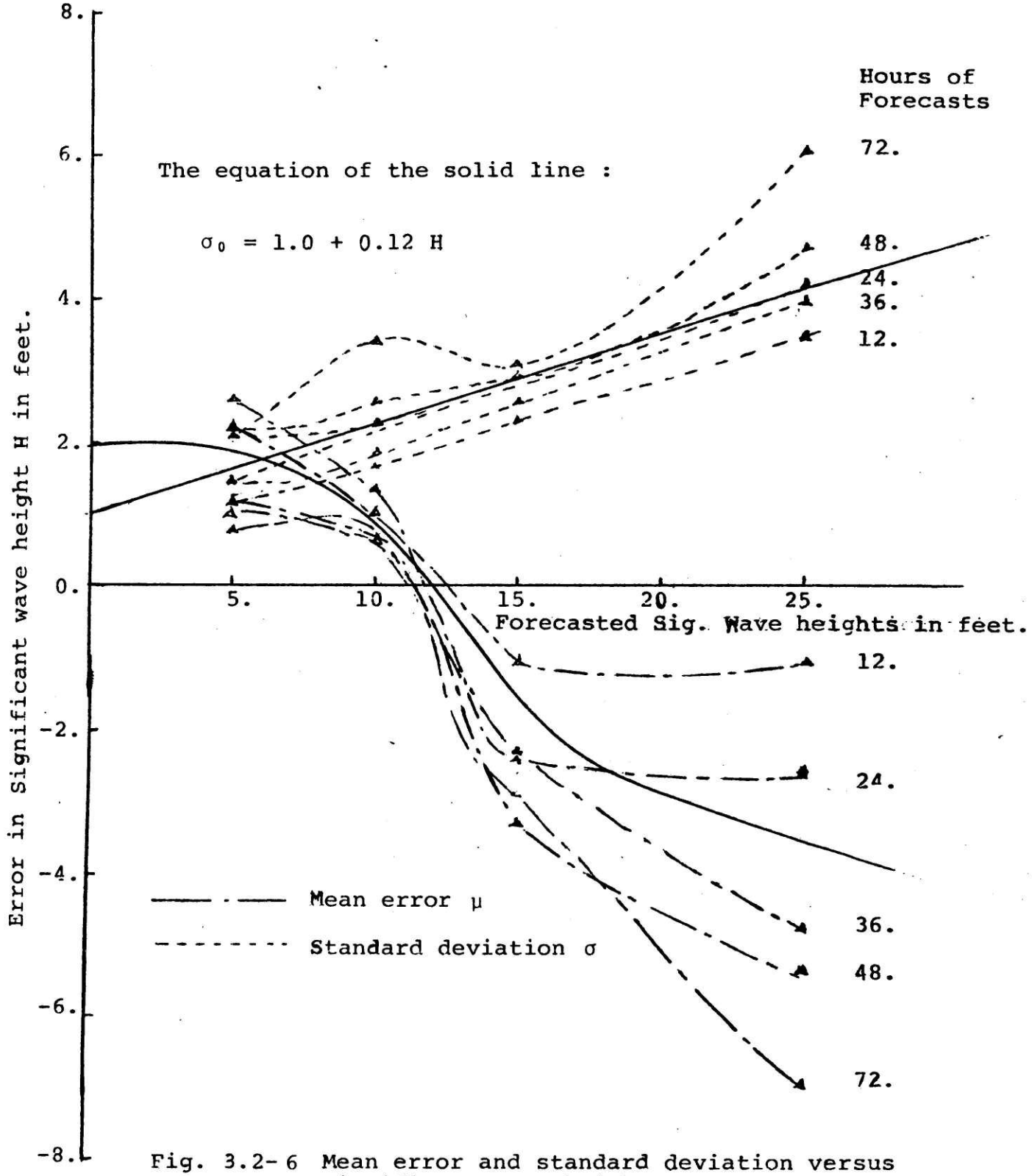


Fig. 3.2-6 Mean error and standard deviation versus significant wave heights.

The later measured actual wave height is $H_n$. When $H_n$ are n such independent observations from the assumed normal population given $\hat{H}$ and DT. To estimate the parameter of the distribution, Baysian Approach is used.

If little is known about the mean and standard deviation of such distribution, then the prior distribution before taking the observation can be respresented as:

$$p(\mu_H, \sigma_H)\, d\mu d\sigma \propto \frac{1}{\sigma_H} d\mu d\sigma$$

i.e. we have assumed $\mu$ and $\sigma$ to be independently distributed, a priori, with $\mu$ and $\log \sigma$ each uniformly distributed. Then it can be shown [26] that after observations, the joint posterior p.d.f. for $\mu$ and $\sigma$ is

$$p(\mu, \sigma | H_n) \propto p(\mu,\sigma)\ \ell(\mu,\sigma | H)$$

$$\propto \sigma^{-(n+1)} \exp\left\{-\frac{1}{2\sigma^2}\left[\nu S^2 + n(\mu-\hat{\mu})^2\right]\right\} \quad \ldots(3.6)$$

where $\ell(\mu,\sigma | H_n) \propto \sigma^{-n} \exp\left[-\frac{1}{2\sigma^2} \sum_{i=1}^{n} (H_i - \mu)^2\right]$

is the likelihood function

$$\nu = n-1$$

$$\hat{\mu} = \sum_{i=1}^{n} H_i / n$$

$$S^2 = \frac{1}{\nu} \sum_{i=1}^{n} (H_i - \hat{\mu})^2 \quad \ldots(3.7)$$

To find the p.d.f. of $\mu$ alone, we integrate out $\sigma$ and it can be shown that the marginal posterior p.d.f. for $\mu$ is in the form of a student t p.d.f. with mean equal to $\hat{\mu}$.

---

[1] It is a symmetrical distribution about the mean. The assumption is reasonable only for all positive value of H. For the negative H's the probability is cummulated at H=0 and H is also set to zero accordingly.

Similarly, to find the p.d.f. of $\sigma$ we integrate out $\mu$ and the resultant marginal posterior p.d.f. for $\sigma$ is in an inverted gama form with mean standard deviation:

$$\hat{\sigma} = E\,(\sigma \mid H_n) = \frac{\sqrt{\nu/2}\;\Gamma\,[(\nu-1)/2]}{\Gamma(\nu/2)} \cdot S \qquad \ldots(3.8)$$

for $\nu > 1$

where $\Gamma$ is the gamma function.

Hence, by obtaining enough observations, the probabilistic variation of significant wave height for a given predicted wave height and forecast time can be characterized. Such p.d.f.s, when discretized, will be used in calculating the p.d.f. of the state variable (time, position) and the corresponding expected value of objective function in our stochastic model.

Similar procedures can be applied when the p.d.f. of more than one parameter is required (e.g. wave height and wave direction). In this case, the p.d.f. is assumed to be a bivariate Normal distribution whose mean and covariance matrix can be calculated by the same Bayesian approach.

With the limited data available, the preliminary analysis leads us to assume the following functional form for the standard deviation of the wave height parameter:

$$\sigma = 1.0 + 0.12 * H + 0.035 * DT \qquad \ldots.(3.9)$$

For the mean error, there is not enough evidence to suggest that the error varies with the forecast time in a consistent way. However, the data shows a definite relation with the wave height parameter H (see Fig.3.2-4. A curve is therefore drawn through the data points to represent the assumed relation which is independent of DT.

Although consistent wave spectra forecasts for times beyond 72 hours are not present, it seems reasonable to extrapolate the standard deviation with eq.(3.9). An alternative method to derive the transition probabilities based on analogue forecast is presented in APPENDIX C.

## 3.3 OTHER OCEAN ENVIRONMENTAL CONDITIONS EFFECTING SHIP PERFORMANCE

### WIND

Ocean surface wind is not only the largest source of wave generation but it also directly contributes to the wind resistance of the ship's superstructure. For large tankers, such resistance can be quite substantial, and may consume a significant amount of the ship power besides the power required to overcome resistance due to wave making and skin friction. FNWC forecasts the wind speed and direction as a part of the output of the directional spectra. For periods beyond 72 hours an analogue model takes over. Fig. 3.3-1 show an example of the model output.

### OCEAN SURFACE CURRENT

The ocean surface current plays an obvious role in determining the ship's gound speed. It is generally believed that the actual ground speed is vectorially affected by the surface current.

Ocean currents are caused by the combined action of several physical environmental forces such as thermhaline, wind and

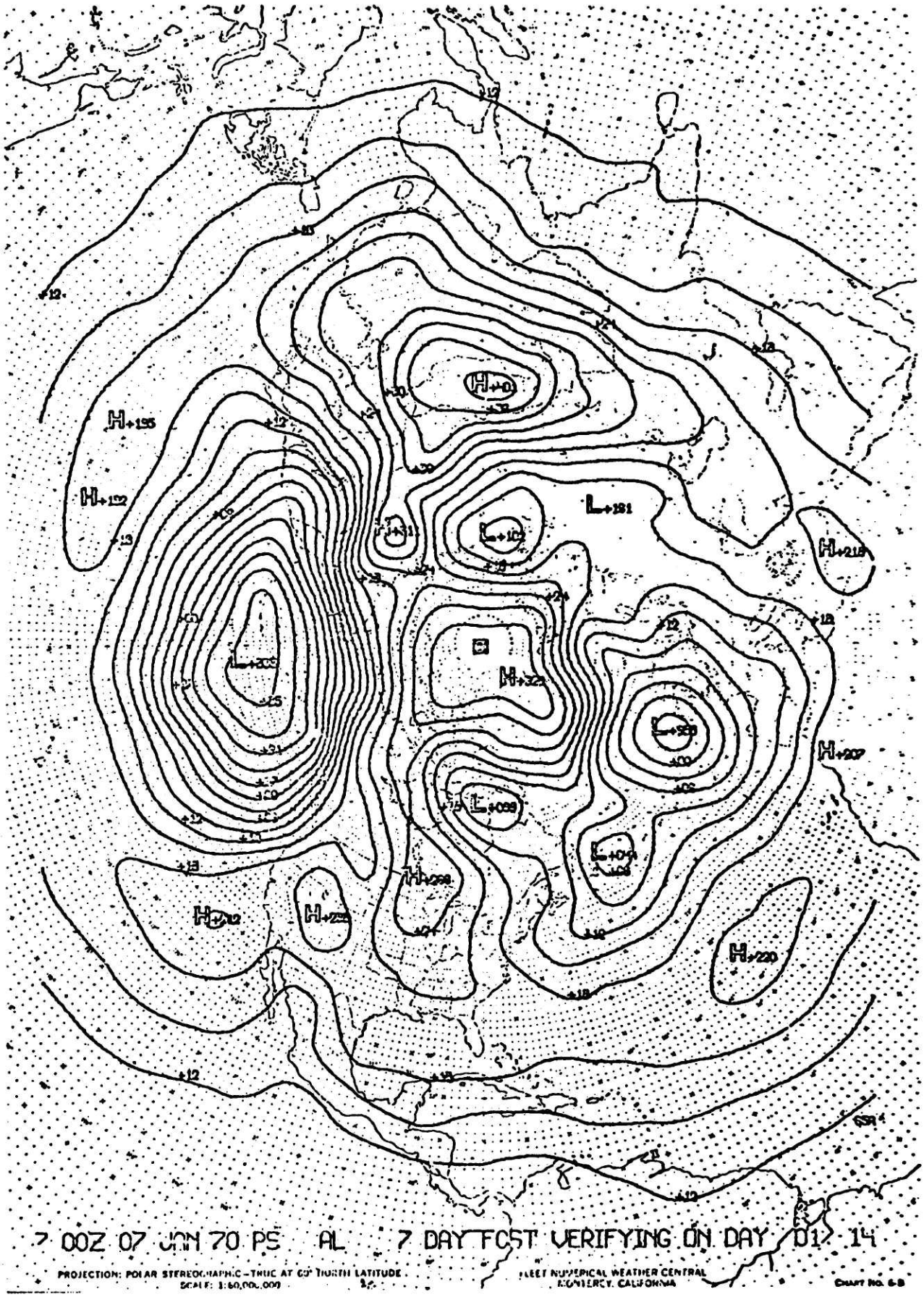


Figure 3.3-1
Surface Pressure Analog Model Seven Day Prognosis Based on the 0000Z 07 JAN 1970 Analysis and Verifying 0000Z 14 JAN 1970. Contour Interval is 3 mb.

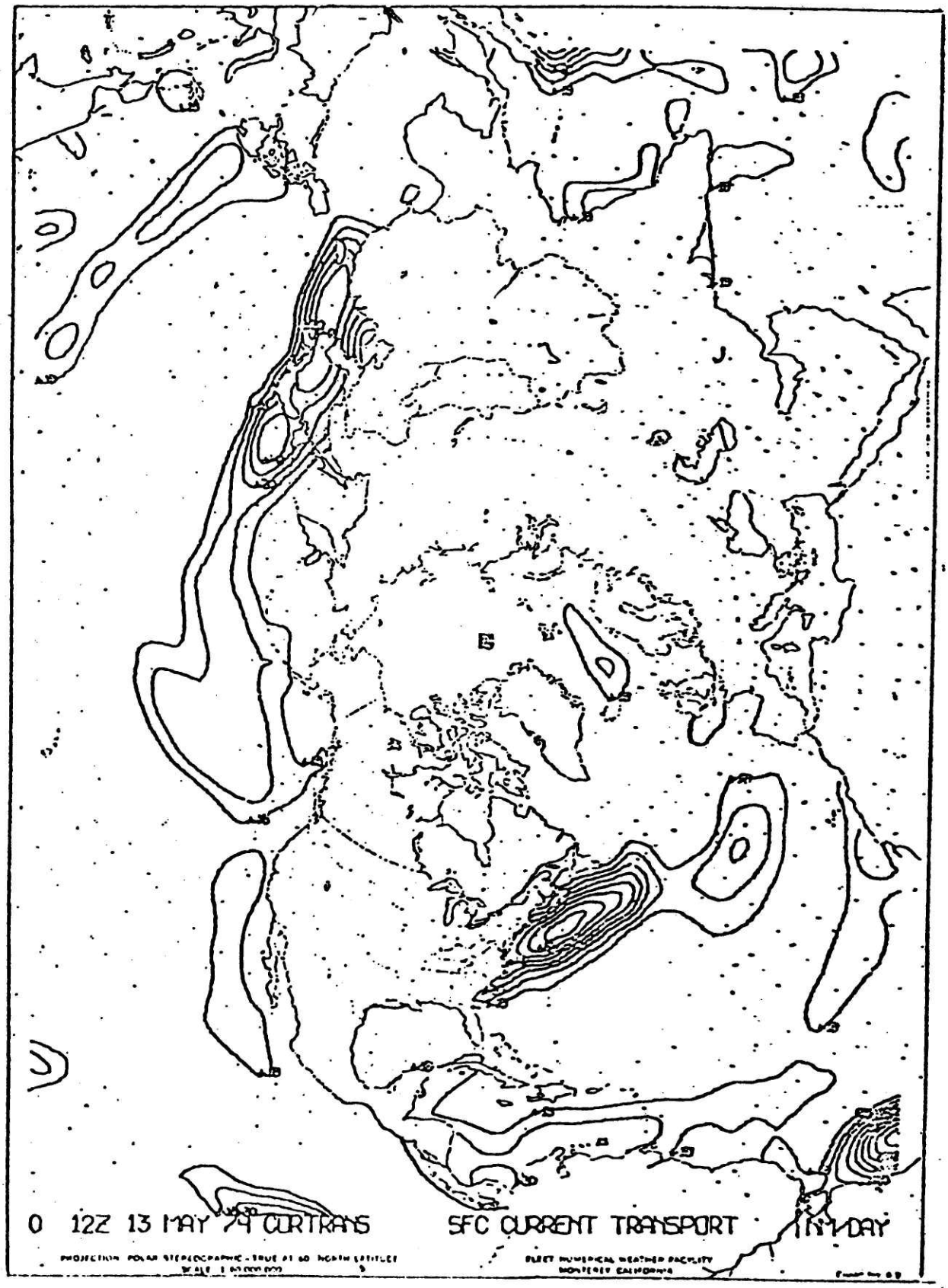


Figure 3.3-2 Ocean Current Transport 24-hr. Prog (B31) (Produced by FNWC.)

mass transport by waves, and the tidal effects are the most important. The movements of ocean current over the years as specificed by speed, direction and season at a particular location are compiled in the form of current tables[46]. A forecasting model to assist day-to-day analysis and prognosis is also available from FNWC. Fig. 3.3-2 shows an example of its product.

OTHER HAZARDS AND DANGERS

Other factors, such as fog, ice and ship wreckage, etc. which would effect the safety of a ship and force it to reduce speed can be represented in codes and specified by location.

## 3.4. A SIMPLE INTERPOLATION SCHEME

The present form of SOWM's grid system and forecasting intervals raises difficulties in providing the data fields between standard grid points as well as time increments. It seems that until a much finer grid system is incorporated into SOWM, some interpolation schemes are always required to evaluate the environmental conditions for the much finer state discriptions in our routing model.

The most sophisticated approach to interpolate the environmental data would probably be relying on a small scale theoretical model, i.e. by formulating wave growth, dissipation propagation mechanism using nearby spectra as boundary conditions, such an approach is in effect building a much larger wave model along the ship's track during the most likely voyage time. It is inevitably a very time-consuming technique, since we cannot practically use the full directional spectra in our routing algorithm, its usefulness is enhanced.

It seems numerical interpolation is more suitable for our application. The possibility of using some powerful curve or surface fitting technique such as Bi-cubic spline have been considered. These methods, while giving numerically better interpolations, often tend to be very sensitive to inputs. With our simplified parameter representation in wave condition such level of detail may not be fruitful, considering the computing efforts that are required to fit the surface.

To avoid numerical difficulties and massive computing efforts, an approximation to the surface fitting techniques is adopted so that it is at least compatible with overall sophistication of the algorithm.

Instead of using simple linear interpolation, a plane is constructed through three surrounding grid points. The interpolation through space is achieved by assuming that the required data value are on this plane which passes through three surrounding grids. For a given specific location, the required data value can be evaluated for all the standard forecast times. The interpolation over time is done by a parabolic interpolation scheme. This assumption is justified when the area under consideration is small, and the data field is varying smoothly. From general obseservation, most of the energy fields, such as mean square wave heights, is of this nature. In essence, the data field surface is approximated by many discrete small planes.

Equation of plane passing through points $(x_1,y_1,z_1)$, $(x_2,y_2,z_2)$, $(x_3,y_3,z_3)$ is given by:

$$\begin{vmatrix} y_2-y_1 & z_2-z_1 \\ y_3-y_1 & z_3-z_1 \end{vmatrix}(x-x_1)+\begin{vmatrix} z_2-z_1 & x_2-x_1 \\ z_3-z_1 & x_3-x_1 \end{vmatrix}(y-y_1)+\begin{vmatrix} x_2-x_1 & y_2-y_1 \\ x_3-x_1 & y_3-y_1 \end{vmatrix}(z-z_1) = 0$$

In our case x, y are longitude and latitudes at which a particular data is to be interpolated. A flow chart showing the proposed interpolation scheme is presented in Fig. 3.4-1.

Notice that above linear interpolation scheme may be reasonable only for data fields which are scalers e.g., mean square wave heights. For those data with a magnitude as well as directions, e.g. current, wind swell etc., a more sophisticated approach may have to be developed in the future.

In the present interpolation scheme, they are simply weighted by respective distances to the three nearby grid points.

Fig. 3.4-1 Flow Chart Showing the data summary and the interpolation procedure.

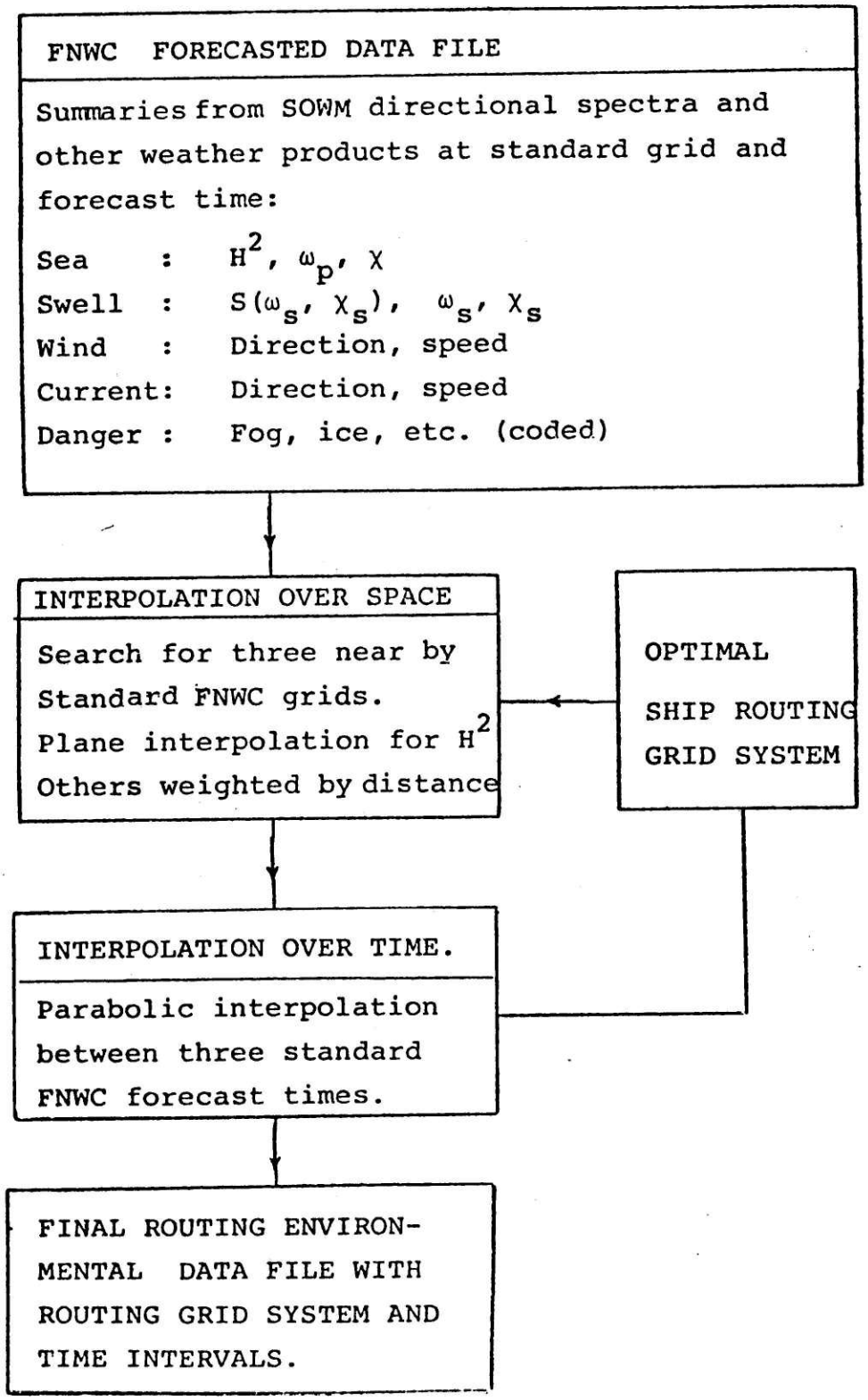

# CHAPTER 4

# SHIP SEAKEEPING SPEEDKEEPING PERFORMANCE ANALYSIS

## 4.1 SHIP'S DYNAMIC INTERACTION WITH ENVIRONMENT

The accurate prediction of seakeeping and speedkeeping performances of a routed ship under various forecasted ocean environment along the route is extremely important to the final result of our optimization. The former establishes a set of constraints in terms of ship motion, seakeeping statistics etc. which the system cannot violate; the latter concerns the ability of the ship to maintain speed in a seaway. Thus, it directly ihfluences the operating cost as well as the terminal cost of our model.

In the past, statistical curve fitting using the data from ships log books were generally used to represent the average performance of a vessel under various observed environmental conditions (e.g. James speed curves). Very often, due to the lack of accurate and complete environmental data, such curves tend to be misleading since it does not explain the causal relationship of the ship's dynamic interaction with the environment. Furthermore, the lack of proper criteria for 'voluntary speed reduction'[1] creates difficulties in establishing the maximum speed that a ship could sustain in a heavy sea.

With the present-state-of-the-art of Naval Architecture and wave analysis, it is possible to look more fundamentally at the speed-power relationship in an arbitrary seaway. In particular, with the development of the powerful ship motion seakeeping computer program [3], it is now possible to predict the ship motion in almost any seastate, thus providing an accurate and consistent input to our ship routing model.

---

[1] Because of excessive ship motion, slamming etc., the captain is forced to reduce speed for the safety of the ship and its crew, even though there is ample power to maintain a higher speed.

The ship speed, in a generalized functional form, may be expressed as:

$$V = V(\vec{D}, \vec{U}, \vec{E}, \vec{M}). \qquad .....(4.1)$$

where:

$\vec{D}$ = Vector specifying ship geometry and loading condition
$\vec{U}$ = Control vector e.g. power output, heading
$\vec{E}$ = Environmental information, e.g. parameterized sea spectra, wind, current, etc.
$\vec{M}$ = Generalized ship motion index

In this chapter, we will first outline the procedure to evaluate the ship motion seakeeping responses $\vec{M}$ of a ship under various loading condition $\vec{D}$. A proposed methodology is then presented to be used for predicting the power requirements of maintaining speed at an arbitrary sea, thus obtaining the speed function without motion constraints. Finally, a set of seakeeping statistics is introduced as system constraints to establish the maximum permissible speed without endangering the ship, cargo, and its crew. The statistics serve as routing criteria which is a function of the ship type, cargo and its mission requirements of the specific ship under consideration.

## 4.2 SHIP MOTION SEAKEEPING RESPONSE EVALUATION

### 4.2.1 SHIP RESPONSE CHARACTERISTICS EVALUATION FOR SHIP ROUTING

The evaluation of the complete dynamic characteristics of ship motion in a seaway was made possible by successful theoretical developments in the area of Naval Architecture. The theory of seakeeping and ship motion can be found in

references [47,48, 49 ]. The existing M.I.T. 5-D ship motion program can predict ship responses specified with the necessary inputs of ship geometry, weight distribution and environmental conditions in terms of ocean wave spectra. The output may be either in the form of Response Amplitude Operator for long crested waves or final motion spectra and seakeeping events for irregular short crested seas described by directional spectra or point spectra together with a spreading function.

There are perhaps several ways in which the ship responses can be numerically computed. The sophistication of the computation procedure depends upon the accuracy and resolution of the desired output information as well as the available input data.

For our routing purpose, where operating economy is an essential feature of a practical system, it is necessary to reduce the on-line computation effort for evaluation of ship responses as much as possible. To accomplish this, it is desirable to express the final seakeeping results in terms of a few environmental parameters such as the ones that have been described in the previous chapter.

Since ship routing is essentially a strategic planning tool rather than tactical decision making once it gets into a storm, some measure of average statistics and mean square values of the responses (areas underneath the response spectra) rather than the actual details of response spectra would be sufficient for the purpose. Furthermore, according to the linear ship motion seakeeping theory, the total responses due to swell and sea may be obtained by adding the separate mean square responses together.

Thus, the total mean square of the response $\sigma^2_{ii}$ under a sea-

way described by sea, $(H_{1/3}, \omega_P, \chi)$

and swell $(S(\omega_s, \chi_s), \omega_s, \chi_s)$ can be expressed as:

$$\sigma_{ii}^2 = \sigma_{swell}^2 + \sigma_{sea}^2 \qquad \ldots\ldots (4.2)$$

where $\sigma_{sea}^2$ is the mean square response obtained by using an assumed theoretical spectra with the same $H_{1/3}$ and $\omega_P$, plus a cosine spreading function about the predominant wave direction $\chi$. (Details of mathematics, see Appendix F). On the other hand, the mean square responses due to swell can be directly computed with the known Response Amplitude Operator $(RAO_{ii})$ at the same frequency of encounter.

$$\omega_e = \left| \omega_s - \frac{\omega_s^2}{g} V \cos \mu \right| \qquad \ldots\ldots (4.3)$$

Where $\mu$ is the relative angle between the ship's heading and swell direction $\chi_s$. To obtain the spectral density in the encounter frequency domain, it is necessary to multiply the corresponding values in the wave frequency domain by the Jacobian $(\partial\omega_e/\partial\omega)$.

$$S(\omega_e, \mu) = S(\omega_s, \chi_s) \cdot \frac{\partial \omega_e}{\partial \omega} \qquad \ldots\ldots (4.4)$$

Since only the mean square value is calculated, the computation is somewhat simplified because there is no longer a need for frequency mapping, and it is simply given by

$$\sigma_{swell}^2 = RAO_{ii}^2(\omega_e, \mu) \cdot S(\omega_e, \mu) \cdot \Delta\omega_e$$

$$= RAO_{ii}^2(\omega_e, \mu) \cdot S(\omega_s, \chi_s) \cdot \Delta\omega \qquad \ldots\ldots (4.5)$$

Where $\Delta\omega$ is the frequency interval in which the swell is present with mean square wave height per unit frequency equal to $S(\omega_s, \chi_s)$.

The above procedure for calculating mean square responses allows us to drastically reduce the amount of on-line computation requirements. Since the values of $\sigma^2_{sea}$ can be pre-calculated for all reasonable combinations of $H_{1/3}$, $\omega p$ and $\mu$ by using theoretical spectra and spreading function, the on-line computation for ship motion constraints would only involve some simple multiplication to calculate the value of $\sigma^2_{swell}$ if necessary and obtain the total mean square response from which other seakeeping statistics are derived.

To summarize, the complete ship motion response characteristics are computed and stored in the following from:

1. Mean square responses at several positions along the ship (e.g. bridge, cargo hold for acceleration, midship for bending moment, bow for slamming, deck wetness etc.) A computer program has been developed to take the outputs from 5-D program in terms of RAOs at several heading and speeds as input and calculate the mean square response by using two parameter spectra and a cosine square spreading function. Figures 4.2-1 shows an example of some typical mean square responses

2. RAOs at discrete heading and speed
   This would essentially be the output from 5-D program except the data may be reduced to contain only the low frequency components (swell).

Hence, during the execution of our routing algorithm, once the sea and swell information are known, the mean square

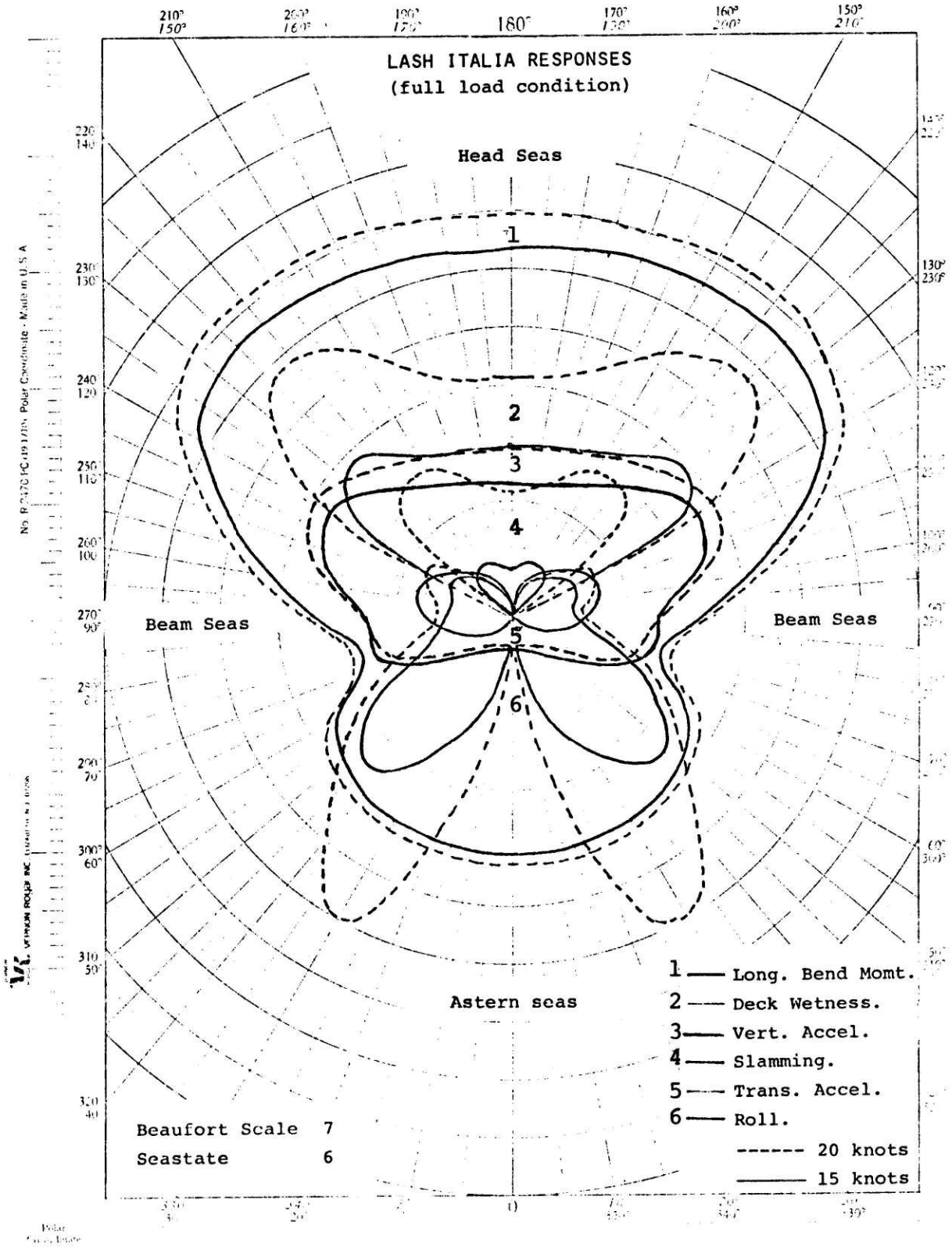


Fig. 4.2-1 An example of some typical mean responses (scales not shown) which can be used for tactical decision making by the onboard personnel.

values of various pertinent responses and other seakeeping statistics can be readily calculated and compared with the preset motion constraints to obtain the maximum ship speed without endangering the cargo, ship and its crew. The question of what constitutes the most appropriate routing criteria and the derivation of some seakeeping statistics will be discussed later in the chapter.

### 4.2.2 EFFECTS OF LOADING CONDITIONS ON MOTION RESPONSES

The U.S. Merchant Marine today consists of a wider variety of ship types then ever before. From the point of view of computing motion responses for our model inputs, it is most important to consider the effect of loading condition on the responses of each type of vessel which inevitably has its own operating requirements.

There are generally six major types of vessels currently under U.S. flag.

1. Tankers have essentially two loading conditions, full and ballasted. As a result, two sets of ship motion response characteristics must be calculated for the two fixed standard loading conditions.

2. Dry bulk carriers like tankers have essentially two loading conditions, full and ballasted. For OBO's and other similar combined carriers, we may need three different conditions, one for each of two alternative cargoes and one for ballasted.

3. General cargo ships loading conditions vary about many standard loading conditions. As a result of this and changes in cargo distribution, there are many combinations of metacentric height GM, longitudinal center of gravity LCG. longitudinal radius of gyration about LCG., longitudinal center of floatation LCF etc. Thus sensitivity must be performed to investigate the changes of these variables around perhaps three to four loading conditions.

4. Container vessels usually carry appreciable deck cargo. The variations of loading conditions can usually be defined by a few loading standards because these volume intensive vessels are generally ballasted to obtain a certain desirable GM independent of the loading. To obtain standard loading conditions, average inbound and outbound loading plans can be used.

5. Barge carriers like containerships usually carry appreciable deck cargo. Although operators attempt to maintain GM within certain small limits, this is seldom possible because of the large percentage of pseudo-bulk high density cargo carried by barge carriers on many routes. As a result, loading conditions vary about several standard loading conditions. Review of actual barge carrier operating conditions indicate that three to four standard conditions will probably suffice.

6. Roll-on/Roll-off carriers even more than containerships are highly volume intensive. As a result and because of the nature of their cargo, Ro-Ro vessel loading conditions always aim at a very close range of GM and other loading condition variables.

Due to the inevitable variations in ship's departure condition from the few calculated ones, ship responses must be modified due to small changes in $K_{yy}$, LCB, LCF, GM etc. For each specific ship, sensitivity study must also be included in characterizing the ship responses by varying the inputs to 5-D ship motion program. Figures 4.2-2 derived from Ref. [50] shows the effect of changes in $K_{yy}$ on ship responses. Figure 4.2-3,4,5 from [50] also shows the variations of LCB, LCB-LCF separations on response characteristics for some standard series type ships.

Hence, the complete ship responses data file may consist of the pertinent ship motion, seakeeping statistics for several standard loading conditions. The results from the sensitivity study can either be plotted or kept in file for modifying the actual response according to the exact loading condition at departure.

## 4.3 SHIP SPEEDKEEPING PERFORMANCE MODEL

### 4.3.1 SHIP SPEED-POWER RELATIONSHIP IN CALM WATER

Recall the generalized speed function in equation (4.1). In the absence of waves and other environmental distrubances, (i.e. the random vector $\vec{E}$ becomes deterministic with its elements all equal to zero), ship speed is simply a function of its geometry and power output.

Generally speaking, the present state-of-the-art in Naval Architecture enables us to estimate fairly accurately the required horsepower for various speeds in calm water. By converting the required effective horsepower (EHP) into shaft horsepower (SHP) with a set of known hull, propeller, relative

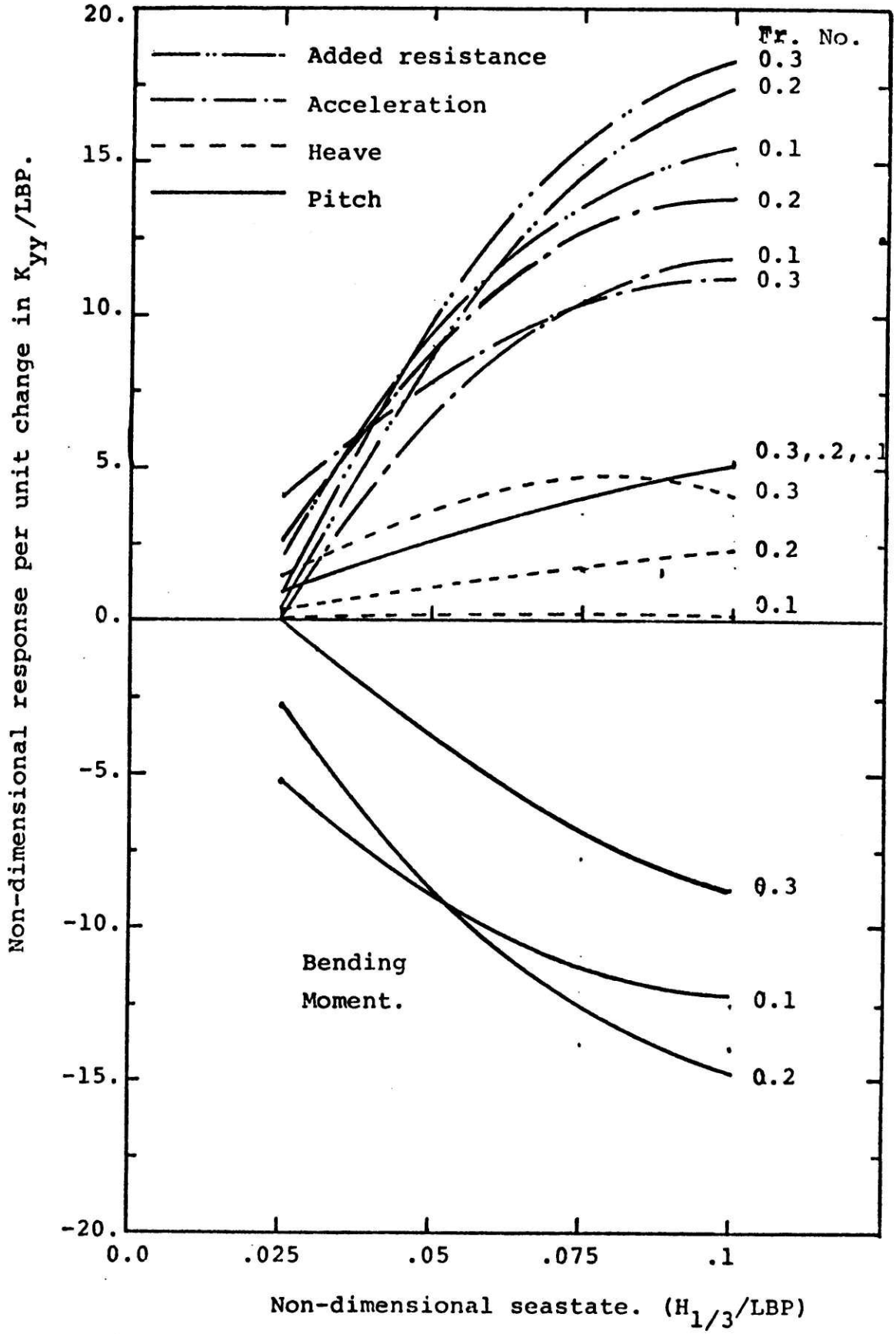


Figure 4.2-2 Effect of changes in longitudinal radius of gyration on ship responses. [50]

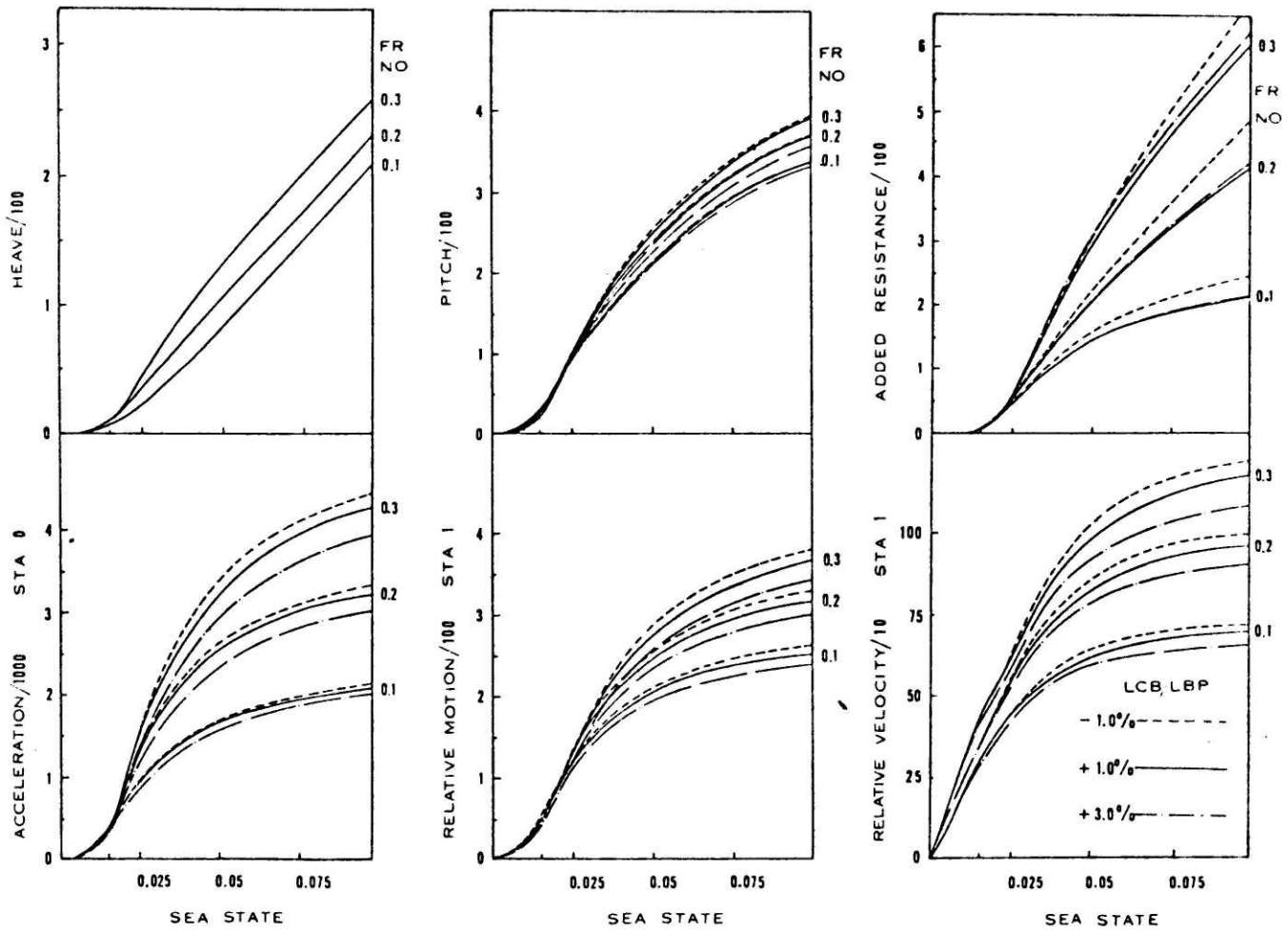


FIGURE 4.2-3 VARIATION OF LCB ON RESPONSE CHARACTERISTICS FOR SHIPS WITH CB = 0.7, L/B = 7.0, B/T = 3.0 [50]

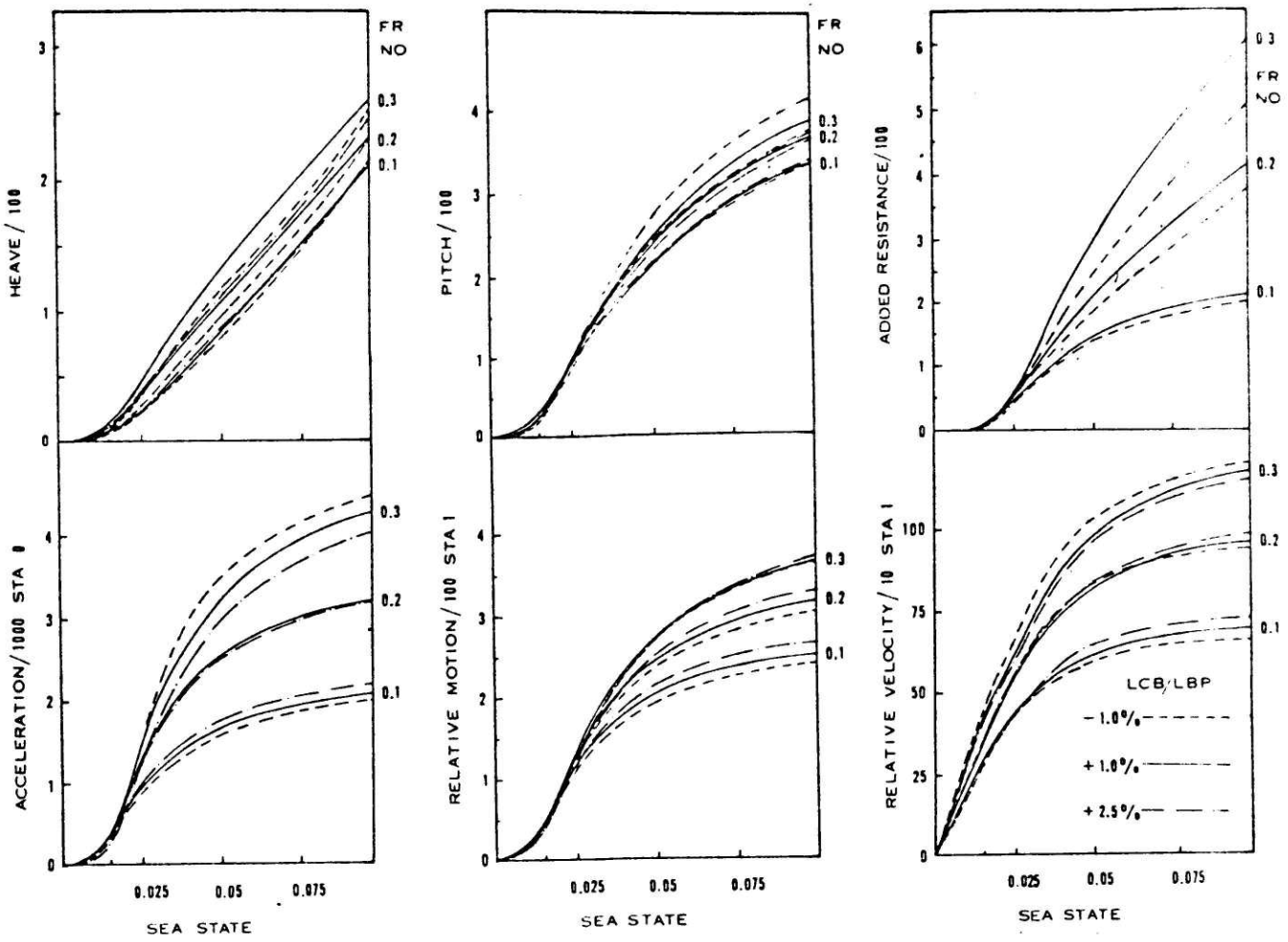


Fig. 4.2-4 Variation of LCB-LCF Separation on Response Characteristics for Ship with CB= 0.7 L/13= 7.0, B/T= 3.0 [50]

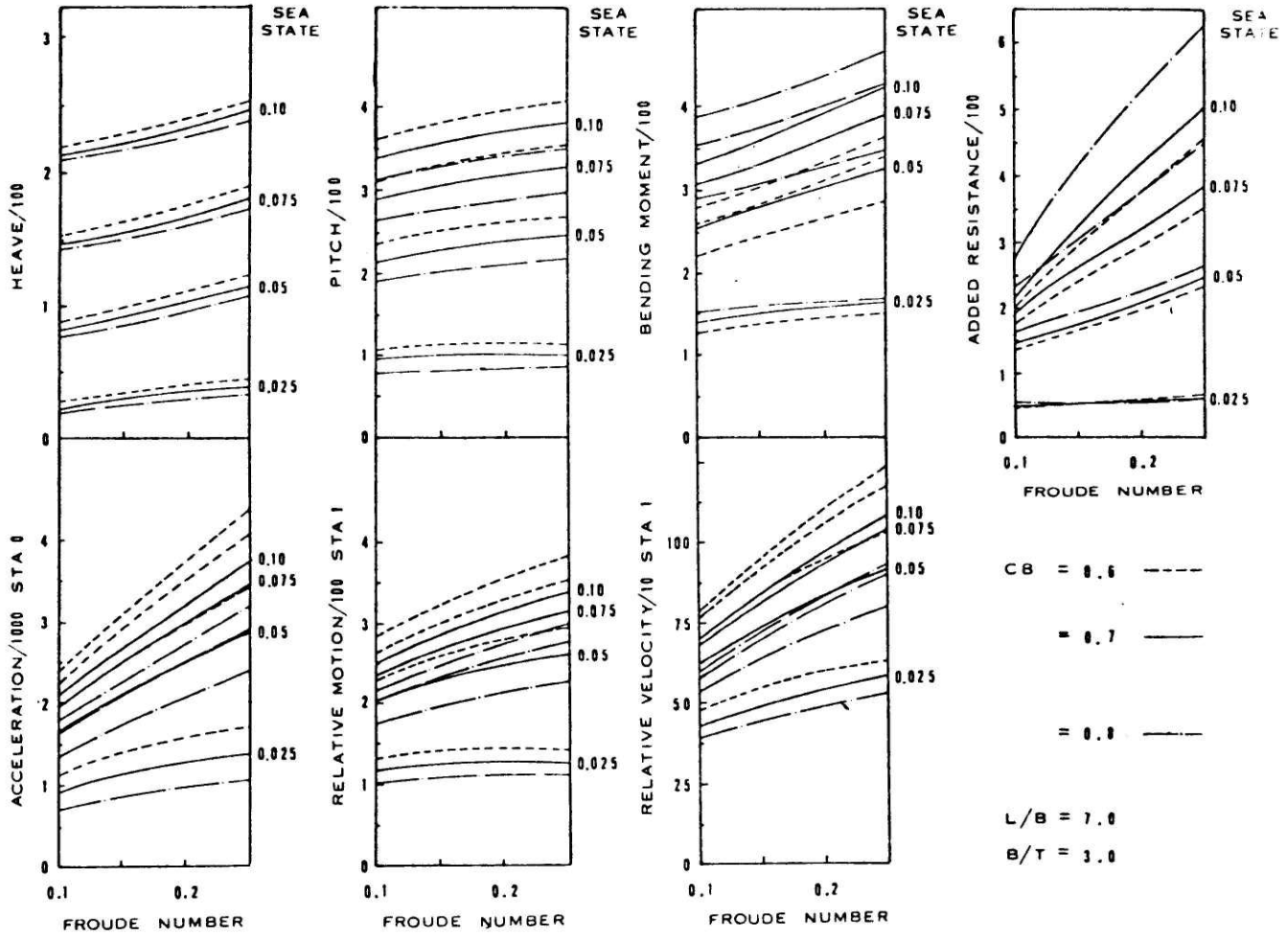


Fig. 4.2-5 Variance of CB on Response Characteristics for Ship with L/B= 7.0 and B/T = 3.0

rotative and shaft transmission efficiencies, the speed function may be derived numerically by equating the available SHP to required SHP.

The effective horsepower required by a ship operating in calm water to maintain at a speed is the result of two sources of resistance:

1. Calm Water Resistance (EHP Calm)

For a first order approximation, the bare hull calm water resistance at various speeds of a given ship geometry and load condition can be computed from the standard hull form series, e.g., [51,52]. The estimate is then augmented about 3% to account for the presence of appendages (single screw - twin screw and side thruster equipped vessels have a larger percentage appendage drag) and so on. Usually, more accurate estimates are carried out by a model test in a towing tank. Figure 4.3.-1 shows a typical plot of the bare hull resistance as a function of ship speed derived from model tests.

2. Resistance Due to Hull Fouling (EHP Foul)

To account for yearly increase[1] in hull fouling which induces additional resistance, the extra EHP required may be estimated by the following expression as suggested by [55].

$$EHP_{foul} = \frac{0.00015 \cdot \rho \cdot v^3 \cdot (1.6889)^3 \cdot \text{Wetted Surface Area}}{2 \cdot 550} \quad \ldots(4.6)$$

where

V = ship's speed in knots

$\rho$ = sea water density in slugs/ft$^3$

[1] It is assumed that the ship is drydocked every year

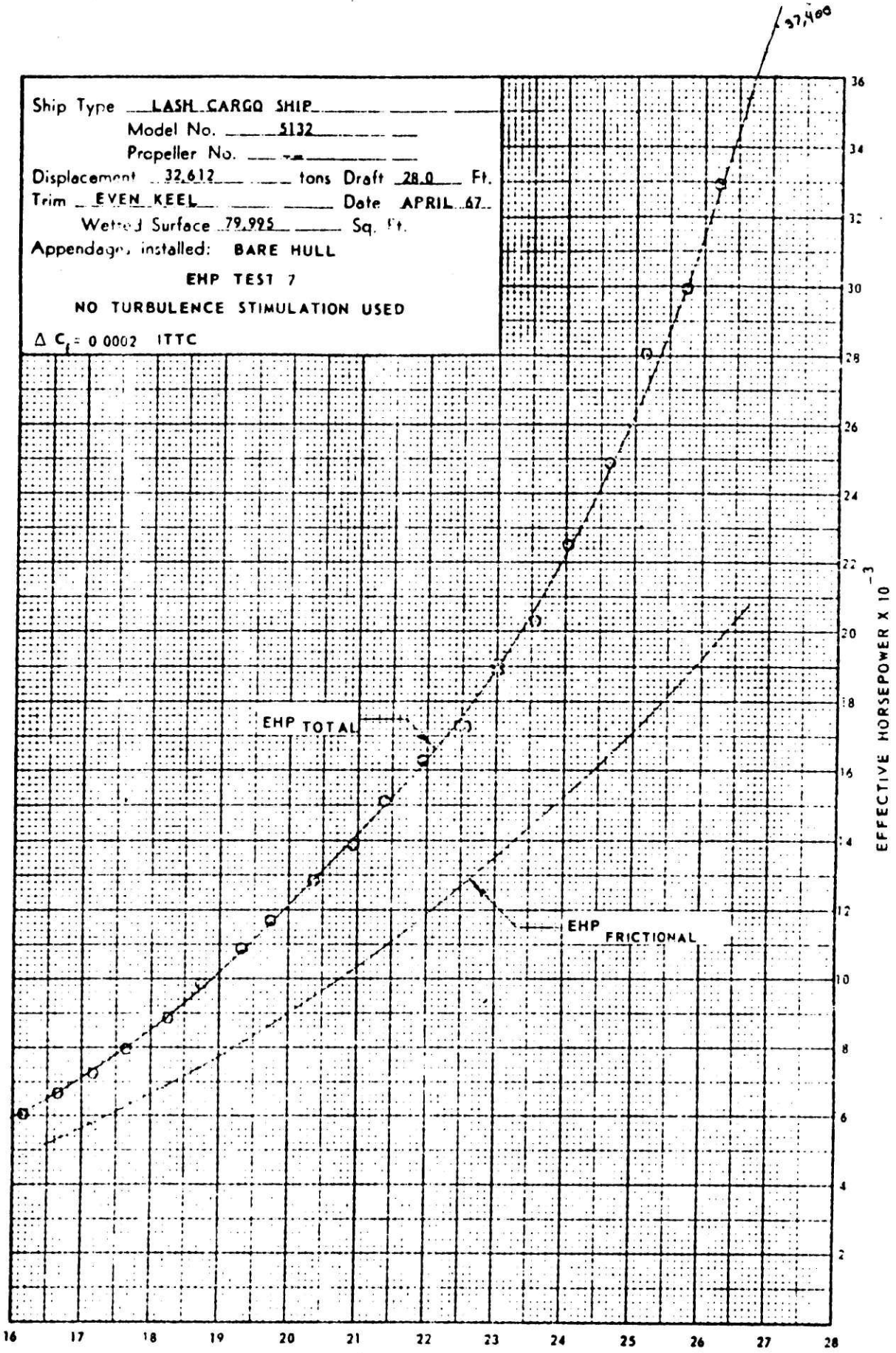


FIGURE 4.3-1 POWER-SPEED RELATIONSHIP OF LASH SHIP OBTAINED FROM MODEL TEST IN CALM WATER [53].

The total required EHP without any environmental excitation is given by the sum of the above components.

$$EHP_{total} = EHP_{calm} + EHP_{foul}$$

To convert from EHP to Brake Horsepower or Indicated Shaft Horsepower (SHP), the notion of propulsive efficiency is used.

$$SHP = EHP/\eta_p \qquad \ldots(4.7)$$

The methods of estimating above efficiency components have been well established for calm water conditions. Experimentally, the coefficients can be obtained by model tests in a simulated environment.

It is now possible, by an iterative procedure of equating the required SHP with ship's power output, to derive the speed function of the form

$$V = V\ (SHP\ ;\ \text{given}\ \vec{D}).$$

Alternatively, the power-speed relationship can be more accurately determined from extensive model tests or directly from the ship's trial record. In this way, the augmentation due to appendages, surface roughness, etc. are automatically included. Figure 4.3-2,3 show a set of typical power-speed relationships obtained from model tests.

### 4.3.2 POWERING OF SHIPS IN ROUGH SEAS

In this section, an attempt is made to look at the fundamental relationships of ship speed-power in waves and review some available methodology for estimating the added resistance and propulsive characteristics of ship in seaways.

FIGURE 4.3-2 POWERING CHARACTERISTICS OF LASH SHIP IN CALM WATER FULL LOAD [54]

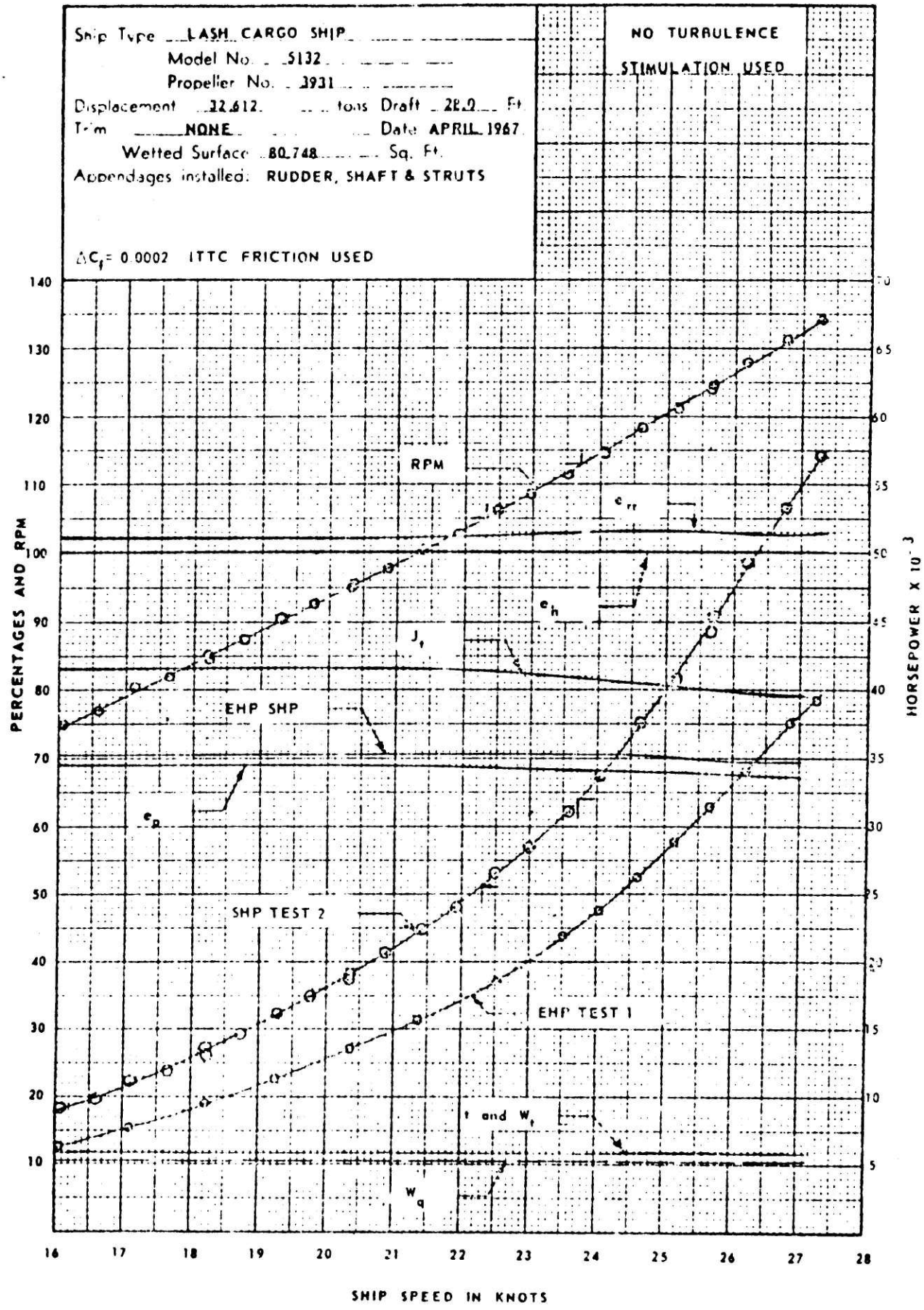

FIGURE 4.3-3 POWERING CHARACTERISTICS OF LASH SHIPS IN CALM WATER HALF LOAD [54]

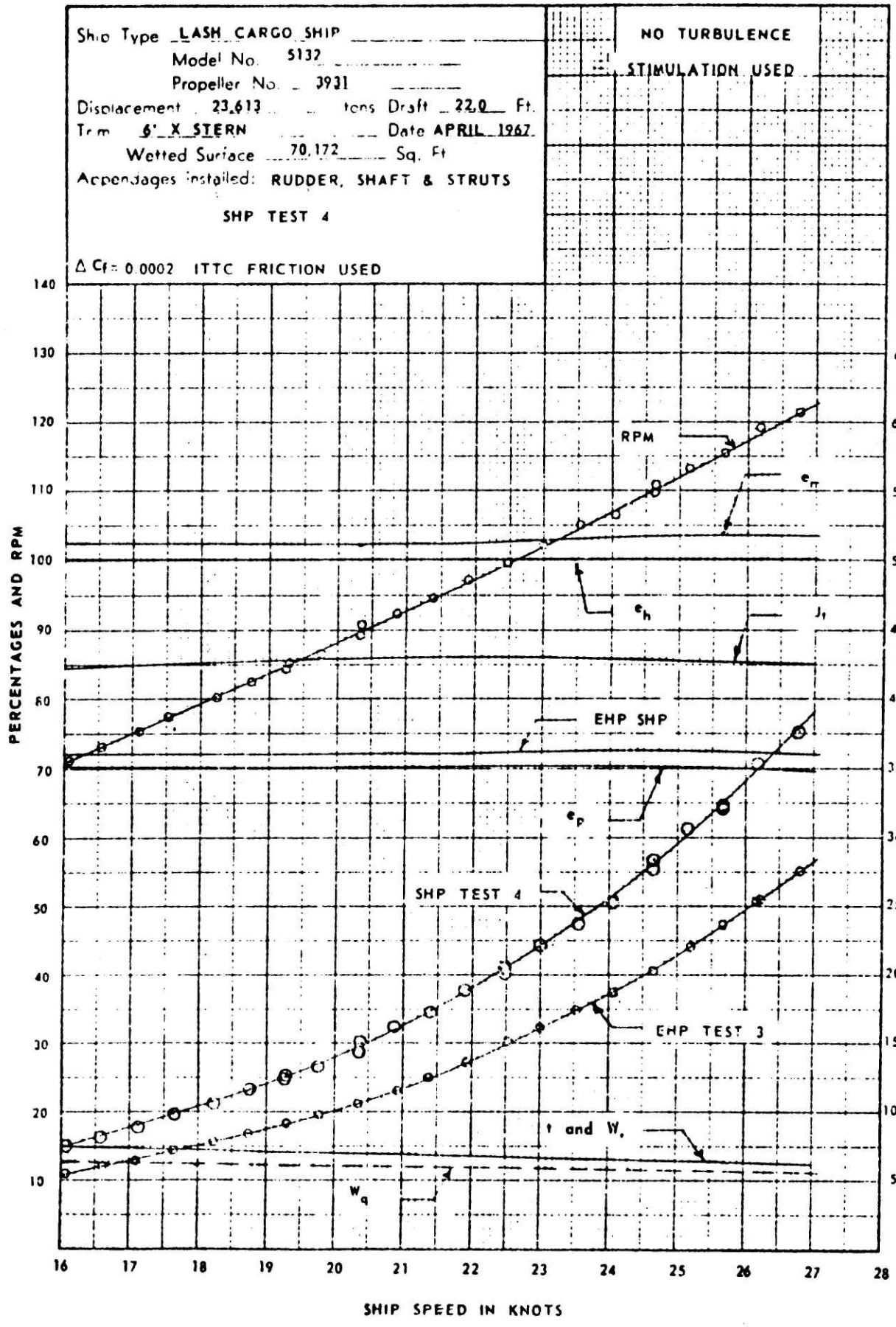

So far, we have only considered the calm water power-speed relationship. Let us now consider the effect of waves on a ship's power requirement to maintain speed. The poundering of waves upon a ship at sea results in two major consequences on a ship's speedkeeping performances.

## 1. Added Resistance in Waves

The theoretical development in the area of wave induced resistance in a seaway has been a major challenge to ship hydrodynamists during the past two decades. In many aspects, this is still an unresolved problem. Various theories [56,57,58,59] developed for regular and irregular head seas have been quite satisfactory insofar as comparing with the results obtained from model experiments.

The theories are mainly based on the principle of linear superposition and assumed that the major contribution to added resistance is from ship's heave and pitch motion, while the lateral ship motion has negligible effects. The experimental data confirmed this linearity and showed that the wave induced resistance is in general proportional to the square of the wave amplitude as predicted by the theory. Ref. [59]. For the case of oblique seas, the problem is much more difficult. Several recent attempts [60,61,62] to formulate the second order steady-state force and moments on a ship moving in an oblique seaway has met various degree of success with limited experimental data [63]. It is conceivable, however, that the problem will be solved in the near future.

Meanwhile, we have to rely on systematic model tests [64,65,59] and ships' log data. The most extensive tests on resistance augmentation in regular and irregular

waves coming from ahead have been carried out for some series 60 hull forms [65]. The added resistance in waves is generally expressed as:

$$R_{wave} = C_w + 1/2\ \rho g V^n$$

where $C_w$, n are coefficients and their values depend on hull geometry and wave characteristics.

2. Variation in Propulsive Efficiencies Due to the Unsteady Flow Field Around the Propelller

This is the second major consequence of wave action upon ship systems. This variation (in most cases, a degradation[1]) results from two concurrent causes:

a. The motion of ship and orbital velocity components of waves create unsteady flow fields in the vicinity of the propeller. The presence of cyclic wake changes propeller operating condition and results in periodic fluctuations of the instantaneous thrust and torque values which consequently lead to the change in propeller RPM and actual operating efficiency.

b. Complex velocity field disturbances caused by combined hull motions in wave changes the value of thrust deduction fraction. Together with the variation in wake fraction, they result in variations of hull efficiency from calm water conditions.

The decrease in propulsive efficiency due to these two phenomena are usually treated independently. By considering the ship motion as a quasi-stationary process Ref. [66] outlines a procedure to compute the changes in propeller efficiency due to heave and pitch motion of the ship.

[1] Traditionally, the design of ship propulsive system is aimed at near optimum for calm water condition and then added 25% more power as service margin to account for rough sea conditions.

Insofar as the effect of the ship motion on thrust deduction fraction t, is concerned, this has not been extensively investigated. It seems from [67] that the value of t is sensitive to configuration of ship appendages in self-propelled model tests. Thus, it is plausible to assume the value in calm water also holds in a seaway. As a result, the variation in hull efficiency can be found directly for a given seastate.

The last, but not the least, term of efficiency is the relative rotative efficiency. This is the residual term that serves to provide the correlation between a propeller's performance in open water and its performance behind a ship. In the absence of any data, it may be assumed that the relative efficiency is independent of seastate. The assumption may also hold for the transmission efficiency $\eta_M$.

Once the efficiencies are computed, the propulsive efficiency of the ship at a given seastate can be determined:

$$\eta_p = \eta_o' \ \eta_H' \ \eta_R \ \eta_M \qquad \ldots(4.8)$$

$$\eta_H' = (1-t)/(1-w) \qquad \ldots(4.9)$$

$w$ = Taylor wake fraction computed for a given seastate

$\eta_o'$ = open water propeller efficiency modified to account for the effect of ships motions.

$\eta_R$ = relative rotative efficiency ([55] suggests a value of 1.026)

$\eta_M$ = shaft transmission efficiency ([55] suggests a value of 0.98 for machinery aft).

To compute the required shaft horsepower to maintain speed in a given seaway, we have by defintiion:

$$SHP_{required} = EHP_{total} / \eta_p \qquad \ldots\ldots(4.10)$$

where EHP is the total effective horsepower required and consists of the following components:

$$EHP_{total} = EHP_{calm} + EHP_{foul} + EHP_{wave} + EHP_{wind} \quad \ldots(4.11)$$

The effective horsepower required to overcome the mean added resistance in waves which can be either computed using the appropriate seakeeping Tables from Ref. [50], or directly from the estimated mean added resistance.

The added resistance due to wind may be expressed in terms of ships drag coefficient and the resultant wind intensity $V_R$:

$$R_{wind} = [C_d A]_\alpha 1/2\ \rho_a V^2_R \quad \ldots(4.12)$$

where

$\rho_a$ = mass density of air

$V_R$ = resultant wind velocity and ship velocity by vector addition

$[C_d A]_\alpha$ = product of the drag coefficient by the frontal area of the ship exposed to the wind when the the resultant direction of the latter makes the angle $\alpha$ with ship's course.

The value can be approximated by

$$[C_d A]_\alpha = [C_x A_T] * \cos^2\alpha + [C_y A_L] * \sin^2\alpha \quad \ldots(4.13)$$

where $C_x$, $C_y$ are the drag coefficients in head and beam wind directions respectively. In the absence of actual data for the ship, the values of $C_x$ and $C_y$ have been estimated by using the multiple regression model [68] and Tables 4.3-4,5show a summary of the regression equations and their associated coefficients.

## TABLE 4.3-4 LATERAL COMPONENT OF WIND FORCE [68]

$$C_Y = B_0 + B_1 \frac{2A_L}{L_{OA}^2} + B_2 \frac{2A_T}{B^2} + B_3 \frac{L_{OA}}{B} + B_4 \frac{S}{L_{OA}} + B_5 \frac{C}{L_{OA}} + B_6 \frac{A_{SS}}{A_L} \pm 1.96 \text{ S.E.}$$

| $\gamma_R^\circ$ | $B_0$ | $B_1$ | $B_2$ | $B_3$ | $B_4$ | $B_5$ | $B_6$ | S.E. |
|---|---|---|---|---|---|---|---|---|
| 10 | 0·096 | 0·22 | – | – | – | – | – | 0·015 |
| 20 | 0·176 | 0·71 | – | – | – | – | – | 0·023 |
| 30 | 0·225 | 1·38 | – | 0·023 | – | –0·29 | – | 0·030 |
| 40 | 0·329 | 1·82 | – | 0·043 | – | –0·59 | – | 0·054 |
| 50 | 1·164 | 1·26 | 0·121 | – | –0·242 | –0·95 | – | 0·055 |
| 60 | 1·163 | 0·96 | 0·101 | – | –0·177 | –0·88 | – | 0·049 |
| 70 | 0·916 | 0·53 | 0·069 | – | – | –0·65 | – | 0·047 |
| 80 | 0·844 | 0·55 | 0·082 | – | – | –0·54 | – | 0·046 |
| 90 | 0·889 | – | 0·138 | – | – | –0·66 | – | 0·051 |
| 100 | 0·799 | – | 0·155 | – | – | –0·55 | – | 0·050 |
| 110 | 0·797 | – | 0·151 | – | – | –0·55 | – | 0·049 |
| 120 | 0·996 | – | 0·184 | – | –0·212 | –0·66 | 0·34 | 0·047 |
| 130 | 1·014 | – | 0·191 | – | –0·280 | –0·69 | 0·44 | 0·051 |
| 140 | 0·784 | – | 0·166 | – | –0·209 | –0·53 | 0·38 | 0·060 |
| 150 | 0·536 | – | 0·176 | –0·029 | –0·163 | – | 0·27 | 0·055 |
| 160 | 0·251 | – | 0·106 | –0·022 | – | – | – | 0·036 |
| 170 | 0·125 | – | 0·046 | –0·012 | – | – | – | 0·022 |
| | | | | | | Mean Standard Error | | 0·044 |

$L_{OA}$ = length overall

B = beam

$A_L$ = lateral projected area

$A_T$ = transverse projected area

$A_{SS}$ = lateral projected area of superstructure

S = length of perimeter of lateral projection of model excluding waterline and slender bodies such as masts and ventilators

C = distance from bow of centroid of lateral projected area

M = number of distinct groups of masts or kingposts seen in lateral projection; kingposts close against the bridge front are not included.

## TABLE 4.3-5

## FORE & AFT COMPONENT OF WIND FORCE [68]

$$C_X = A_0 + A_1 \frac{2A_L}{L_{OA}^2} + A_2 \frac{2A_T}{B^2} + A_3 \frac{L_{OA}}{B} + A_4 \frac{S}{L_{OA}} + A_5 \frac{C}{L_{OA}} + A_6 M \pm 1{\cdot}96 \text{ S.E.}$$

| $\gamma_R^\circ$ | $A_0$ | $A_1$ | $A_2$ | $A_3$ | $A_4$ | $A_5$ | $A_6$ | S.E. |
|---|---|---|---|---|---|---|---|---|
| 0 | 2·152 | −5·00 | 0·243 | −0·164 | – | – | – | 0·086 |
| 10 | 1·714 | −3·33 | 0·145 | −0·121 | – | – | – | 0·104 |
| 20 | 1·818 | −3·97 | 0·211 | −0·143 | – | – | 0·033 | 0·096 |
| 30 | 1·965 | −4·81 | 0·243 | −0·154 | – | – | 0·041 | 0·117 |
| 40 | 2·333 | −5·99 | 0·247 | −0·190 | – | – | 0·042 | 0·115 |
| 50 | 1·726 | −6·54 | 0·189 | −0·173 | 0·348 | – | 0·048 | 0·109 |
| 60 | 0·913 | −4·68 | – | −0·104 | 0·482 | – | 0·052 | 0·082 |
| 70 | 0·457 | −2·88 | – | −0·068 | 0·346 | – | 0·043 | 0·077 |
| 80 | 0·341 | −0·91 | – | −0·031 | – | – | 0·032 | 0·090 |
| 90 | 0·355 | – | – | – | −0·247 | – | 0·018 | 0·094 |
| 100 | 0·601 | – | – | – | −0·372 | – | −0·020 | 0·096 |
| 110 | 0·651 | 1·29 | – | – | −0·582 | – | −0·031 | 0·090 |
| 120 | 0·564 | 2·54 | – | – | −0·748 | – | −0·024 | 0·100 |
| 130 | −0·142 | 3·58 | – | 0·047 | −0·700 | – | −0·028 | 0·105 |
| 140 | −0·677 | 3·64 | – | 0·069 | −0·529 | – | −0·032 | 0·123 |
| 150 | −0·723 | 3·14 | – | 0·064 | −0·475 | – | −0·032 | 0·128 |
| 160 | −2·148 | 2·56 | – | 0·081 | – | 1·27 | −0·027 | 0·123 |
| 170 | −2·707 | 3·97 | −0·175 | 0·126 | – | 1·81 | – | 0·115 |
| 180 | −2·529 | 3·76 | −0·174 | 0·128 | – | 1·55 | – | 0·112 |
| | | | | | | | Mean Standard Error | 0·103 |

### 4.3.3. SHIP SPEED AS A FUNCTION OF ENVIRONMENTAL PARAMETERS

From the above calculations of ship power requirements in waves, it is possible to establish the functional relationship between ship speed and specific environmental parameters. By a similar procedure of equating the available power output and the required SHP to maintain certain speed, the complete ship speed function can be expressed as follows:

$$V = V(SHP, \mu, H^2, T) \qquad .....(4.15)$$

where $\mu$ = wave to ship track angle

$H^2$ = mean square wave height of the seaway

T = predominant wave period

From the ship's log record actual speed versus wave height can be used to check the accuracy of the calculated speed function. Some statistical inferences should also be applied to estimate more realistic ship speed in waves.

For the purpose of the research project, an empirical approach to model the ship speed in a seaway was adopted in our preliminary routing model. Figure 4.3-6 shows some simple speed curves for various power setting and headings at various sea severities characterized by significant wave heights. The simplification was partly because our aim was to develop a ship routing model not a ship design methodology, and partly due to the unavailability of widely accepted tools for estimating the ship powering requirements in severe seaways.

Fig. 4.3-6 An example of ship speed function for various power output, heading under different sea conditions.

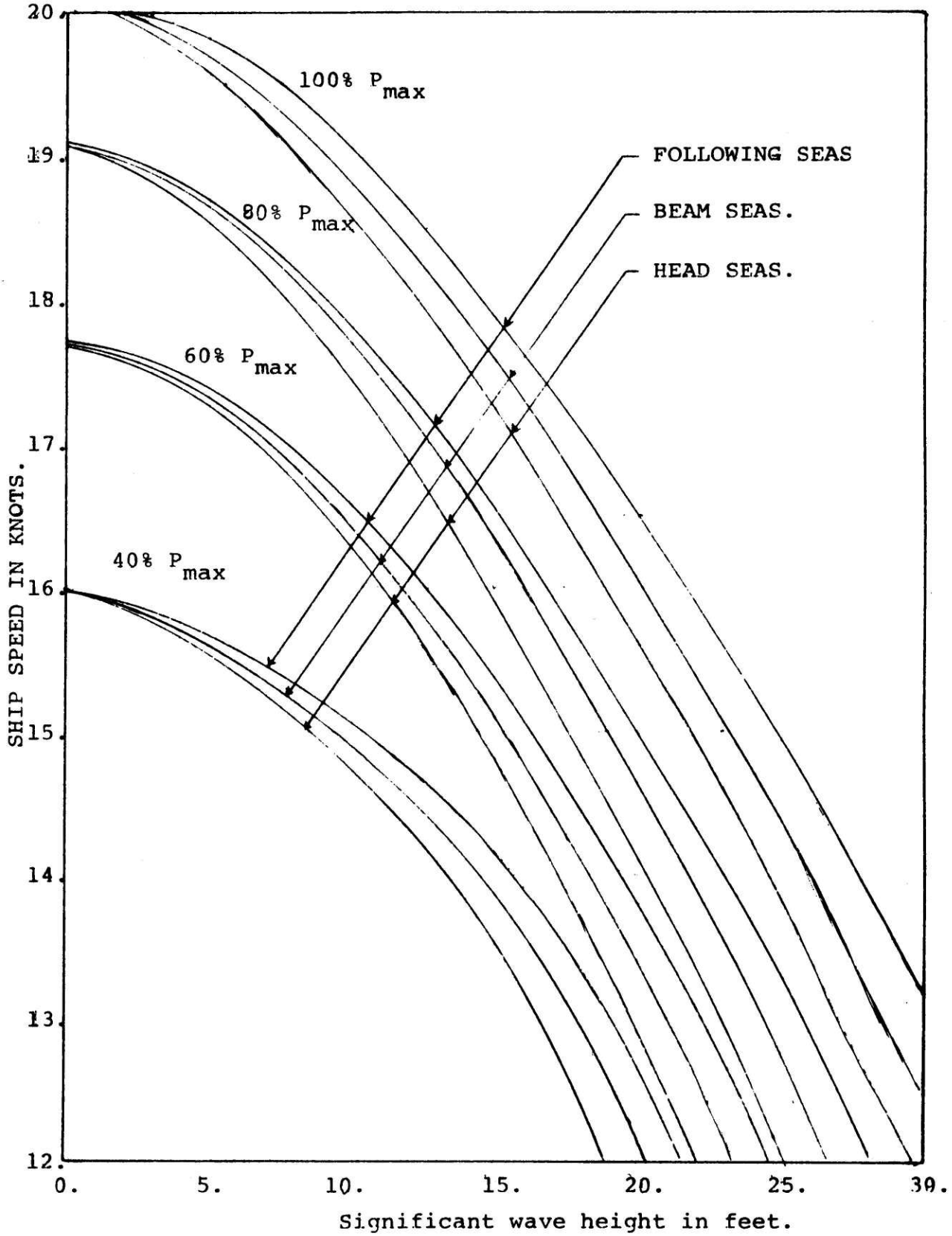

It must be realized, however, that while such statistical curve fitting through the recorded wave height speed and power output from the past voyages may serve the purpose of testing the algorithm, further developments in this area will invariably increase the accuracy of the results.

## 4.4 SHIP ROUTING CRITERIA

During the past decade, the application of ship motion seakeeping theory has been largely made use of in establishing proper ship design criteria. Most seakeeping literature deals exclusively with the extremal value statistics of the ship responses during its lifetime. Little or no attention has been paid in establishing a set of sound operational criteria from a ship operator's point of view.

Various empirical operating criteria have been suggested in the past [69,70,71]. Table 4.4-1 summarizes some of the recommended seakeeping criteria for commercial operation. These criteria are derived from extensive operating experiences of actual ship trials. However, while they serve as an excellent bounds of the most "safe and efficient operating region" for similar ship types and loading conditions, they cannot in general realistically be applied to other situations when the design, loading and cargo conditions are significantly different. In order to establish some causal relationship between operational criteria and human responses, cargo or structural damages, we will look at some major issues of ship motion and seakeeping events that are most concerned by ship operators.

Table 4.4-1

RECOMMENDED SEAKEEPING CRITERIA FOR COMMERCIAL OPERATION

| Response | Recommended Criteria | |
|---|---|---|
| | Aertssen [69] | Hoffman [70] |
| Slamming rate and midship whipping stress | 6/100 pitches<br>2.9 kpsi | 1 in 15 min. > 3.5 kpsi<br>2 in 15 min. > 2.25 kpsi<br>Lower threshold 1.75 kpsi |
| Vertical bow accel. | .5g | .5g max. or .15g rms |
| Lateral acceleration | --- | .5g max. or 15g rms |
| Bow submergence rate | 5/100 | ------- |
| Bow Impact (just below deck) | --- | 15 occ. in 15 min.<br>Max. > 3.5 kpsi<br>Lower threshold 1.5 kpsi |

| | Chryssostomidis [71] |
|---|---|
| Vertical Acceleration at bridge | < 0.125g R.M.S. |
| Vertical acceleration anywhere along the ship's length | 1/10 highest values < 1.0 g<br>$H^{1}/_{10} = 1.80\sqrt{8\ mo\ (1-\varepsilon^2/2)}$<br>$\sqrt{mo} \leq 0.217$ , $\varepsilon$ = broadness factor |
| Probability of deck wetness | < 0.01 |
| Probability of slamming | < 0.01 |

1. Acceleration & Roll

Acceleration, both linear and angular, are major concerns to the onboard safety of the crew as well as cargo carried. The former leads to motion sickness and direct damage to cargo. Whereas the latter influences the task performance efficiency of the crew.

Much of the research that has been conducted is in the field of human factor research for aircraft and space vehicle pilots. Current efforts for the Navy are also reported [ 72] in developing some motion sickness indices for use in studies about crew effectiveness due to both linear and angular acceleration. Figure 4.4-1 shows an example of human tolerance to oscillations.

Roll response of a ship in a seaway may be vastly different depending on its speed and course. It is generally a finely tuned response and also very critical to the capability of the ship as its crew meet the performance requirements. From the point of view of crew-working efficiency, excessive roll will degrade the motor capability of operating personnel and results in a reduced rate of effciency. Figure 4.4-2 shows the effect of roll on personnel capabilities.

As far as the cargo damage is concerned, it depends on its form, type of packaging and the storage location onboard. Some general upper limits of shipboard acceleration that various cargo types may be subjected to under normal operating conditions must be developed in the future.

2. Deck Wetness

The problem of deck wetness concerns a ship operator

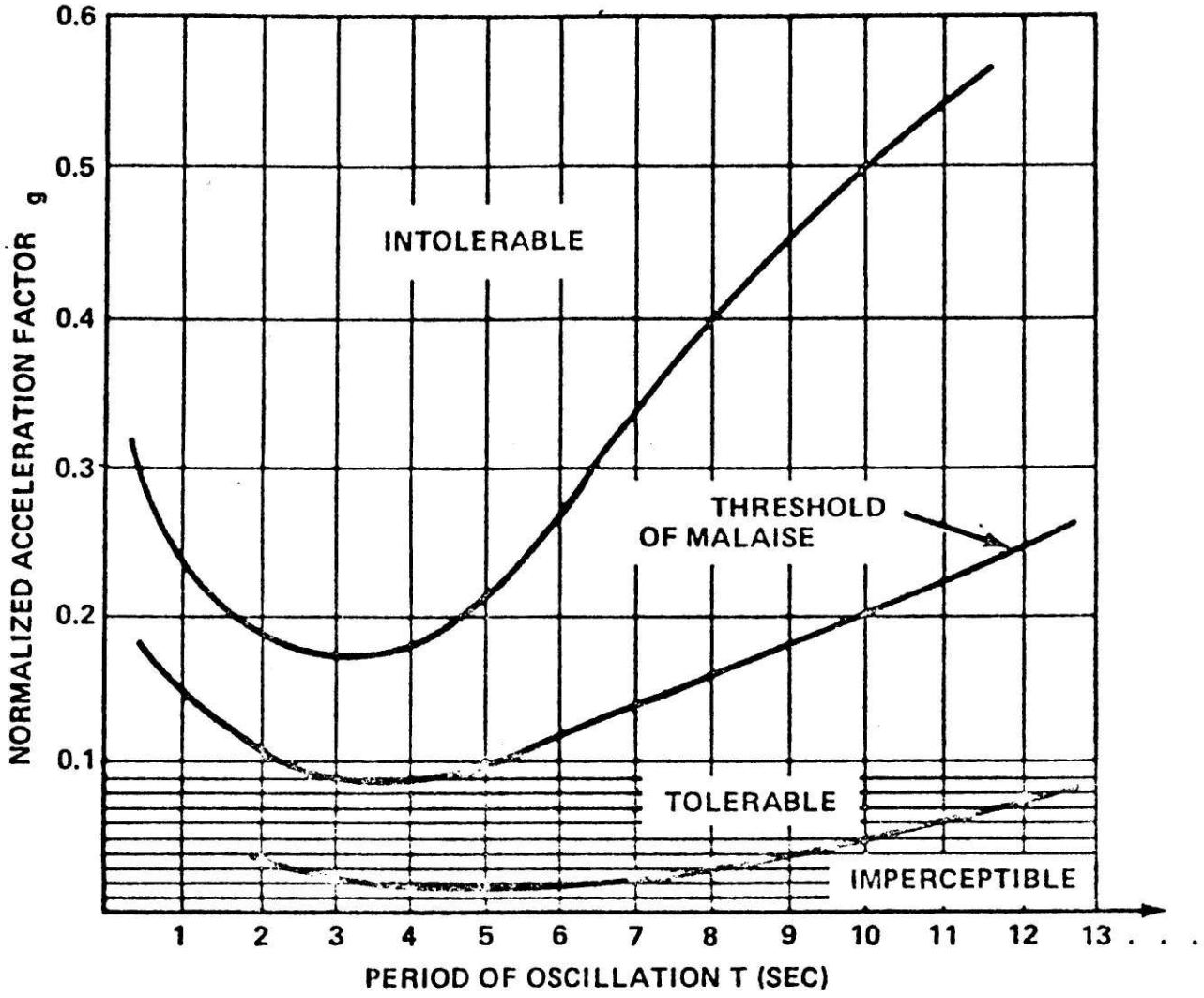


Figure 4.4-1 Physiological response to periodic vertical acceleration. [66].

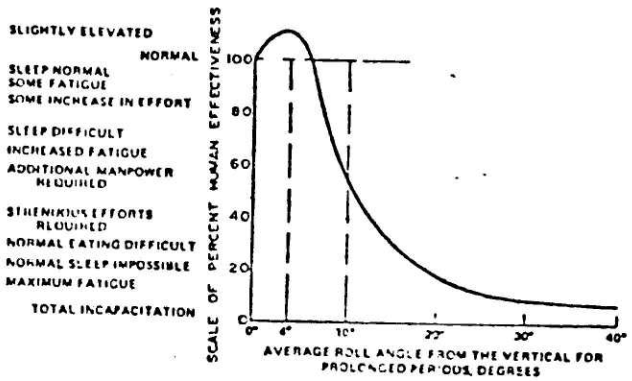


Figure 4.4-2 Effect of rolling on personnel capabilities. [71].

when he feels that damage to deck machinery or working conditions on deck is threatened by water coming onboard [74]. It is essentially a function of relative motion between waves and the ship bow with certain freeboard forward, f. The probability of deck wetness can be expressed by the following formula [75).

$$P_{wet} = \exp(-f_w^2/2\sigma_{rm}^2) \qquad \ldots(4.16)$$

where $\sigma_{rm}^2$ = mean square value of the relative motion between wave and ship bow. It is equal to the area under neath the relative motion spectrum $M_o$. To account for the spectral broadness, it is sometimes modified by a broadness factor $\varepsilon$. [47].
$\sigma_{rm}^2 = (1-\varepsilon^2/2)M_o$.

By assuming a modified Rayleigh probability law, the probability density function of pressure due to green water on the deck q (psi), are also derived in [75]

$$f(q) = \frac{\alpha^2}{\sigma_{rm}^2}(q + q^*)\exp\left\{\frac{-\alpha^2}{2\sigma_{rm}^2}[(q + q^*)^2 - q^{*2}]\right\} \qquad \ldots(4.17)$$

where q = Pressure due to green water on the deck in psi
$q^* = f_w/\alpha$
$f_w$ = freeboard at the ship bow in ft.
$\alpha$ = constant = 2.32(ft/psi)

3. Slamming & Whipping

Another factor which may persuade the captain to take similar actions is slamming [66]. This is generally caused by excessive impact pressure on the ship's bottom shell, particularly when the bow re-enters the water in large relative motions caused by heavy seas.

For a ship without stress-monitoring equipment, it is only detected by the high frequency second order whipping phenomenon of the main hull girder.

From a statistical point of view, slamming is a phenomenon very similar to deck wetness. An essential difference between these two seakeeping events is that deck wetness is a function of relative motion between wave and ship bow, while slamming is a function of relative motion as well as velocity. The probability of slamming may be expressed as:

$$P_{slam} = \exp\left[-\left(f^2/2\sigma^2_{rm} + V_{cr}{}^2/2\sigma^2_{rv}\right)\right] \qquad \ldots(4.16)$$

where $f$ = the draft where slam is experienced

$\sigma^2_{rv}$ = mean square value of the relative velocity between wave and the slamming location

$V_{cr}$ = the threshold critical velocity for slam to occur. It is assumed equal to 12 ft/sec for a 500 ft ship and scaled according to Froude number for other ship lengths.

4. Propeller Racing & Vibration

To the engineers, propeller racing and vibration are their main concern. These two seakeeping events often occur sequentially when the propeller is out of water due to heavy heave and pitch, especially for a ship of light load. The instantaneous reduction of loadings on propeller blades out of the water may cause propeller racing and induce location vibration of stern structure and shafting.

In the most severe case, the governor may shut down the engine due to overspeeding. When the possibility of such an event taking place reaches a certain level, the chief engineer may request the captain's action to re-

duce the danger of engine shutdown.

The statistical treatment of propeller racing probability is identical to that of deck wetness (see eq. (4.16). The only change is that the formula is now applied for relative motion at a draft of the propeller plane which the racing is likely to occur.

Generally, as indicated in [66], deck wetness and slamming are the dominant parameters which contribute to speed reduction for the full load condition. Acceleration and slamming are those for light conditions; while propeller racing is less critical unless in the very light condition.

All the above ship responses and seakeeping events can be calculated by the available ship motion seakeeping programs and expressed in terms of the spectral parameters that we used to construct the input spectra.

Hopefully, in the future, with the help of the new shipboard heavy weather monitoring instrumentation [76], proper criteria and constraints can be established for various types of ship and cargos. By using these criteria as inputs to our routing algorithm, upper limits on ship speed can be imposed when there exists potential danger to the cargo, ship and its cargo in forecasted sea conditions. Fig. 4.4-3 shows a pictorial representation of the speed functions being superimposed by the motion constraints.

Fig. 4.4-3 Required S.H.P. to maintain speed in seaways.

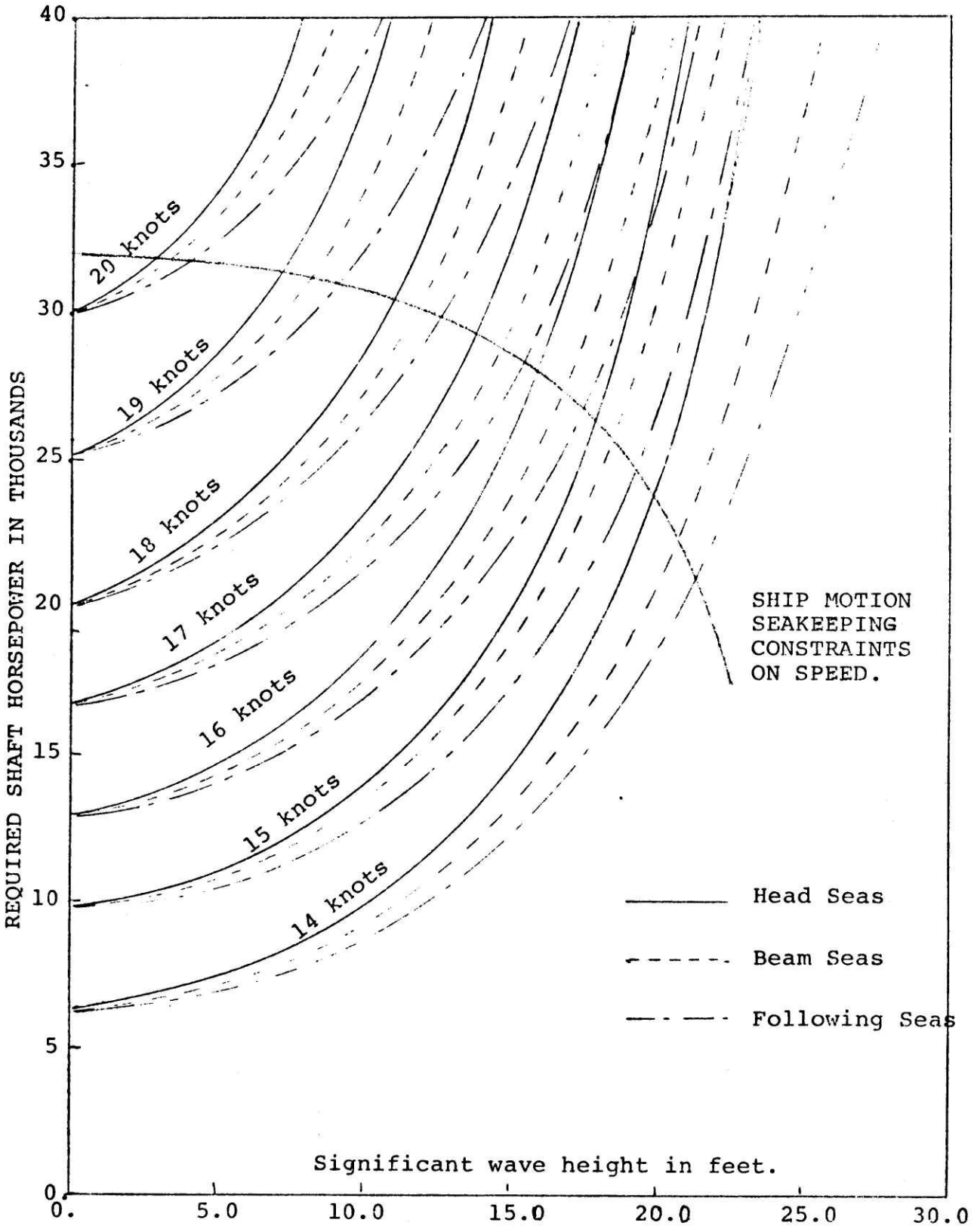

# CHAPTER 5

# SYSTEMS IMPLEMENTATION

## 5.1 SYSTEM MODULES FOR PREPARING INPUT DATA FILES

To implement the ship routing procedure that has been described, computer and data processing facilities complete with telecommunication system seems imperative. Too little automation may require many highly skilled professionals, while excessive machine process can result in unnecessary large numbers of errors which may be vital to ship's safety.

The proposed system calls for standard modules which initially prepares the necessary input files to the routing optimization model. There are five separate standard modules to deal with the five areas that we have discussed.

1. Grid Generation Model

   An interactive computer program has been developed to generate a grid system between any origin-destination pair in the ocean. The grid will cover a band alongside any nominal track specified by the user in terms of a set of co-ordinates. Fig 6.1-1 shows an example of the program outputs. After the modification has been made, the grids will be used in the routing algorithm as state descriptions. The distance between grids are based on the great circle distance calculation. The final results are stored on a sequential data file.

2. Environmental Data Interpolation Model

   Due to the fineness of our routing grid system, environmental information provided by FNWC has to

```
* GRID SYSTEM GENERATION FOR THE STOCHASTIC OPTIMAL SHIP ROUTING ALGORITHM *

   THE GRID WILL COVER A BAND ALONG A TRACK DESCRIBED BY UP TO 12 SETS OF COORDINATES.
   THE USER IS ALSO EXPECTED TO SPECIFY THE DISTANCES BETWEEN
   THE GRIDS ALONG THE TRACK (DX), AS WELL AS PERPENDICULAR TO IT (DY), IN NAUTICAL MILES.


*ENTER THE NUMBER OF COORDINATES (N),  FREE FORMAT
?
4
*ENTER THE COORDINATES : LONGITUDE (E+VE,W-VE), LATITUDE  (N+VE,S-VE) IN DEGREES.
?
-10.0,35.5
?
-37.0,42.0
?
-58.0,35.0
?
-76.0,32.5
*ENTER VALUES OF DX,DY, IN NAUTICAL MILES, AND THE NUMBER OF GRIDS IN EACH COLUMN.
?
100.,30.,15


* GRID SYSTEM HAS BEEN GENERATED WITH :

                LONGITUDE   LATITUDE
  ORIGIN :          -10.00      35.50  DEGREES.
  DESTINATION :     -76.00      32.50  DEGREES.
  G.C. DISTANCE =   3227.43  NAUTICAL MILES.
  G.C. BEARING =    287.18  DEGREES.
  DX =  100.00 N.M.     DY =   30.00 N.M.
  NO. OF STAGES =  32   NO. OF STATES =  15
  DISTANCE ALONG SPECIFIED TRACK = 3287.04 N.M.

*DO YOU WANT THE GRID SYSTEM TO BE PLOTED ? YES/NO
 IF YES CLEAR THE SCREEN OR START A NEW PAGE THEN HIT RETURN.
yes
```

Fig. 5.1-1 (a) Sample ouputs from the Grid generation program GRIDS.

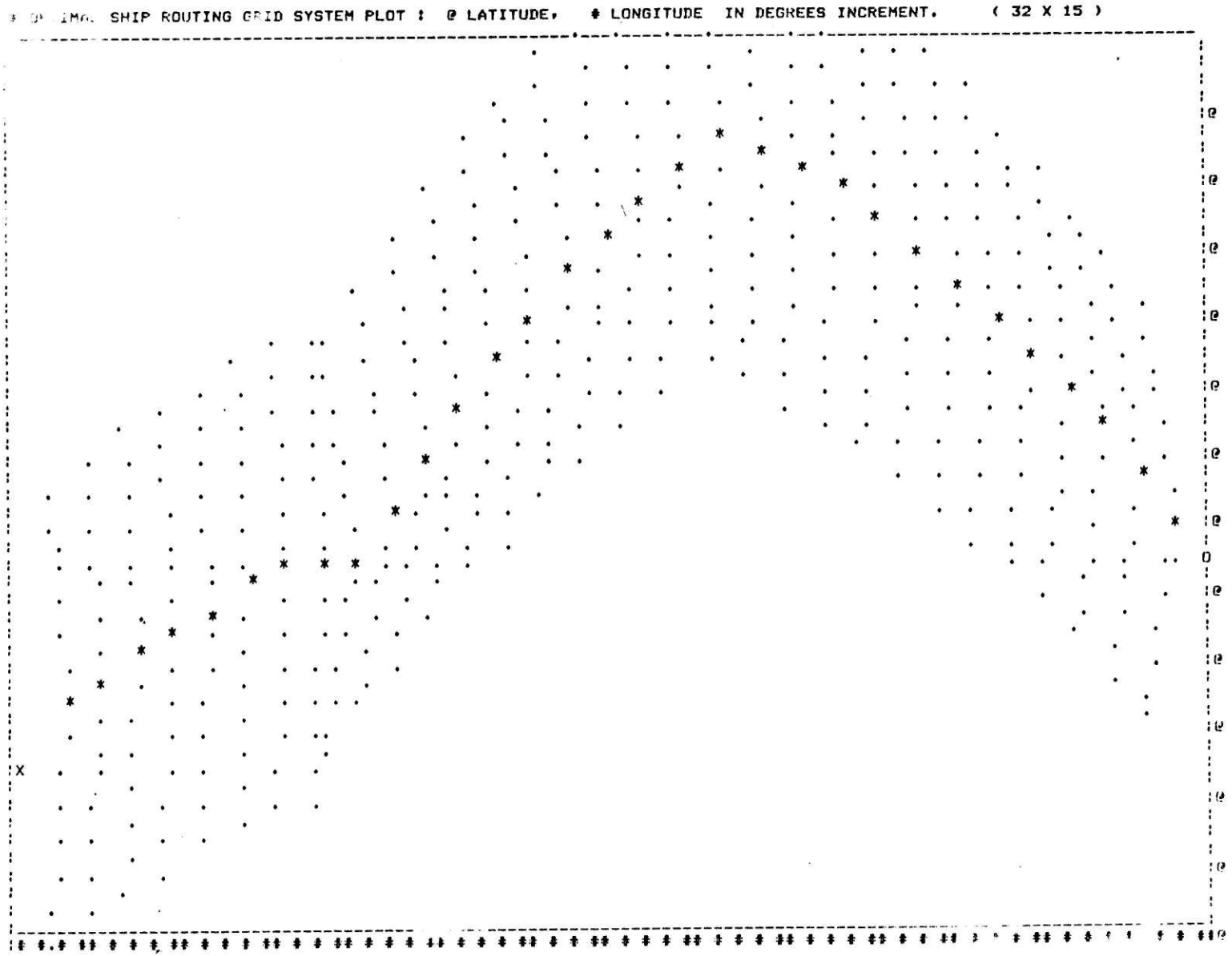


Fig. 5.1-1 (b) Sample ouputs from the grid generation program GRIDS.

be interpolated over space as well as time. Two separate computer programs have been developed for this purpose.

First, the FNWC's forecasted directional spectra information are reduced to parameter of sea and swell as indicated in Chapter 3 . The summary of wave information plus other ocean environmental data then becomes the input to the Data Interpolation Program. Together with the routing grid system, the average conditions of wave, wind, current, etc. for each state transition (grid points and time interval) are interpolated and stored on a direct access data file to be read-in later by the routing program.

3. Ship Seakeeping, Speedkeeping Performance Model

The procedure for computing the ship motion responses has been programmed in conjunction with the MIT 5-D program to evaluate ship performance in various sea conditions. The mean square responses are evaluated and tabulated as a function of discrete intervals of $H_{1/3}$, $\omega_p$, $\mu$ for several speed and loading conditions. Together with some relevant Response Amplitude Operators, they are stored on a random access disc file. The appropriate set of responses can be modified once the ship's departure conditions become known. The final modified ship responses file are then transferred into a routing data file ready to be read-in by the routing program.

4. Operating Criteria Selection Model

Based on the type of cargo and operating conditions of the vessel, a set of operating criteria is recommended for each voyage. The criteria are tabulated according

to cargo types and other mission related factors. This information hopefully will be developed in the future, based on the extensive data recorded by the new Ship Instrumentation Package [76]. The user can then use it as a default option or modify the criteria for the specific ship under consideration.

## 5. Cost Function Derivation Model

The cost function essentially consists of two points; namely, operating cost and terminal cost function. For the present model, the former only consists of a fuel cost[1] and the latter can be regarded as delay penalty.

A set of empirical relationships have been developed (see APPENDIX F ) to estimate the delay penalty cost which can be considered as a function of owners capital opportunity costs, manning insurance costs, stevedoring schedule and so on. Figure 5.1-2 shows an example of a typical terminal cost as a function of delay in hours. The discontinuity exists because of the stevedoring schedules (assuming 8 hours a shift, 2 shifts a day). The slope of the line is cost per hour due to delay. Depending upon the type of the service the ship is currently engaged in, the competitive market situation and the financial management practices of the owner, this figure can vary from a couple of hundred dollars to a few

[1] Due to lack of the cost data to relate ship motion, seakeeping events to possible cargo ship damages, these are not included in the operating cost function. The motions are considered as hard constraints. In the future, with the new onboard heavy weather monitoring system, realistic operating cost functions which include ship motion may be estimated and used as a part of the entire cost minimization procedure.

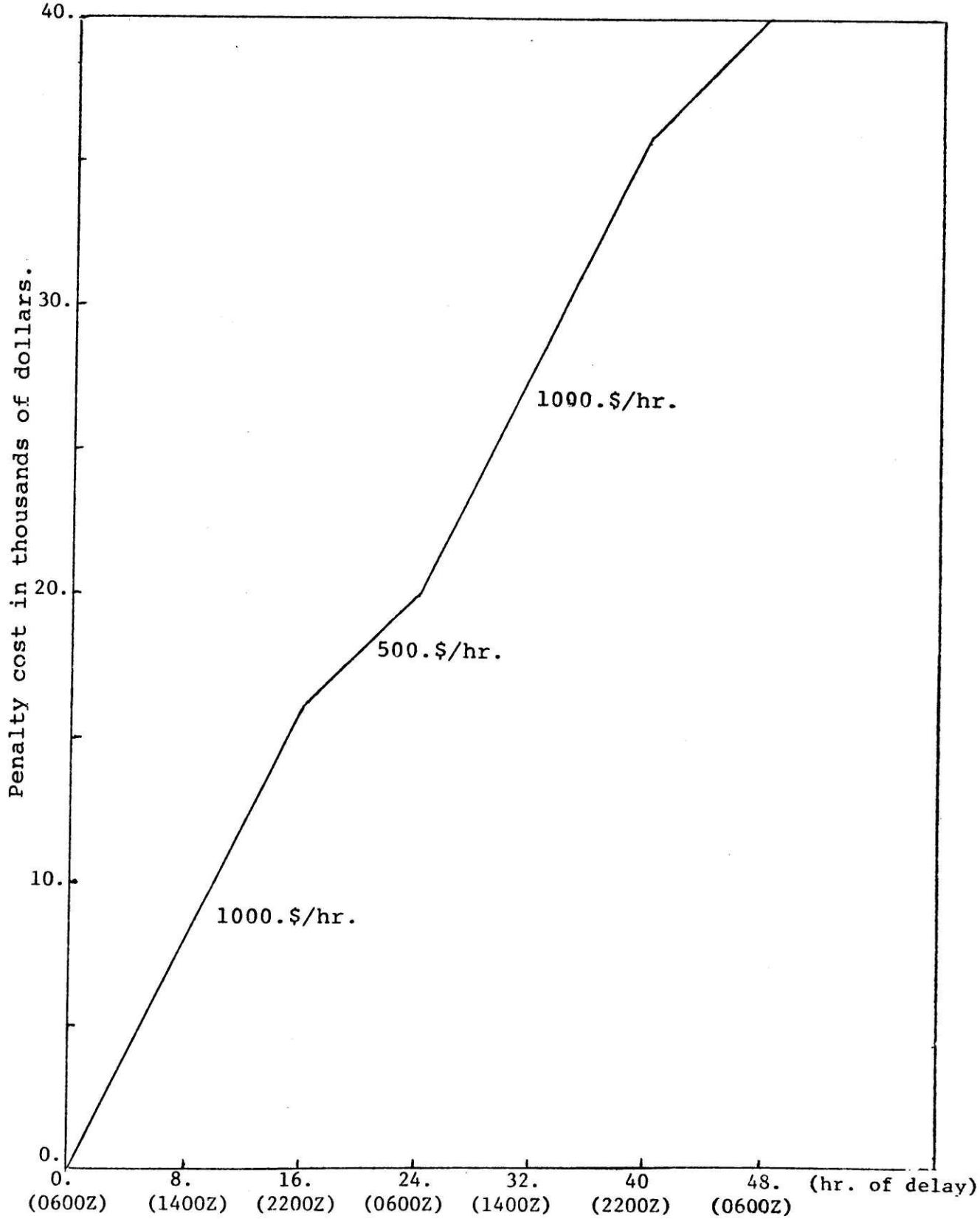


Fig. 5.1-2 An example of delay penalty cost at the terminal.

thousand per hour. The appropriate terminal cost function thus becomes one of the most important trade-offs between the fuel cost and delay penalty in the minimum cost ship routing algorithm.

## 5.2 PROGRAMMING STRUCTURE

Any good theoretical model cannot be successfully implemented without a well planned computer system. For our routing system which requires substantial input data processing and on-line computation, the system programming structure must provide enough flexibility to achieve the maximum utilization of the available resources. The resources may be limited in many ways including the size and availability of computer hardware or shortage of professional meteorologists and Naval Architects etc.

The proposed routing system and computer file structure thus attempts to reduce the amount of manual input by standardization and machine processing while retaining sufficient man-machine interaction for modifying and checking the results. Figure 5.2-1 shows a schematic representation of the programming structure. Each individual input files are connected to three integrated computer programs which constitutes our routing system.

1. PROGRAM ROUTE

   This is an interactive program which provides an opportunity for the user to enter and modify any information concerning the ship, cargo, route and the desired routing criteria plus the appropriate cost functions. Figure 5.2-2 shows an example of a session on the terminal. The routing data file is then stored on a disc file to be used later by the stochastic dynamic

Fig. 5.2-1 Optimal Ship Routing Systems
Programming Structure

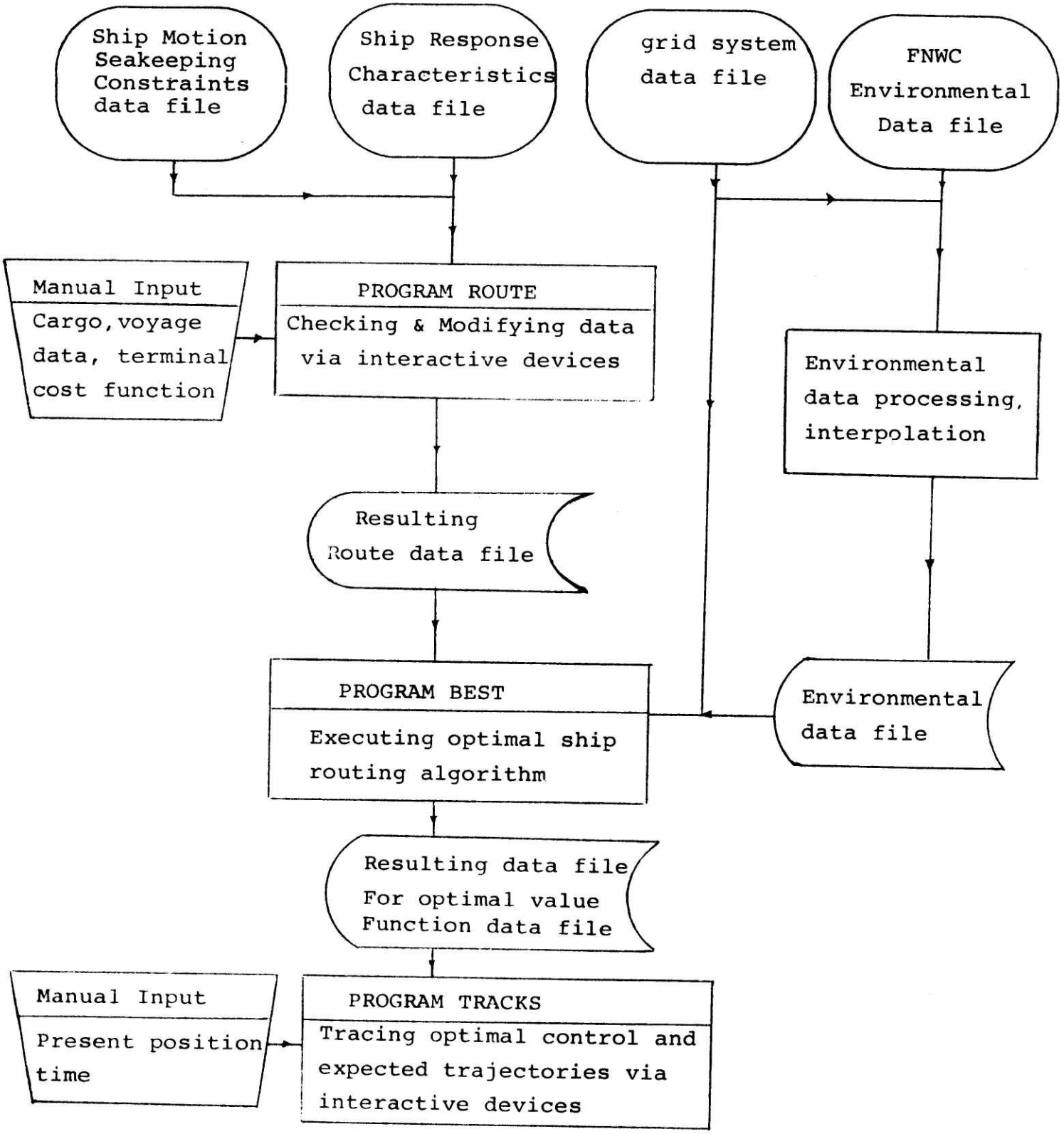

```
*****************************************
* OPTIMAL SHIP ROUTING INPUT INFORMATION *
*****************************************


ENTER VESSEL NAME,CODE AND AFFILIATION.    FORMAT(5A4,I5,5A4)
*                    *    *                    *
  LASH ITALIA          007      PRUD. GRACE

ORIGIN DESTINATION AND VOYAGE CODE.    FORMAT(5A4,5A4,I5)
*                    *                    *     *
 STR. OF GIBRALTAR     NEW YORK             1000

INITIAL POSITION :  LONGITUDE AND LATITUDE. FORMAT(2F7.2)
*      *      *
 -10.0    35.5

EXPECTED DEPARTURE TIME,EXPECTED ARRIVAL TIME. (MONTH-DAY-HOUR IN GMT)
TOTAL TRAVEL TIME IN HOURS.    FORMAT(2I8,F7.1)
*       *       *       *
03191800 3261800   168.

LOADING CONDITIONS :  FULL(1),HALF(2),OR BALLAST(3),MEAN DRAUGH,TRIM,GM.
                      UNITS IN FEET.        FORMAT(I5,3F10.2)
*    *          *          *          *
     1    -    35.      3.0        5.

MAX.POWER OUTPUT,SPECIFIC FUEL CONSUMPTION.    FORMAT(2F15.3)
*              *              *
   32000.           0.45

FUEL ON BOARD IN TONS, FUEL PRICE IN $/TON.    FORMAT(2F10.2)
*         *         *
    1000.    86.

CARGO INFORMATION : IN HOLD, ON DECK (SEE CODES).        FORMAT(2I10)
*         *         *
        100        200

Z CORD. FOR : DECK WETNESS.     PROP. RACING.     SLAMMING    VCR (FT/S)
FORMAT(4F10.2) *          *           *          *          *
                    16.          10.         10.       15.


 *** END OF DATA REQUEST. HIT RETURN FOR DISPLAY ***
```

Fig. 5.2-2 Sample session of executing Program ROUTE on a terminal.

```
**************************************
* OPTIMAL SHIP ROUTING INPUT DATA FILE *
**************************************

DATA #                          * CONTENT *

 1      LASH ITALIA              CODE=    7    OWNER :  PRUD. GRACE LINE

 2    FROM:  STR. OF GIBRALTAR  TO:    CHALESTON USA.      VOYAGE CODE= 1000

 3    INITIAL POSITION :  LONG.= -10.00 DEG.    LATI.=  35.50 DEG.

 4    SCH.TIME DEPT.= 3191800 SCH.TIME ARR.= 3261800 TOTAL TR.TIME =168.0 HR.

 5    LOADING CONDITIONS :  FULL     MEAN DRAUGH=35.00  TRIM= 3.00  GM= 5.00 FT

 6    MAX.POWER OUTPUT=  32000.00  HP.    SFC =0.450  LBS/HP HOUR

 7    FUEL ON BOARD=    1000.00  TONS    AV. FUEL PRICE=86.00  $/TON

 8    CARGO INFORMATION :  (CODES) IN HOLD =    10     ON DECK =    20

      BASED ON THE CARGO INFORMATION AND SHIP CONDITIONS,
      THE FOLLOWING SEAKEEPING CRITERIAS WERE SELECTED:

      A.    RMS VERTICAL ACCELERATION < 0.125 G.
      B.    RMS TRANSVERSE ACCELERATION < 0.125 G.
      C.    MIDSHIP BENDING MOMENT < .250E+11 LBS FT.
      D.    PR OBABILITY OF SLAMMING < 0.0100
      E.    PROBABILITY OF PROP. RACING < 0.0100
      F.    PROBABILITY OF DECK WETNESS <0.0100
      G.    MAX. ROLL ANGLE <  20.0 DEGREES.


*ANY CHANGES IN THE DATA SET ?  IF YES TYPE THE DATA # , IF NO MORE TYPE 0.
0
```

Fig. 5.2-2 (cond.) Summary of the input data file created by Program ROUTE.

programming routing algorithm.

2. PROGRAM BEST

Having prepared the necessary input data for the route optimization, program BEST is a batch version of the dynamic programming algorithm which can be submitted from a terminal. The program reads in the ship response and environmental data, then performs cost minimization with ship constraints according to the recursive equation of our stochastic dynamic programming. The resulting optimal value function is written onto a disc file for later tracing out the optimal controls at each state and other useful information.

3. PROGRAM TRACKS

The program TRACKS is again an interactive program to be called after the execution of PROGRAM BEST has terminated. There are perhaps two ways that this program can be utilized. Before the ship's departure it can be used to carry out sensitivity studies on the costs of various departure time and the expected travel time. Once underway, the feedback property of the dynamic programming algorithm allows us to trace out the optimal controls at the present time, position from the nearest state. Besides the recommended optimal controls, other useful information, such as wave height, etc. along the expected trajectory are also printed. Figure 5.2-3 shows an example of the output from PROGRAM TRACKS.

From the operational point of view, the above programming structure has several advantages.

```
                              ********************************
                              * OPTIMAL SHIP ROUTING OUTPUT *
                              ********************************

 SHIP NAME ID. =    1    VOYAGE NO. ID. =  1000

 ETD = 3191800      ETA = 3261800

* ENTER INDICES FOR THE INITIAL STARTING GRID (IS,JS):
?
1,1

* INPUTED GRID INDICES :     IS =  1   JS =  1
  CORRESPONED TO :    LONGITUDE =  1000 W    LATITUDE =  3530 N

* IS THE POSITION CORRECT ?      (YES/NO)
yes

* INPUT TERMINAL COST FUNCTION : *                    * INITIAL OPTIMAL CONTROL INFORMATION : *

ARRIVAL TIME  EARLY ARR.  TERMINAL     SEQUENCE STARTING TIME  POWER OUTPUT   NEXT GRID    GC. COURSE  EXPT.VOY.
   (GMT)      OR DELAY   COST ($)        K        (GMT)        (% PMAX)     LONGI.LATIT.     (DEG)     COST ($)

    32613       -5.5          0.         1       31906          80 %     1208 W  3627 N      299       74855.
    32615       -3.3          0.         2       31907          80 %     1208 W  3627 N      299       75063.
    32617       -1.1          0.         3       31908          80 %     1208 W  3627 N      299       75299.
    32619        1.0       1044.         4       31909          80 %     1208 W  3627 N      299       75575.
    32621        3.2       3212.         5       31910          80 %     1208 W  3627 N      299       75902.
    32623        5.4       5379.         6       31911          80 %     1208 W  3627 N      299       76287.
    32702        7.5       7546.         7       31912          80 %     1208 W  3627 N      299       76737.
    32704        9.7       9713.         8       31913          80 %     1208 W  3627 N      299       77256.
    32706       11.9      11881.         9       31914          80 %     1208 W  3627 N      299       77840.
    32708       14.0      14048.        10       31915          80 %     1208 W  3627 N      299       78473.
    32710       16.2      16107.        11       31916          80 %     1208 W  3627 N      299       79144.
    32712       18.4      17191.        12       31917          80 %     1208 W  3627 N      299       79842.
    32715       20.5      18275.        13       31918          80 %     1208 W  3627 N      299       80565.
    32717       22.7      19358.        14       31918          80 %     1208 W  3627 N      299       81301.
    32719       24.9      20884.        15       31919          80 %     1208 W  3627 N      299       82040.
    32721       27.1      23051.        16       31920          80 %     1208 W  3627 N      299       82774.
    32723       29.2      25218.        17       31921          80 %     1208 W  3627 N      299       83504.
    32801       31.4      27386.        18       31922          80 %     1208 W  3627 N      299       84228.
    32804       33.6      29553.        19       31923          80 %     1208 W  3627 N      299       84942.
    32806       35.7      31720.        20       32000          80 %     1208 W  3627 N      299       85636.
    32808       37.9      33887.        21       32001          80 %     1208 W  3627 N      299       86294.
    32810       40.1      36055.        22       32002          80 %     1208 W  3627 N      299       86906.
    32812       42.2      38222.        23       32003          80 %     1208 W  3627 N      299       87478.
    32814       44.4      40389.        24       32004          80 %     1208 W  3627 N      299       88030.
    32817       46.6      42556.        25       32005          80 %     1157 W  3558 N      286       88632.

* DO YOU WISH TO TRACE OUT THE EXPECTED OPTIMAL TRAJECTORY ? (YES/NO)
yes

* SENSITIVITY STUDY :  ENTER (UP TO 6) OF THE POTENTIAL TRACKS TO BE INVESTIGATED.  AND THEIR ASSOCIATED K VALUES
?
6,1,5,10,15,20,25
```

Fig. 5.2-3 Sample output from Program TRACKS executed from a terminal.

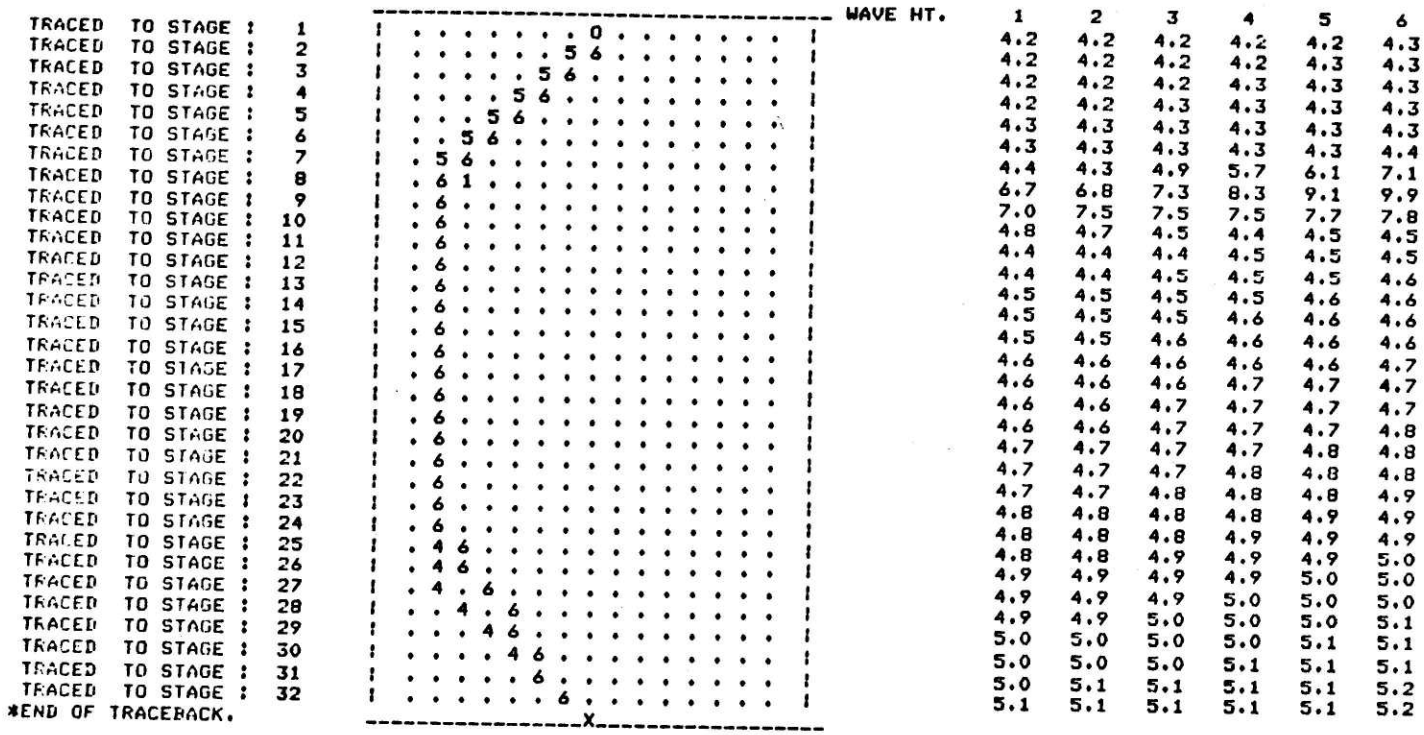

```
TRACED  TO STAGE :  1
TRACED  TO STAGE :  2
TRACED  TO STAGE :  3
TRACED  TO STAGE :  4
TRACED  TO STAGE :  5
TRACED  TO STAGE :  6
TRACED  TO STAGE :  7
TRACED  TO STAGE :  8
TRACED  TO STAGE :  9
TRACED  TO STAGE : 10
TRACED  TO STAGE : 11
TRACED  TO STAGE : 12
TRACED  TO STAGE : 13
TRACED  TO STAGE : 14
TRACED  TO STAGE : 15
TRACED  TO STAGE : 16
TRACED  TO STAGE : 17
TRACED  TO STAGE : 18
TRACED  TO STAGE : 19
TRACED  TO STAGE : 20
TRACED  TO STAGE : 21
TRACED  TO STAGE : 22
TRACED  TO STAGE : 23
TRACED  TO STAGE : 24
TRACED  TO STAGE : 25
TRACED  TO STAGE : 26
TRACED  TO STAGE : 27
TRACED  TO STAGE : 28
TRACED  TO STAGE : 29
TRACED  TO STAGE : 30
TRACED  TO STAGE : 31
TRACED  TO STAGE : 32
*END OF TRACEBACK.
```

WAVE HT.

| 1 | 2 | 3 | 4 | 5 | 6 |
|---|---|---|---|---|---|
| 4.2 | 4.2 | 4.2 | 4.2 | 4.2 | 4.3 |
| 4.2 | 4.2 | 4.2 | 4.2 | 4.3 | 4.3 |
| 4.2 | 4.2 | 4.2 | 4.3 | 4.3 | 4.3 |
| 4.2 | 4.2 | 4.3 | 4.3 | 4.3 | 4.3 |
| 4.3 | 4.3 | 4.3 | 4.3 | 4.3 | 4.3 |
| 4.3 | 4.3 | 4.3 | 4.3 | 4.3 | 4.4 |
| 4.4 | 4.3 | 4.9 | 5.7 | 6.1 | 7.1 |
| 6.7 | 6.8 | 7.3 | 8.3 | 9.1 | 9.9 |
| 7.0 | 7.5 | 7.5 | 7.5 | 7.7 | 7.8 |
| 4.8 | 4.7 | 4.5 | 4.4 | 4.5 | 4.5 |
| 4.4 | 4.4 | 4.4 | 4.5 | 4.5 | 4.5 |
| 4.4 | 4.4 | 4.5 | 4.5 | 4.5 | 4.6 |
| 4.5 | 4.5 | 4.5 | 4.5 | 4.6 | 4.6 |
| 4.5 | 4.5 | 4.5 | 4.6 | 4.6 | 4.6 |
| 4.5 | 4.5 | 4.6 | 4.6 | 4.6 | 4.6 |
| 4.6 | 4.6 | 4.6 | 4.6 | 4.6 | 4.7 |
| 4.6 | 4.6 | 4.6 | 4.7 | 4.7 | 4.7 |
| 4.6 | 4.6 | 4.7 | 4.7 | 4.7 | 4.7 |
| 4.6 | 4.6 | 4.7 | 4.7 | 4.7 | 4.8 |
| 4.7 | 4.7 | 4.7 | 4.7 | 4.8 | 4.8 |
| 4.7 | 4.7 | 4.7 | 4.8 | 4.8 | 4.8 |
| 4.7 | 4.7 | 4.8 | 4.8 | 4.8 | 4.9 |
| 4.8 | 4.8 | 4.8 | 4.8 | 4.9 | 4.9 |
| 4.8 | 4.8 | 4.8 | 4.9 | 4.9 | 4.9 |
| 4.8 | 4.8 | 4.9 | 4.9 | 4.9 | 5.0 |
| 4.9 | 4.9 | 4.9 | 4.9 | 5.0 | 5.0 |
| 4.9 | 4.9 | 4.9 | 5.0 | 5.0 | 5.0 |
| 4.9 | 4.9 | 5.0 | 5.0 | 5.0 | 5.1 |
| 5.0 | 5.0 | 5.0 | 5.0 | 5.1 | 5.1 |
| 5.0 | 5.0 | 5.0 | 5.1 | 5.1 | 5.1 |
| 5.0 | 5.1 | 5.1 | 5.1 | 5.1 | 5.2 |
| 5.1 | 5.1 | 5.1 | 5.1 | 5.1 | 5.2 |

```
*DO YOU WANT THE FINAL OPTIMAL TRAJECTORIES TO BE PRINTED OUT ON THE TERMINAL ?  YES/NO
 IF NO THE OUTPUT WILL BE STORED ON AN ALLOCATED DISC FILE.
yes
```

Fig. 5.2-3 Sample outputs from Program TRACKS executed from a terminal. (continue.)

```
**********************************************************
* EXPECTED OPTIMAL SHIP TRAJECTORY INFORMATION OUTPUT *
**********************************************************
```

ROUTE NO. 1 REFERENCE : K= 1 SHIP ID.= 1 VOYAGE ID.= 1000
INITIAL STARTING TIME = 31906 GMT EXPECTED ARRIVING TIME = 32617 GMT
TOTAL VOYAGE TIME = 179.3 HOURS STD. DEVIATION = 3.1 HOURS. DELAY FROM SCHEDULE = -0.7 HOURS.
ESTIMATED TOTAL VOYAGE COST = 74855. $

| STAGE (I) | TR.TIME (HR) | GMT (M-D-H) | LONGITUDE (DEG.MIN) | LATITUDE (DEG.MIN) | WAVE.HT (FT) | DIR. (DEG) | POWER (%PMAX) | AV.SPD (KNOTS) | COURSE (DEG) | CURF (KNOTS) | VOY.COST ($$$) | WARNING (CODE) |
|---|---|---|---|---|---|---|---|---|---|---|---|---|
| 1 | 6.2 | 31906 | 1000 W | 3530 N | 4.2 | NNE | 80 % | 19.0 | 299 | 0.0 | 74855. | 0 |
| 2 | 6.2 | 31912 | 1208 W | 3627 N | 4.2 | NNE | 80 % | 19.0 | 298 | 0.0 | 72220. | 0 |
| 3 | 6.1 | 31918 | 1418 W | 3723 N | 4.2 | NNE | 80 % | 19.0 | 298 | 0.0 | 69776. | 0 |
| 4 | 6.0 | 32001 | 1627 W | 3817 N | 4.2 | NNE | 80 % | 18.9 | 298 | 0.0 | 67427. | 0 |
| 5 | 5.9 | 32007 | 1836 W | 3910 N | 4.3 | NNE | 80 % | 18.9 | 297 | 0.0 | 64904. | 0 |
| 6 | 5.0 | 32012 | 2045 W | 4000 N | 4.3 | NNE | 80 % | 18.9 | 282 | 0.0 | 62683. | 0 |
| 7 | 4.9 | 32017 | 2245 W | 4020 N | 4.4 | NEE | 80 % | 19.1 | 281 | 0.0 | 60622. | 0 |
| 8 | 5.7 | 32022 | 2446 W | 4037 N | 6.7 | NEE | 80 % | 18.7 | 295 | 0.0 | 58807. | 0 |
| 9 | 5.4 | 32104 | 2654 W | 4121 N | 7.0 | NEE | 60 % | 17.2 | 278 | 0.0 | 56438. | 0 |
| 10 | 5.3 | 32109 | 2856 W | 4134 N | 4.8 | NNE | 60 % | 17.4 | 276 | 0.0 | 54553. | 0 |
| 11 | 5.2 | 32115 | 3058 W | 4144 N | 4.4 | NNE | 60 % | 17.5 | 275 | 0.0 | 52716. | 0 |
| 12 | 5.2 | 32120 | 3300 W | 4152 N | 4.4 | NNE | 60 % | 17.5 | 273 | 0.0 | 50889. | 0 |
| 13 | 5.2 | 32201 | 3503 W | 4157 N | 4.5 | NNE | 60 % | 17.5 | 272 | 0.0 | 48754. | 0 |
| 14 | 5.2 | 32206 | 3706 W | 4200 N | 4.5 | NNE | 60 % | 17.6 | 270 | 0.0 | 46874. | 0 |
| 15 | 5.4 | 32212 | 3909 W | 4200 N | 4.5 | NNE | 60 % | 17.6 | 269 | 0.0 | 45002. | 0 |
| 16 | 5.2 | 32217 | 4116 W | 4158 N | 4.6 | NNE | 80 % | 19.0 | 268 | 0.0 | 43001. | 0 |
| 17 | 5.2 | 32222 | 4330 W | 4154 N | 4.6 | NNE | 80 % | 19.0 | 266 | 0.0 | 40783. | 0 |
| 18 | 5.2 | 32303 | 4543 W | 4147 N | 4.6 | NNE | 80 % | 19.0 | 265 | 0.0 | 38559. | 0 |
| 19 | 5.3 | 32309 | 4756 W | 4138 N | 4.6 | NNE | 80 % | 19.0 | 263 | 0.0 | 36300. | 0 |
| 20 | 5.2 | 32314 | 5009 W | 4126 N | 4.7 | NNE | 80 % | 19.0 | 262 | 0.0 | 33998. | 0 |
| 21 | 5.3 | 32319 | 5220 W | 4112 N | 4.7 | NNE | 80 % | 19.0 | 261 | 0.0 | 31706. | 0 |
| 22 | 5.7 | 32400 | 5431 W | 4056 N | 4.7 | NNE | 60 % | 17.5 | 259 | 0.0 | 29047. | 0 |
| 23 | 5.3 | 32406 | 5641 W | 4037 N | 4.8 | NNE | 80 % | 19.0 | 258 | 0.0 | 26996. | 0 |
| 24 | 5.5 | 32411 | 5849 W | 4016 N | 4.8 | NNE | 80 % | 19.0 | 240 | 0.0 | 24624. | 0 |
| 25 | 5.3 | 32417 | 6047 W | 3924 N | 4.8 | NNE | 80 % | 19.0 | 255 | 0.0 | 22049. | 0 |
| 26 | 5.5 | 32422 | 6252 W | 3858 N | 4.9 | NNE | 80 % | 19.0 | 238 | 0.0 | 19603. | 0 |
| 27 | 6.0 | 32504 | 6445 W | 3802 N | 4.9 | NNE | 60 % | 17.5 | 237 | 0.0 | 16973. | 0 |
| 28 | 5.7 | 32510 | 6636 W | 3705 N | 4.9 | NNE | 60 % | 17.5 | 252 | 0.0 | 14318. | 0 |
| 29 | 6.0 | 32515 | 6834 W | 3634 N | 5.0 | NNE | 60 % | 17.5 | 235 | 0.0 | 11837. | 0 |
| 30 | 5.7 | 32521 | 7020 W | 3533 N | 5.0 | NNE | 60 % | 17.5 | 250 | 0.0 | 9146. | 0 |
| 31 | 6.0 | 32603 | 7215 W | 3458 N | 5.0 | NNE | 60 % | 17.5 | 232 | 0.0 | 6605. | 0 |
| 32 | 8.1 | 32609 | 7356 W | 3354 N | 5.1 | NNE | 80 % | 18.9 | 237 | 0.0 | 4085. | 0 |
| 33 | 0.0 | 32617 | 7630 W | 3230 N | 0.0 | -- | 0 % | 0.0 | 0 | 0.0 | 0. | 0 |

Fig. 5.2-3 (continue) Sample outputs from Program TRACKS.

ROUTE NO. 5 REFERENCE : K= 20 SHIP ID.= 1 VOYAGE ID.= 1000
INITIAL STARTING TIME = 32000 GMT EXPECTED ARRIVING TIME = 32702 GMT
TOTAL VOYAGE TIME = 169.8 HOURS STD. DEVIATION = 2.9 HOURS. DELAY FROM SCHEDULE = 8.1 HOURS.
ESTIMATED TOTAL VOYAGE COST = 85636. $

| STAGE (I) | TR.TIME (HR) | GMT (M-D-H) | LONGITUDE (DEG.MIN) | LATITUDE (DEG.MIN) | WAVE.HT (FT) | DIR. (DEG) | POWER (%PMAX) | AV.SPD (KNOTS) | COURSE (DEG) | CURF (KNOTS) | VOY.COST ($$$) | WARNING (CODE) |
|---|---|---|---|---|---|---|---|---|---|---|---|---|
| 1 | 6.2 | 32000 | 1000 W | 3530 N | 4.2 | NNE | 80 % | 18.9 | 299 | 0.0 | 85636. | 0 |
| 2 | 6.2 | 32006 | 1208 W | 3627 N | 4.3 | NNE | 80 % | 18.9 | 298 | 0.0 | 83129. | 0 |
| 3 | 6.1 | 32013 | 1418 W | 3723 N | 4.3 | NNE | 80 % | 18.9 | 298 | 0.0 | 80605. | 0 |
| 4 | 6.0 | 32019 | 1627 W | 3817 N | 4.3 | NNE | 80 % | 18.9 | 298 | 0.0 | 78233. | 0 |
| 5 | 5.9 | 32101 | 1836 W | 3910 N | 4.3 | NNE | 80 % | 18.9 | 297 | 0.0 | 75942. | 0 |
| 6 | 5.8 | 32107 | 2045 W | 4000 N | 4.3 | NNE | 80 % | 18.9 | 297 | 0.0 | 73793. | 0 |
| 7 | 4.9 | 32112 | 2253 W | 4049 N | 6.1 | NEE | 80 % | 18.8 | 281 | 0.0 | 70850. | 0 |
| 8 | 4.8 | 32117 | 2453 W | 4106 N | 9.1 | NEE | 100 % | 19.4 | 280 | 0.0 | 68933. | 0 |
| 9 | 4.8 | 32122 | 2654 W | 4121 N | 7.7 | NNE | 100 % | 19.4 | 278 | 0.0 | 66758. | 0 |
| 10 | 4.9 | 32203 | 2856 W | 4134 N | 4.5 | NNE | 80 % | 18.9 | 276 | 0.0 | 64521. | 0 |
| 11 | 4.8 | 32208 | 3058 W | 4144 N | 4.5 | NNE | 80 % | 18.9 | 275 | 0.0 | 63489. | 0 |
| 12 | 4.9 | 32213 | 3300 W | 4152 N | 4.5 | NNE | 80 % | 18.9 | 273 | 0.0 | 61396. | 0 |
| 13 | 4.8 | 32217 | 3503 W | 4157 N | 4.6 | NNE | 80 % | 18.9 | 272 | 0.0 | 59190. | 0 |
| 14 | 4.8 | 32222 | 3706 W | 4200 N | 4.6 | NNE | 80 % | 19.0 | 270 | 0.0 | 56905. | 0 |
| 15 | 5.0 | 32303 | 3909 W | 4200 N | 4.6 | NNE | 80 % | 19.0 | 269 | 0.0 | 55818. | 0 |
| 16 | 5.3 | 32308 | 4116 W | 4158 N | 4.6 | NNE | 80 % | 19.0 | 268 | 0.0 | 53239. | 0 |
| 17 | 5.2 | 32313 | 4330 W | 4154 N | 4.7 | NNE | 80 % | 19.0 | 266 | 0.0 | 51502. | 0 |
| 18 | 5.3 | 32319 | 4543 W | 4147 N | 4.7 | NNE | 80 % | 19.0 | 265 | 0.0 | 48400. | 0 |
| 19 | 5.3 | 32324 | 4756 W | 4138 N | 4.7 | NNE | 80 % | 19.0 | 263 | 0.0 | 46597. | 0 |
| 20 | 5.0 | 32405 | 5009 W | 4126 N | 4.8 | NNE | 100 % | 20.0 | 262 | 0.0 | 44735. | 0 |
| 21 | 5.0 | 32410 | 5220 W | 4112 N | 4.8 | NNE | 100 % | 20.0 | 261 | 0.0 | 41394. | 0 |
| 22 | 5.0 | 32415 | 5431 W | 4056 N | 4.8 | NNE | 100 % | 20.0 | 259 | 0.0 | 39473. | 0 |
| 23 | 5.0 | 32420 | 5641 W | 4037 N | 4.9 | NNE | 100 % | 20.0 | 258 | 0.0 | 35894. | 0 |
| 24 | 5.2 | 32501 | 5849 W | 4016 N | 4.9 | NNE | 100 % | 20.0 | 240 | 0.0 | 33924. | 0 |
| 25 | 5.0 | 32506 | 6047 W | 3924 N | 4.9 | NNE | 100 % | 20.0 | 255 | 0.0 | 31573. | 0 |
| 26 | 5.2 | 32511 | 6252 W | 3858 N | 5.0 | NNE | 100 % | 20.0 | 238 | 0.0 | 27743. | 0 |
| 27 | 5.3 | 32517 | 6445 W | 3802 N | 5.0 | NNE | 100 % | 20.0 | 237 | 0.0 | 25286. | 0 |
| 28 | 5.0 | 32522 | 6636 W | 3705 N | 5.0 | NNE | 100 % | 20.0 | 252 | 0.0 | 22795. | 0 |
| 29 | 5.3 | 32603 | 6834 W | 3634 N | 5.1 | NNE | 100 % | 20.0 | 235 | 0.0 | 20703. | 0 |
| 30 | 5.0 | 32608 | 7020 W | 3533 N | 5.1 | NNE | 100 % | 20.0 | 250 | 0.0 | 18143. | 0 |
| 31 | 5.3 | 32613 | 7215 W | 3458 N | 5.1 | NNE | 100 % | 20.0 | 232 | 0.0 | 13910. | 0 |
| 32 | 7.7 | 32618 | 7356 W | 3354 N | 5.1 | NNE | 100 % | 19.9 | 237 | 0.0 | 11261. | 0 |
| 33 | 0.0 | 32702 | 7630 W | 3230 N | 0.0 | -- | 0 % | 0.0 | 0 | 0.0 | 0. | 0 |

Fig. 5.2-3 (continue) Sample outputs from Program TRACKS.

ROUTE NO. 6 REFERENCE : K= 25 SHIP ID.= 1 VOYAGE ID.= 1000
INITIAL STARTING TIME = 32005 GMT EXPECTED ARRIVING TIME = 32711 GMT
TOTAL VOYAGE TIME = 173.8 HOURS STD. DEVIATION = 3.0 HOURS. DELAY FROM SCHEDULE = 16.8 HOURS.
ESTIMATED TOTAL VOYAGE COST = 88632. $

| STAGE (I) | TR.TIME (HR) | GMT (M-D-H) | LONGITUDE (DEG.MIN) | LATITUDE (DEG.MIN) | WAVE.HT (FT) | DIR. (DEG) | POWER (%PMAX) | AV.SPD (KNOTS) | COURSE (DEG) | CURR (KNOTS) | VOY.COST ($$$) | WARNING (CODE) |
|---|---|---|---|---|---|---|---|---|---|---|---|---|
| 1 | 5.2 | 32005 | 1000 W | 3530 N | 4.3 | NNE | 80 % | 18.9 | 286 | 0.0 | 88632. | 0 |
| 2 | 6.3 | 32010 | 1157 W | 3558 N | 4.3 | NNE | 80 % | 18.9 | 298 | 0.0 | 86225. | 0 |
| 3 | 6.2 | 32017 | 1407 W | 3654 N | 4.3 | NNE | 80 % | 18.9 | 298 | 0.0 | 84369. | 0 |
| 4 | 6.1 | 32023 | 1617 W | 3748 N | 4.3 | NNE | 80 % | 18.9 | 298 | 0.0 | 81452. | 0 |
| 5 | 5.9 | 32105 | 1827 W | 3841 N | 4.3 | NNE | 80 % | 18.9 | 297 | 0.0 | 79178. | 0 |
| 6 | 5.8 | 32111 | 2036 W | 3931 N | 4.4 | NNE | 80 % | 18.9 | 297 | 0.0 | 77064. | 0 |
| 7 | 5.8 | 32117 | 2245 W | 4020 N | 7.1 | NEE | 80 % | 18.6 | 296 | 0.0 | 75017. | 0 |
| 8 | 5.1 | 32122 | 2453 W | 4106 N | 9.9 | NEE | 80 % | 18.0 | 280 | 0.0 | 72313. | 0 |
| 9 | 5.1 | 32203 | 2654 W | 4121 N | 7.8 | NNE | 80 % | 18.2 | 278 | 0.0 | 70952. | 0 |
| 10 | 4.9 | 32208 | 2856 W | 4134 N | 4.5 | NNE | 80 % | 18.9 | 276 | 0.0 | 68923. | 0 |
| 11 | 4.8 | 32213 | 3058 W | 4144 N | 4.5 | NNE | 80 % | 18.9 | 275 | 0.0 | 67052. | 0 |
| 12 | 4.9 | 32218 | 3300 W | 4152 N | 4.6 | NNE | 80 % | 18.9 | 273 | 0.0 | 65144. | 0 |
| 13 | 4.9 | 32223 | 3503 W | 4157 N | 4.6 | NNE | 80 % | 18.9 | 272 | 0.0 | 63153. | 0 |
| 14 | 4.8 | 32304 | 3706 W | 4200 N | 4.6 | NNE | 80 % | 19.0 | 270 | 0.0 | 61107. | 0 |
| 15 | 5.0 | 32309 | 3909 W | 4200 N | 4.6 | NNE | 80 % | 19.0 | 269 | 0.0 | 59038. | 0 |
| 16 | 5.3 | 32314 | 4116 W | 4158 N | 4.7 | NNE | 80 % | 19.0 | 268 | 0.0 | 57636. | 0 |
| 17 | 5.2 | 32319 | 4330 W | 4154 N | 4.7 | NNE | 80 % | 19.0 | 266 | 0.0 | 54987. | 0 |
| 18 | 5.3 | 32400 | 4543 W | 4147 N | 4.7 | NNE | 80 % | 19.0 | 265 | 0.0 | 53247. | 0 |
| 19 | 5.3 | 32405 | 4756 W | 4138 N | 4.8 | NNE | 80 % | 19.0 | 263 | 0.0 | 50474. | 0 |
| 20 | 5.2 | 32411 | 5009 W | 4126 N | 4.8 | NNE | 80 % | 19.0 | 262 | 0.0 | 48632. | 0 |
| 21 | 5.3 | 32416 | 5220 W | 4112 N | 4.8 | NNE | 80 % | 19.0 | 261 | 0.0 | 46806. | 0 |
| 22 | 5.3 | 32421 | 5431 W | 4056 N | 4.9 | NNE | 80 % | 19.0 | 259 | 0.0 | 43853. | 0 |
| 23 | 5.3 | 32503 | 5641 W | 4037 N | 4.9 | NNE | 80 % | 19.0 | 258 | 0.0 | 41934. | 0 |
| 24 | 5.5 | 32508 | 5849 W | 4016 N | 4.9 | NNE | 80 % | 18.9 | 240 | 0.0 | 40014. | 0 |
| 25 | 5.3 | 32513 | 6047 W | 3924 N | 5.0 | NNE | 80 % | 18.9 | 255 | 0.0 | 37770. | 0 |
| 26 | 5.5 | 32519 | 6252 W | 3858 N | 5.0 | NNE | 80 % | 18.9 | 238 | 0.0 | 34593. | 0 |
| 27 | 5.5 | 32600 | 6445 W | 3802 N | 5.0 | NNE | 80 % | 18.9 | 237 | 0.0 | 32288. | 0 |
| 28 | 5.3 | 32606 | 6636 W | 3705 N | 5.1 | NNE | 80 % | 18.9 | 252 | 0.0 | 29945. | 0 |
| 29 | 5.6 | 32611 | 6834 W | 3634 N | 5.1 | NNE | 80 % | 18.9 | 235 | 0.0 | 27919. | 0 |
| 30 | 5.3 | 32617 | 7020 W | 3533 N | 5.1 | NNE | 80 % | 18.9 | 250 | 0.0 | 25494. | 0 |
| 31 | 5.3 | 32622 | 7215 W | 3458 N | 5.2 | NNE | 100 % | 19.9 | 232 | 0.0 | 22016. | 0 |
| 32 | 7.7 | 32703 | 7356 W | 3354 N | 5.2 | NNE | 100 % | 19.9 | 237 | 0.0 | 19572. | 0 |
| 33 | 0.0 | 32711 | 7630 W | 3230 N | 0.0 | -- | 0 % | 0.0 | 0 | 0.0 | 0. | 0 |

* END OF OPTIMAL SHIP ROUTING OUPUT *

*** GOOD LUCK AND BON VOYAGE ***
READY

Fig. 5.2-3 (continue) Sample outputs from Program TRACKS.

1. It reduces on-line core requirements. Since the model is split into three sequential parts, each of which requires less storage location than the entire program, a much smaller computer with direct access devices will be adequate.

2. It facilitates better scheduling of jobs. The execution of actual routing algorithm (i.e. program BEST) can be done sequentially according to the time of ship departure, whereas input data files can be prepared at other convenient times before hand.

3. It utilizes the computing facilities. Under Multiple programming with variable number of tasks operating systems, it is possible to fully utilize the complete capacities because of the different core requirements, execution time and mode of operation of the programs ROUTE, BEST and TRACKS.

## 5.3 PROPOSED SYSTEM SETUP

Figure 5.3-1 shows the entire set-up of the Optimal Routing System linking communication sattelite and/or radio transmission. Notice that human inputs should be made available whenever possible to reduce unexpected errors.

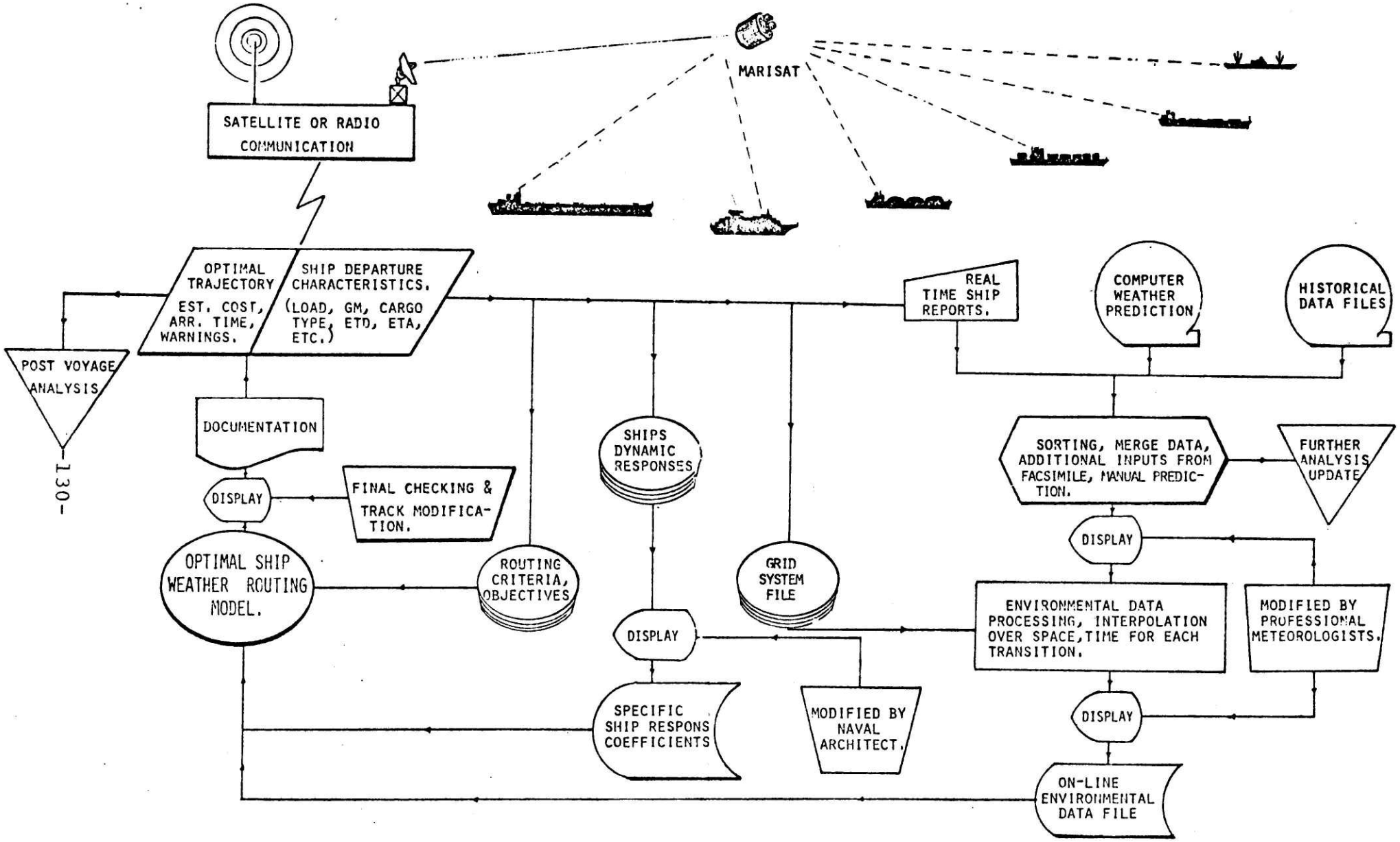


Fig. 5.3-1 Proposed set-up for a real-time ship routing system.

# CHAPTER 6

## CONCLUSION AND RECOMMENDATION FOR FUTURE DEVELOPMENT

A dynamic programming algorithm has been developed for solving the stochastic ship routing problem. The algorithm takes account of the stochastic varations in the forecasted wave height parameter and minimizes the expected total voyage cost under the constraints of ship motion seakeeping criteria. The algorithm is believed to be more general and realistic than existing ship routing methods. The preliminary test runs using simulated data demonstrated that even if a 1% savings in fuel cost (about $800) on a Trans-Atlantic voyage would fully justify the use of such system[1], thus establishing its economic feasibility for possible real-time implementations in the future.

Before the proposed routing system can be fully implemented on a large scale, however, there are still many areas where further tests and evaluation are required. In particular, further calibration studies should be carried out under the real-time operating conditions. Questions such as grid size, coverage, and time intervals should be investigated in relation to the overall compatibility of the level of details of various input data and the required output information. The analyis should center on the question whether the additional computation effort is worthwhile in real dollar terms to achieve a 'more accurate' solution which may have to be updated several times during a voyage.

---

[1] A typical Trans-Atlantic voyage of the LASH ship requires around 7 days at a fuel cost of $80,000. Suppose the ship track is updated once every day, the total computing cost is around $200 and would be considerably less if a special purpose computer is used.

The calibration of the complete routing model should also take into consideration of the type of routing criteria and objective function. For commercial ship operations, the factors considered are far less complicated than for a military application. The primary concern here is to develop a set of causal relationship between the physical ship motion responses to expected cargo ship damage as well as human response onboard. The present seakeeping criteria in many ways lack the causal content and tend to be ambiguous. Hopefully, with the extensive data gathering capability by the new shipboard instrumentation,further research efforts will provide realistic ship motion constraints for various types of services and operational requirements.

On the whole, it is important to bear in mind that the decision for real-time implementation should base on the real advantages in terms of dollars saved over any other existing routing systems. To help reach this Yes of No decision, the following steps for evaluating the proposed routing system are recommended.

Step 1 : Route Comparision with Other Existing Routing Methods

This test can be easily carried out with the cooperations of commercial routing companies. By providing access to all the input data and cost functions to the routing agencies, each of them are required to come up with a route using their system. The output from the Dynamic Programming outputs are then compared with various other alternative routes in order to explore the potential savings or lack of "human insight" by the computer model.

Step 2 : Route Evaluation Based on Hindcasted Data

Of course, the potential savings or errors made by any routing system cannot be verified until the stochastic nature reveals itself for the entire voyage. One simple method of evaluating various systems without actually risking the ship is to calculate the total ship motion responses etc. of the recommended routes using hindcasted environmental data from the wave model. Such comparison should be done over many voyages during different times of the year so that statistically valid conclusion can be drawn based on the large sample.

Step 3 : Actual Testing Implementation on Ships at Sea

If the results from the previous tests show conclusive advantages of the proposed Dynamic Programming routing system in real dollar savings over any other existing systems, then the next step is to carry out actual tests on a ship with proper instrumentation and communication equipments. This requires the full cooperation of the onboard personnel to carry out the recommended control policies along the route and make detailed records if alternative action is justified. Other assistance are also required to develop a realistic delay penalty cost function which is consistent with the financial and management practice of the ship owner.

Finally, it should be emphasized that efforts lead to a successful implementation of the proposed ship routing system would depend on the cooperation and inputs from ship operators, the U.S. Navy, commercial ship routing agencies and the academic establishment. The decision at various stages of development should be based on the hard performance statistics in terms of dollars saved under the operating conditions.

After all, it is this incentive that has brought any real improvements in the state-of-the-art of ship routing techniques since Henry the Navigator.

## REFERENCES


1. R.W. James. The Present Status of Ships Routing. INTEROCEAN '70. Paper presented at the International Conference, 15 Nov., 1970.

2. S. Laranoff and N. Stevenson. An Evaluation of a Hemispheric Operational Wave Spectral Model. Tech. Note No. 75-3, FNWC, Monterey, California. June 1975

3. C. Chryssostomidis,T.A. Loukakis and A. Steen. The Seakeeping Performance of a Ship in a Seaway. Report to be published by Maritime Administration.

4. W.E. Bleick and F.D. Faulkner. Minimal-Time Ship Routing. Technical Report, Naval Postgraduate School, August, 1964.

5. F.D. Faulkner. Determining Optimmum Ship Routes. Operations Research, Vol. 10, No. 6, p. 799-807. November-December, 1962.

6. H.D. Hamilton. Minimum-Time Ship Routing by Calculus of Variation Methods. USNPS, Thesis, 1961. Monterey, Calif.

7. E.W. Seibel. Thesis. United States Naval Postgraduate School, 1963. Monterey, Calif.

8. R.A. Gregor. Optimum Ship Routing by the Method of Steepest Ascent. Thesis, USNPGS, 1967, Monterey, Calif.

9. F.W. Nagle. A Numerical Study in Optimum Track Ship Routing Climatology. ENVPREDRSCHFAC, 10-70, TR/RP, No. 78, USNPGS. Technical Paper, October 1972.

10. W. Dupin. Optimum Ship Weather Routing. Marine Technology Society, Int. Maritime Inf. Symposium, p. 162-167. Washinton, D.C.

11. Bendix Marine Service, Sales Brochure

12. Fujitsu Limited. Development of Optimum Ship Route Setting System. Japan Shipbuilding & Marine Engineering, Vol. 7, No. 2, 1973.

13. F.E. Jaquotot, F.B. Donete, J.M. Palnneix and F. Tourman. Optimisation de la route à bord du "Castillo de la Mota" Fonctions et calculs de prévision du comportement a la mer. Bulletin De L'Association Technique Maritime Et Aeronautique No. 73, session de 1973.

14. R.F. Zobel. Weather Routing of Ships on the North Atlantic. Proc. Royal Society of Edinbrough, Series B., 1971/1972.

15. C. DeWit. Optimal Meteorological Ship Routing. Int. Shipping & Shipbuilding Progress, p.334-351, Vol.18, No. 205, 1971.

16. R. Zoppoli. Minimum-Time Routing as N-Stage Decision Process. Journal of Applied Meteorology, Vol. 11, p. 429-435, April 1972.

17. R.W. James. Application of Wave Forecasts to Marine Navigation. Naval Hydrographic Office, SP-1, 1970.

18. L.S. Pontryagin, et al. The Mathematical Theory of Optimal Processes. (translated by K.N. Trirogoff). Interscience, New York, 1962

19. W. Marks, et al. An Automated System for Optimum Ship Routing SNAME, Trans., 1968, Vol. 76.

20. R. Bellman. Dynamic Programming. Princeton University Press, Princeton, N.J., 1957.

21. R. Bellman. Adaptive Control Processes: A Guided Tour Princeton University Press, Princeton, N.J., 1961.

22. R. Bellman and S. Dreyfus. Applied Dynamic Programming Princeton University Press, Princeton, N.J., 1962.

23. J.W. Devanney III, Marine Decision Under Uncertainty. M.I.T. Sea Grant publication. 1971.

24. J.W. Devanney III, Dynamic Programming Under Constant Risk Aversion. Report #73-12. Commodity Transportation & Economic Development Laboratory. M.I.T. June 1973.

25. R.A. Howard. Dynamic Programming and Markov Process John Wiley and Sons, Inc. New York, 1960.

26. A. Zellner. An Introduction to Bayesian Inference In Econometrics. John Wiley & Sons. Inc., New York, 1971.

27. H. Chernoff and L.E. Moses, Elementary Decision Theory, John Wiley and Sons Inc., New York, 1959.

28. J.T. Tou. Optimum Design of Digital Control Systems. Academic Press, New York, 1963

29. Z.G. Wachnik and E.E. Zarnick. Ship Motions Prediction in Realistic Short-Crested Seas. SNAME, Transaction, Vol. 72, 1965

30. Report of Seakeeping Committee. 13th ITTC, p.815, Berin Hamburg, 1972.

31. D. Hoffman. Evaluation of the Spectral Ocean Wave Model (SOWM) as a Tool for Ship Response Prediction. NMRC Report, March, 1976.

32. W.J. Pierson, Jr. Known and Unknown Properties of the Two-dimensional Wave Spectrum and Attempts to Forecast the Two-dimensional Wave Spectrum for the North Atlantic Ocean. 5th Symposium of Naval Hydrodynamics ONR 1964.

33. W.J. Pierson & L. Moskowitz, A Proposed Spectral Form of Fully Developed Wind Seas Based on the Similarity Theory of S.A. Kitargorodsky , Journal of Geophysical Research, Vol. 69, No. 24, 12/1964.

34. M.S. Longnet-Higgins, On the Statistical Distribution of Maxima of Random Function , Proc. Roy Society Series A, Vol. 237, 1956.

35. C.L. Bretschneider, Wave Variability & Wave Spectra for Wind-Generated Gravity Waves , Beach Erosion Board Corps of Engineers, Tech. Memo, No. 118, 1959.

36. G. Neumann, Zur Charakteristik des Seeganges , Arch. Meterol. Geophys. Bioklimatol, A 7, 1954.

37. M.V. Mirokhim & Kholodilin, Probability Characteristic of Ship Inclination due to Erupting Wave Impulse , Proceedings of 14th ITTC, 1975.

38. I.N. Davidan, L.I. Lopatukhim, et al, The Results of Experimental Studies on the Probabilistic Characteristics of Wind Waves , Paper 39, Symposium on Theoretical Wave Making Resistance, Tokyo, 1976.

39. M.K. Ochi & E.N. Hubble, On Six-Parameter Wave Spectra , Proceedings of 15th Conference on Coastal Engineering, 1976.

40. Hasselman et al, Measurements of Wind-Wave Growth & Swell Decay During the Joint North Sea Wave Project (JONSWAP , Deutsches Hydrograph Inst., 1973.

41. J. Darbyshire, The One-Dimensional Wave Spectrum in the Atlantic Ocean & In Coastal Waters, Proceedings of Conference on Ocean Wave Spectra, 1961.

42. J.R. Scott, A Sea Spectrum for Model Tests & Long Term Ship Prediction, Journal of Ship Research, Vol. 4, No.3, 1965.

43. Nordenstrøm, N., Methods for Predicting Long Term Distributions of Wave Loads & Probability of Failure for Ships, DNV, Rep. 71-2-3, Appendix IV & Appendix V.

44. T.A. Loukakis, Experimental & Theoretical Determination of of Wave Form & Ship Responses Extremes, Dept. of Naval. Arch. & Marine Eng., Report 69-7, 1970.

45. E.H. Vanmerke, Properties of Spectral Moments with Applications at Random Vibration. Journal of AMSC. Engineering Mechanics Division., April 1972.

46. D. Hoffman. Analysis of Measured and Calculated Spectra. Paper 3, Symposium on Dynamics Responses of Marine Vehicles London, 1975.

47. T.A. Loukakis. Computer Aided Prediction of Seakeeping Performance in Ship Design M.I.T. Dept. of Naval Arch. & Marine Eng. Report No. 70-3, 1970.

48. W.G. Price and R.E.D. Bishop Probabilistic Theory of Ship Dynamics Chapman and Hall, London 1974.

49. J.N. Newman, Lecture Notes in Marine Hydrodynamics, Dept. of Ocean Engineering, M.I.T. 1974.

50. T. Loukakis & C. Chryssostomidis, Seakeeping Standard Series for Cruiser Stern Ship, Transaction, SNAME, 1975 Vol 83.

51. F.H. Todd, Series 60: Methodological Experiments with Models of Single-Screw Merchant Ships, DTMB Report No. 1712, Washington, D.C. 1963.

52. H. Lackenby & M.N. Parker, BSRA Methodical Series - An Overall Presentation Variations of Resistance with Breath - Draght Ration & Length Displacement Ratio, Trans., RINA, Vol. 108, 1966.

53. D.W. Hankley, Resistance & Propulsion Characteristics of the LASH Cargo Ships- Represented by Model 5132, NSRDC Report p-211-H-01, May, 1967.

54. G.A. Hampton & L.B. Crook. Powering Characteristics for the LASH Cargo Ship Represented by Model 5132 Fitted with Design Propeller 4395, NSRDC Report, T & E, p-211-H-06, March, 1969.

55. H. Marcus, The Excess Resistance of a Ship in A Rough Sea, International Shipbuilding Progress, Vol.4, No.35, July, 1957.

56. L. Vassilopoulos, The Application of Statistical Theory of Nonlinear Systems to Ship Motion Performance in Random Seas, First Ship Control System Symposium, U.S. Marine Eng. Lab. Annapolis, Maryland, 1966.

57. J. Strom-Tejsen, H.Y. Yeh & D.D. Moran, Added Resistance in Waves, Transaction, SNAME, Vol. 81, 1973.

58. J. Gerritsma & W. Beukelman, Analysis of the Resistance Increase in Waves of a Fast Cargo Ship, Report 169-S, Netherlands Ship Research Center, TNO, 1972.

59. N. Salvesen, Second-Order Steady-State Forces & Moments on Surface Ships in Oblique Regular Waves, Int'l Symp. on the Dynamics of Marine Vehicles & Structures in Waves, University College, London, 1974.

60. W.C. Lin & A.M. Reed, The Second Order Steady Forces & Moment on a Ship Moving in an Oblique Seaway, 11th ONR Symposium, 1976.

61. R. Hosoda, The Added Resistance of Ship in Regular Oblique Waves, Journal of Soc. of Naval Arch., Japan, Vol. 133, June, 1973

62. S. Nakamura, Added Resistance & Propulsive Performance of Ship in Waves, Int'l Seminar on Wave Resistance, Feb. 1976, Tokyo, Japan.

63. D.C. Murdey, Seakeeping Experiments on the BSRA Methodical Series 0.85 Block Coefficient Parent Form, RINA, Trans. Vol. 114, 1972.

64. O.J. Sibul, An Experimental Study of Ship Resistance & Motion in Waves - A Test for Linear Superposition. Univer. of Calif. Berkeley, College of Eng. Report No. NA-66-3, Jan. 1966.

65. M.F. VanSlijs, Performance & Propeller Load Fluctuations of A Ship in Waves, Report 163S, Netherlands Ship Research Center, TNO, Delft, Feb., 1972.

66. M. St. Denis, On the Environmental Operability of Seagoing Systems, Technical & Research Bulletin, No. 1-32, Published by SNAME. Jan. 1976.

67. R.M. Isherwood, Wind Resistance of Merchant Ships, RINA Transaction, 1973.

68. G. Aertssen & M.F. Van Sluys, Service Performance and Seakeeping Trials on Large Container, Spring meeting 19-2 RINA London

69. D. Hoffman, The Impact of Seakeeping on Ship Operations SNAME paper. New York Metropolitan Section, February, 1976.

70. C. Chryssostomidis, Seakeeping Considerations in a Total Design Methodology Ninth Symposium on Naval Hydrodynamics. Paris, August 1972.

71. J.B. Hadler & T.H. Sarchin, Seakeeping Criteria and Specification Seakeeping (1953-1973) T & R Symp S-3 SNAME

72. F. Warhurst, & A.J. Cerasini, Evaluation of the Performance of Human Operators as a Function of Ship Motion NSRDC report 2828, April 1969.

73. C.L. Crane, Jr. Report on Instrumentation and Analysis to Determine Reasons for a Ship Slowing Down in Heavy Weather, SNAME T & R Bulletin No. 4-3, 1961

74. L.J. Tick, Certain Probabilities Associated with Bow Submergence and Ship Slamming in Irregular Seas Journal of Ship Research, Vol. II No. 1, 1958.

75. M.K. Ochi, Prediction of Occurrence and Severity of Ship Slamming at Sea Fifth Symposium on Naval Hydrodynamics, ONR, USA and S. Kipsmodelltanken, Norway, Bergen, 1964.

76. D. Hoffman & E.V. Lewis, Heavy Weather Damage Warning Systems, Report NMRC KP-143, Setember 1975.

77. A. E. Bryson, Y.C. Ho, Applied Optimal Control Revised edition, Halsted Press. 1975.

APPENDIX A

APPROXIMATING STATE VALUE BY ITS EXPECTATION

When the controls are strong, there is little uncertainty in getting to a state j under control k. In this case, it is possible to replace the random variable j by its expected value, $\sum_{j=1}^{N} P_{ij}^{K} \; j$ for each control k, resulting in a deterministic system.

For the purpose of discussion, consider a one dimensional problem with a single stage return $q_i^k$ when control k is chosen in state i. Then, for the probabilistic and the deterministic system respectively, the gain g and objective function are given by:

$$\text{Probablistic: } g + C_i = q_i^k + \sum_j P_{ij}^k \; C_j \qquad \ldots(A1)$$

$$\text{Deterministic: } g^* + C_i^* = q_i^{k*} + \sum_j P_{ij}^k \; C^*[\mu^k(i)] \ldots(A2)$$

where $\mu^k(i)$ = Expected state that the system will in if control k is chosen at state i

By Taylor expansion

$$g - g^* + C_i - C_i^* = \sum_j P_{ij}^k (C_j - C_j^*) + \sum_j P_{ij}^k \{C_j - C^*[\mu^k(i)]\}$$

$$\simeq \sum_j P_{ij}^k (C_j - C_j^*) + \sum_j P_{ij}^k \; C^{*\prime\prime}[\mu^k(i)][j - \mu^k(i)]^2/2!$$

$$\therefore \Delta g + \Delta C \simeq \sum_j P_{ij}^k \; (C_j - C_j^*) + C^{*\prime\prime}[\mu^k(i)] \sigma_k^2 \; (i)/2! \qquad \ldots\ldots(A3)$$

where $\sigma_k^2$ (i) = variance of the state that system will be in if control k is chosen at state i.

$C^*_j{}''$ = the second derivative of C* with respect to j.

Now if the control is strong, there is less uncertainty in the state transition, i.e. the value of $\sigma_k^2$ (i) is small. Since the difference between the deterministic and stochastic discription resulted in a change of gain and objective function, ($\Delta g$, $\Delta C$ respectively), as $\sigma_k^2$(i) tends to zero, the difference between the true optimal value function C and the approximated value C* becomes very small.

APPENDIX B

REDUCTION OF STATE SPACE BY PENALTY METHOD

In the stochastic model, the random state variable, time should have an infinite range in order to completely describe the feasible state space. This is because there always exists a non-zero probability, however small, that the ship is going to arrive at a grid later than the so-called 'latest time'. This means that we could have a infinitely large state space to ensure that the system will not go out of the bounds. In practice, this is obviously not allowed in evaluating the optimal value function by our stochastic recursion equation. It is therefore necessary to specify the bounds of the feasible state space in order to reduce the problem size. We propose to implement this by a penalty method which imposes a large penalty cost whenever the system is outside the bounds.

Because the nature of the recursion equation, the imposed penalty in a state of stage n could effect the optimal value function in remaining stages. The following is a derivation of a set of necessary conditions which ensure the bounds are large enough so that the penalties on the states which has a small probability of going out of bounds could not significantly effect the true optimal value function.

For the purpose of discussion let us consider a simple one dimension problem. Suppose that the entire set of feasible states can be partitioned into three mutually exclusive subsets X,Y,Z of which Z comprises only state known to be out of bounds. Let Y comprise of the state in which there is a non-zero probability of transition into Z, where a large penalty M will be imposed.

At the start of the recursion, we let the minimum cost function be $C_{N+1}(j)$; also let $P_{ij}^{k_n \ldots k_N}$ be the probability that if we start initially in state i and then execute N-n successive controls $k_n \ldots k_{n+1} \ldots k_N$, we will be in state j.

Suppose A or B contains j at N + 1. The recursion equation is given by

$$C_n(i) = \min_k \left[ q_i^k + \sum_j P_{ij}^k \, C_{n+1}(j) \right] \qquad \ldots\ldots (B.1)$$

Now, if we split the minimum cost function $C_{n+1}(j)$ into two parts:

$$C_{n+1}(j) = c_{n+1}(j) + L_{n+1}$$

where $L_{n+1}$ is the loss at stage n+1 then:

$$C_n(i) = \min_k \left\{ q_i^k + \sum_j P_{ij}^k \left[ c_{n+1}(j) + L_{n+1} \right] \right\} \qquad \ldots\ldots (B.2)$$

Furthermore, let q* be the smallest single stage loss obtainable at any state then:

$$C_n(i) \geq q^* + \min_k \left[ \sum_j P_{ij}^k \left[ c_{n+1}(j) + L_{n+1} \right) \right]$$

Recall the first order Markov property; we can rewrite the minimization of expected value cost in two parts, one for the present stage n, and the other for the later stages. We have:

$$C_n(i) \geq q^* + E[L_{n+1}] + \min_{k(n)} \left\{ \sum_{j(n)} P_{ij(n)}^k \min_k \left[ q_{j(n)}^{k(n)} + \sum_{j(n+1)} P_{ij(n+1)}^k C_{n+2}(j) \right] \right\}$$

Similar mathematical manipulation can be carried out for $C_{n+2}(j)$; $C_{n+3}$, ..... until $C_{N+1}(j)$.

Hence we may derive :

$$C_n(i) \geq nq^* + \sum_{s=n}^{n} E[L_s] + \sum_j P_{ij}^{k_n, k_{n+1} \cdots k_N} \; C_{N+1}(j). \qquad \ldots.(B.3)$$

At any stage $s, n \leq s \leq N$, if the system goes out of the bounds into Z, we impose a high penalty cost M. i.e. $C_{s+1}(j) = M$ $j \in Z$. The difference in $C_N(i)$ after N-s iterations would be:

$$\sum_j P_{ij}^{k_s \cdot k_{s+1} \cdots k_N} * M \qquad j \in Z, \quad n \leq s \leq N \qquad \ldots.(B.4)$$

It is also interesting to note that if we let $M \to \infty$, then after N-s interaction, all states in Y and Z will be $\infty$. Only the states in X will have finite values which will converge. In fact, rigorously X is an empty set by definition of stochastic process.

From equation (D.4), we have derived two necessary conditions to ensure that the bounds on state variable time had been large enough.

1. $P_{cr} = P_{ij}^{k_s \cdot k_{s+1} \cdots k_N}$ is small. $j \in Z$.

2. $P_{cr} \cdot M$ is also small for some large M.

APPENDIX C

DERIVATION OF STATE TRANSITION PROBABILITY BASED ON ANALOGUE FORECAST

When consistent wave spectra forecasts are not available, the ocean environment conditions are usually forecasted by analogue methods. The analogue forecasts rely largely on experienced meteorologists and vast computer data banks of historical wave information. By searching and comparing similar weather patterns in the past, the forecaster may be able to estimate the most likely wave height $\hat{H}$, a lower bound $H_{min}$ and a upper bound $H_{max}$ on some inherent confidence level.

Based on these three estimates, we postulate that the wave height parameter distributes with a Gamma p.d.f. The distribution is chosen not because of its closeness to reality which cannot easily be verified, but rather due to its simplicity and powerful properties to approximate many situations.

Essentially, we will utilize the extremely rich family of functions which lie on the positive real axis. The parameter of the distribution can be expressed in terms of the most probable wave height $\hat{H}$ and the two extremes: $H_{min}$, $H_{max}$.

The Gamma p.d.f. in a general form can be written as:

$$f(H) = A\, H^{b}\, e^{-CH}\, U(H)$$

$$U(H) = \begin{cases} 1 & H \geq 0 \\ 0 & H < 0 \end{cases} \qquad \ldots(C.1)$$

where

$$A = \frac{C^{b+1}}{\Gamma(b+1)}$$

$\Gamma$ = Gamma Function

The mode, i.e. the maximum f of the function is located at

$$\hat{H} = b/c. \qquad \ldots.(C.2)$$

The expected value is given by:

$$E(H) = \frac{b+1}{C} \qquad \ldots.(C.3)$$

and variance

$$\sigma_H^2 = \frac{b+1}{C^2} \qquad \ldots.(C.4)$$

To express the parameter b, c in terms of the three estimates, it is necessary to provide additional information on the variance of the distribution $\sigma_H 2$.

Let the standard derivation be 1/6 of the range $H_R = H_{max} - H_{min}$.[1] Then from (E.4)

$$\sigma_H^2 = \frac{b+1}{C^2} = [1/6\ (H_{max} - H_{min})]^2 \qquad \ldots.(C.5)$$

with equation (E.2), it can be shown that the parameters b, and c are given by

$$C = \frac{\hat{H} \pm \sqrt{9\ \hat{H}^2 + H_R^2}}{1/6\ H_R^2} \qquad \ldots.(C.6)$$

$$b = \hat{H} \cdot C.$$

Hence, by discretizing the above Gamma p.d.f, we can derive the state transition probabilities and carry out the recurrsion same as before.

---

[1] The normal distribution translated at $\pm$ 2.66 has standard deviation equal to 1/6 of its range i which corresponds to arround 99% confidence level. This assumption is also used in PERT to derive the parameter for Beta distribution.

APPENDIX D

PROPERTIES OF THE GENERALIZED TWO PARAMETER SPECTRAL FORMULATION FOR OCEAN WAVES

The generalized two parameter sea spectra formulation has the following form: Ref. [43].

$$S(\omega) = \alpha\ \omega^{-a}\ \exp\ (-\beta\ \omega^{-b}) \qquad \ldots.(D\ 1)$$

where S(W) is the spectral density as a function of wave frequency $\omega, \alpha, \beta$, a and b are constants.

Moments defined as: $M_i = \int_0^\infty S(\omega) * \omega^i\ d\omega$ is given by

$$m_i = \alpha\Gamma(k)/(b\beta^{-k}) \qquad \ldots.(D\ 2)$$

where $\Gamma(\cdot)$ = Gamma Function

$$k = (a - i - 1)/b \qquad k > 0$$

$$m_o = \alpha\Gamma(a-1/b)/[b\beta^{(a-1/b)}]$$

$$m_1 = \alpha\Gamma(a-2/b)/[b\beta^{(a-2/b)}]$$

$$m_2 = \alpha\Gamma(a-3/b)/[b\beta^{(a-3/b)}]$$

$$m_4 = \alpha\Gamma(a-5/b)/[b\beta^{(a-5/b)}]$$

In seakeeping work provided that the wave process is Gaussian and narrow band, some characteristics wave heights and period may be defined in terms of these moments [34].

| | |
|---|---|
| mean square wave heights | $H^2 = 8\ m_o$ |
| significant wave height | $H\ 1/3 = 4\ m_o^{1/2}$ |
| energy-average period | $T_{-1} = 2\pi\ (m-1/m_o)$ |
| average mean period | $T_1 = 2\pi\ (m_o/m_1)$ |
| average zero crossing period | $T_2 = 2\pi\ \sqrt{m_o/m_2}$ |
| apparent period between crests | $T_4 = 2\pi\ \sqrt{m_2/m_4}$ |

For processes that are not strictly narrow band, the motion of broadness $\varepsilon$ was introduced in [43] and it is defined as:

$$\varepsilon = (1 - \frac{m_2^2}{m_o m_4})^{1/2} \qquad \ldots.(D.3)$$

Then, the characteristic wave heights for processes other than ideally narrow band process ($\varepsilon>0$) are given by:

$$H^2 = 8(1 - \varepsilon^2/2)m_o \qquad \ldots.(D.4)$$

$$H\ 1/3 = 4(1 - \varepsilon^2/2)^{1/2}\ m_o^{1/2} \qquad \ldots.(D.5)$$

Alternatively, a bandwidth parameter may be introduced Ref.[45] to characterize the dispersion or spread of $s(\omega)$ about its central frequency

$$q = (1 - \frac{m_1^2}{m_o\ m_2})^{1/2} \qquad \ldots.(D.6)$$

For Pierson-Moskowitz spectrum and Bretschneider spectrum, a=5, b=4, then

$$m_i = \frac{\alpha}{4\beta^{(1-i/4)}} \Gamma(1-i/4)$$

$$m_o = \alpha/4\beta$$

$$m_1 = \alpha/4\beta^{3/4}$$

$$m_2 = \alpha\pi^{1/2}/4\beta^{1/2}$$

$$m_4 = \text{unbounded as } \omega \to \infty$$

$$q = [1.0 - \frac{\Gamma(0.75)^2}{\Gamma(1)\Gamma(0.5)}]^{1/2}$$

$$= 0.39088$$

It has been argued in [44] that Truncation of frequency beyond three times the modal frequency would only contribute less than 1% of error. In this case, the spectral broadness function, $\varepsilon$, is given by:

$$\varepsilon = (1.0 - m_2^2/m_o m_4)^{1/2}$$

$$\simeq = 0.59$$

For the Neuman spectrum, a=6, b=2, the value of broadness parameters are given by:

Broadness or bandwidth measure then becomes:

$$\varepsilon^2 = [1.0 - \frac{m_2^2}{m_o m_4^2}]$$

$$= 1.0 - \frac{\Gamma((a-3)/b)^2}{\Gamma((a-1)/b)\ \Gamma((a-5)/b)}$$

$$q^2 = [1.0 - \frac{m_1^2}{m_o m_2}]$$

$$= 1.0 - \frac{\Gamma((a-2)/b)}{\Gamma((a-1)/b)\Gamma((a-3)/b)}$$

The constant $\alpha$, $\beta$ of the parameters can be expressed in terms of $H_{1/3}$, $T_2$

$$\alpha = H_{1/3}^2\ b/16\ (2\pi/T_2)^{(a-1)}\ [\frac{\Gamma((a-1)/b)^{(a-3)}}{\Gamma((a-3)/b)^{(a-1)}}]^{1/2} \qquad \ldots(D.7)$$

$$\beta = (2\pi/T_2)^b [\frac{\Gamma((a-1)/b)}{\Gamma((a-3)/b)}]^{1/2} \qquad \ldots(D.8)$$

and peak frequency:

$$\omega_p = (b\beta/a)^{1/b} = b/a\ 2\pi/T_2\ [\frac{\Gamma((a-1)/b)}{\Gamma(a-3)/b)}]^{1/2} \qquad \ldots(D.9)$$

$$\varepsilon = [1.0 - \frac{\Gamma(3/2)^2}{\Gamma(5/2)\Gamma(1/2)}]^{1/2}$$

$$= 0.816$$

$$q = [1.0 - \frac{\Gamma(2)^2}{\Gamma(5/2)\Gamma(3/2)}]^{1/2}$$

$$= 0.3888$$

For the Nozresenski-Netsvetayer spectrum, a=6,b=4:

$$q = [1.0 - \frac{\Gamma(1)^2}{\Gamma(5/4)\Gamma(3/4)}]^{1/2}$$

$$= 0.31573$$

and the Davidan-Lopatukhim spectrum, a=6, b=5.

$$q = [1.0 - \frac{\Gamma(4/5)^2}{\Gamma(1)\Gamma(3/5)}]^{1/2}$$

$$= 0.2997$$

For the Darbyshire type of spectrum proposed in [42] and moments have been estimated by numerical integration [43] and the value of q equals:

$$q = [1.0 - m_1^2 / m_o m_2]^{1/2}$$

$$= 0.47$$

Notice that for all the above spectral formulations, both measures of spectral broadness or bandwidth parameters namely $\varepsilon$ and q are constant independent of $H_{1/3}$ and T. This is contrary to what is found from the actual measured data where the value $\varepsilon$ tended to increase at high value of $H_{1/3}$, see Table D.1.

Although the parameter $\varepsilon$ itself still has some problems because $m_4$ is unbounded, the variations in $\varepsilon$ and q do indicate the importance of the spread of energy content in the frequency domain as it differs from formulation to formulation.

TABLE D.1 CHARACTERISTICS OF NEW WAVE SPECTRA FAMILY WITH EIGHT SPECTRA PER GROUP [4]

| GROUP NO. | HIGHTS FT. | $H_1$ | $T_1$ | $\varepsilon$ | NO. OF RECORDS IN SAMPLE |
|---|---|---|---|---|---|
| 1 | > 3 | 2.22 | 6.97 | 0.5782 | 11 |
| 2 | 3 - 6 | 5.20 | 7.33 | 0.5784 | 49 |
| 3 | 6 - 9 | 7.53 | 8.46 | 0.6368 | 57 |
| 4 | 9 - 12 | 10.63 | 8.31 | 0.6345 | 59 |
| 5 | 12 - 16 | 14.04 | 9.03 | 0.6806 | 48 |
| 6 | 16 - 21 | 17.83 | 8.80 | 0.6803 | 46 |
| 7 | 21 - 27 | 24.04 | 9.50 | 0.7075 | 31 |
| 8 | 27 - 34 | 28.93 | 9.93 | 0.7328 | 11 |
| 9 | 34 - 42 | 37.23 | 11.21 | 0.7638 | 9 |
| 10 | 42 > | 48.08 | 11.61 | 0.7870 | 8 |

APPENDIX E. Calculation of Mean Square Responses Using Two Parameter Spectra and Cosine Square Spreading Function

Wave Spectra Formulation

Recall that in Chapter 4 we haved assumed that the wave spectrum is considered to be a separable function of wave frequency and direction.

$$S(\omega,\mu) = S_1(\omega)\ S_2(\mu). \qquad \text{for } 0 \leq \omega \leq \infty, \quad -\frac{\Pi}{2} \leq \mu \leq \frac{\Pi}{2} \qquad \ldots.(E.1)$$

where

$S_1(\omega)$ may have the formulation of a two-parameter family spectra.

$$S_1(\omega) = \alpha\omega^{-5}\exp(-\beta\omega^{-4}) \qquad \ldots(E.2)$$

by definition and assuming the crest-to-trough wave heights have a Rayleigh distribution, then the parameters are related to the significant wave height and peek frequency by:

$$\alpha = \omega\rho^4 (H_{1/3})2 \qquad [ft^2/sec^4].$$

$$\beta = 5/4\ \omega\rho^4 \qquad [sec^{-4}]$$

$$\ldots(E.3)$$

$\omega$ is circular wave frequency in $[Sec^{-1}]$.

The spreading function has been assumed a cosine square form.

$$S_2(\mu) = \frac{2}{\Pi}\ Cos^2\ \mu \qquad \ldots(E.4)$$

where

$\mu$ = wave direction relative to predominant direction $\chi$

Responses

According to linear superpostion theory, all the responses in the frequency domain may be expressed simply as the product of the transfer function squared.

$$S_{ii}(\omega,\mu) = [RAO^2_{ii}(\omega,\mu)] \cdot S(\omega,\mu) \quad \ldots(E.5)$$

where $RAO_{ii}(\omega,\mu)$ = response amplitude operater (amplitude of response ii per unit wave amplitude).

Thus the mean square responses is the sum of each response at different $\omega$ and $\mu$.

$$\sigma^2_{ii} = \int_0^\infty \int_{-\pi/2}^{\pi/2} S_{ii}(\omega,\mu)\, d\mu\, d\omega$$

$$= \int_{-\pi/2}^{\pi/2} S_2(\mu) \left[ \int RAO^2_{ii}(\omega,\mu) S_1(\omega)\, d\omega \right] d\mu$$

$$= \frac{\pi}{2} \int_{-\pi/2}^{\pi/2} \cos^2 \mu \int_0^\infty RAO^2_{ii}(\omega,\mu) S_1(\omega; H_{1/3}, \omega_p) d\omega\, d\mu \quad \ldots (E.6)$$

Notice that above expression is only strictly true for zero ship speed. To account for the ship's mean forward velocity and relative angle between ship and wave, the frequency has to be mapped into frequency fo encounter by

$$\omega_e = \left| \omega - \frac{\omega^2}{g} V \cos \mu_r \right| \quad \ldots(E.7)$$

Since we are only interested in mean square values, the computation becomes somewhat simplified because there is no need for frequency mapping, and only the RAO's are referred to by

the encounter frequency.

Hence,

$$\sigma_{ii}^2 = \frac{\pi}{2} \int_{-\pi/2}^{\pi/2} \mathrm{Cos}^2\ \mu \int_0^{\infty} RAO_{ii}^2(\omega e, \mu) S_1(\omega; H_{1/3}\omega p)\, d\omega\ d\mu \quad \ldots(E.8)$$

The above expression can be readily evaluated by numerical integration. APPENDIX contains a listing of the FORTRAN program for calculating the ship responses for a given set of $H_{1/3}$, $\omega_p$ and $\chi$ .

APPENDIX F

DERIVATION OF TERMINAL COST FUNCTION

In our model, the terminal cost for a ship on a particular voyage is essentially a function of the trade-off between the extra fuel cost for sailing at maximum power and the owner's opportunity cost and related expenses if the ship arrives later than the schedule.

For owner-operators, e.g. oil company, the opportunity costs of his fleet is directly related to the tanker spot market. By reducing the fleet's cruising speed, the oil company may save considerable fuel cost in their own fleet operation. While making up the lost ten-mile capacity by chartering ships in the depressed spot market.

However, for other types of ship operations, such classic trade-offs in the use of resources can not easily be made. In particular, for a ship engaging in a liner service, the derivation of terminal cost becomes very complicated. The delay penalty for a liner ship should include not only the owner's opportunity cost and related expenses, but also the 'user cost' if schedules are not well kept. The 'user cost' in the competitive liner business can be very large and has far reaching effects on a company's future revenue. It is this kind of uncertainty in the market plus the labour practices at the unloading port which create difficulties in estimating the terminal cost function for our routing model.

On the other hand, if we disregard the intricate market situation, etc. for a moment and only consider the following:

1. Capital Cost

Depending on the management and financial arrangements, the daily finance cost of a vessel ownership can be more than $10,000/day. If such a figure is not available, the following is an approximated cost of financing a new ship:

(Owner's Cost Excluding Subsidy (CDS) = Foreign Cost)

| | | | |
|---|---|---|---|
| General Cargo Ships | = | $500 R + 30800\sqrt{H}$ | = K |
| Container Ships | = | $620 R + 34000\sqrt{H}$ | = K |
| Barge Carriers | = | $670 R + 36000\sqrt{H}$ | = K |
| Tankers Small (10-35000 DWT) | = | $430 R + 28000\sqrt{H}$ | = K |
| Tankers Medium (36-120000 DWT) | = | $380 R + 26000\sqrt{H}$ | = K |
| Tankers Large (121-500000 DWT) | = | $300 R + 24000\sqrt{H}$ | = K |
| Dry Bulk Carriers Small (10-35000 DWT) | | $460 R + 29600\sqrt{H}$ | = K |
| Dry Bulk Carriers Medium (36-120000 DWT) | = | $400 R + 28800\sqrt{H}$ | = K |
| Dry Bulk Carriers Large (121-500000 DWT) | = | $330 R + 27000\sqrt{H}$ | = K |

H = SHP  R = Cubic Number = $\frac{L.B.D.}{100}$

To determine U.S. construction or capital costs before CDS or without CDS the above costs should be multiplied (for 1977 orders 1979 delivery)by

| | | |
|---|---|---|
| U.S. Cost Multiplier | General Cargo Liner | = 1.80 |
| | Containership | = 1.92 |
| | Barge Carrier | = 1.96 |
| | Tanker Small | = 1.80 |
| | Medium | = 1.84 |
| | Large | = 1.88 |

| | | |
|---|---|---|
| Dry Bulk Carrier | | |
| | Small | = 1.80 |
| | Medium | = 1.84 |
| | Large | = 1.88 |

Considering daily finance cost of vessel ownership, linear depreciation of capital cost over 20 years with a 4% salvage value and interest on the unpaid balance at i% is usually assumed. As a result average depreciation and interest costs per day are for a vessel equal to:

$$F = 1.3 \times 10^{-3} K(.1 + i) \text{ in } \$/\text{day}$$

where K is first or capital cost of ship

Insurance Costs

Of the total Insurance Cost (premiums) paid for a general cargo ship (liner) for example, 48% goes for (H&M) hull and machinery coverage, while the remaining 52% goes for (P&I) protection and indemnity. Different proportions of H&M and P&I coverage apply to containerships, barge carriers, tankers and bulk carriers. Total daily insurance cost is nearly linear with first or capital cost of the vessel and can be approximated by

| | | | |
|---|---|---|---|
| General Cargo Ships | | $I = 0.2166 \times K \times 10^{-4}$ | $/day |
| Containerships | | $I = 0.201 \times K \times 10^{-4}$ | $/day |
| Barge Carriers | | $I = 0.21 \times K \times 10^{-4}$ | $/day |
| Tankers | Small | $I = 0.23 \times K \times 10^{-4}$ | $/day |
| | Medium | $I = 0.24 \times K \times 10^{-4}$ | $/day |
| | Large | $I = 0.26 \times K \times 10^{-4}$ | $/day |
| Dry Bulk Carriers | | | |
| | Small | $I = 0.18 \times K \times 10^{-4}$ | $/day |
| | Medium | $I = 0.19 \times K \times 10^{-4}$ | $/day |
| | Large | $I = 0.19 \times K \times 10^{-4}$ | $/day |

3. Manning or Crew Costs

The crew size of a general cargo, containership, or barge carrier can generally be estimated using the expression

$$N = 26.8 + \frac{0.35}{1000} + 0.15\sqrt{H}$$ to the nearest integer for US practice

Tanker and Dry Bulk Carrier manning size can be determined by

$$N = 29 + \frac{0.3R}{1000} + 0.2\sqrt{H}$$ to the nearest integer for US practice

It should be noted though that manning is increasingly subject to owner/union negotiation and only limited by minimum Coast Guard manning standards. The above should therefore only be used as a standard.

Average Annual Cost of Crew including all fringe benefits, repatriation, overtime, compensatory time, relief, and other payments averaged (1977) to

$44,200/man/year

or $121.10/man/day

on subsidized (ODS) vessels, basically. U.S. flag liners on essential trade routes, owners costs or crew are only about 38% of the above. As a result Daily Crew Costs can be estimated as follows:

For Cargo Ships, Containerships, Barge Carriers

$CL = 3245.5 + 0.042\ R + 18.1\sqrt{H}$ Unsubsidized

$CL = 1233.1 + 0.016\ R + 6.88\sqrt{H}$ Subsidized or Foreign Flag

For Tankers and Dry Bulk Carriers

$CL = 3512 + 0.036\ R + 24.2\sqrt{H}$

4. Additional Operating Costs due to late arrival

Because of the delayed arrival, additional shifts or overtime for unloading or loading is necessary to make up the schedule. The added cargo handling costs should be included in the terminal cost or delay penalty.

Depending upon the rates and labour practices in different ports around the world, the additional direct operating cost may be a certain percentage of the total cargo handling cost.

Bulk Carriers (in $/ship assuming full load handled)

Import Loading Costs $= 2.2DWT(0.63 + 0.27R)/d^{0.43} = LC_I$

Discharge Costs $= 17.74DWT/d^{0.43} = DC_F$

Export Loading Costs $= 2.0DWT/d^{0.43} = LC_E$

Discharge Costs $= 2.2DWT(5.6 + 2.4R)/d^{0.43} = DC_E$

Tankers (In $/ship assuming full load handled)

Loading Costs $= 0.8DWT/d^{0.43} = LC$

Discharge Costs $= 1.6DWT/d^{0.43} = DC$

Containership (in $ for number of TEU's handled)

Import Loading Costs $= 2 \cdot TEU(28 + 52R)$

Discharge Costs $= 160 \cdot TEU$

Export Loading Costs $= 160 \cdot TEU$

Discharge Costs $= 2 \cdot TEU(28 + 52R)$

General Cargo

Loading or Discharging Costs $= 32(0.15 + 0.85R)$ $/ton

Loading or Discharging Costs $= 32$ tons$(0.15 + 0.85R)$

where

DWT = Deadweight Load in Tons

d = cargo density in $lbs/ft^3$

R = ratio of port labor cost in foreign country to port labor cost in US

TEU = 20' container equivalent

It follows therefore, by adding all the cost components and converting them into $/hour, a delay cost curve can be derived. Fig. 5.1-2 shows a typical example of the cost function. Notice the inconsistencies in the curve occur at the stevedore working shifts. After two shifts at (1800Z). the curve levels off with the slope equal to the extra overtime loading/unloading cost. The whole cycle repeats for the next day starting at(0600 Z). The delay cost per hour is assumed linear with time and changes its value according to the shifts.

Obviously, other forms of cost function are also permitted. For example, by using a quadratic or cubic function, it increases the delay penalty for later arrivals.